RESEARCH STUDY ON COLD DRAWING

PHENOMENA IN HIGH POLYMERS

by

R. D. Andrews, Jr., S. W. Allison, D. H. Ender

R.M. Kimmel, and W. Whitney

Massachusetts Institute of Technology
Fibers and Polymers Division
Department of Mechanical Engineering
Cambridge, Massachusetts 02139

DEC 29 1966

UNITED STATES ARMY
NATICK LABORATORIES
Natick, Massachusetts 01760

Clothing and Organic Materials Division
C&OM-25

AD _____

TECHNICAL REPORT
67-10-CM

RESEARCH STUDY ON COLD DRAWING PHENOMENA IN
HIGH POLYMERS

by

R. D. Andrews, Jr., S. W. Allison, D. H. Ender,
R. M. Kimmel, and W. Whitney

Massachusetts Institute of Technology
Fibers and Polymers Division
Department of Mechanical Engineering
Cambridge, Massachusetts 02139

Contract No. DA19-129-AMC-238(N)

FOREWORD

The ability of polymeric materials to yield and draw can play an important role in the dissipation of energy during ballistic impact. In addition, knowledge of the mechanisms operating to produce yielding in amorphous and crystalline polymers can advance our scientific understanding to a point where improved polymeric materials may be prepared.

The work covered in this report was performed over a two-year period by Dr. R. D. Andrews, Mr. S. W. Allison, Mr. D. H. Ender, Mr. R. H. Kimmel, and Dr. W. Whitney of Massachusetts Institute of Technology under Contract DA19-129-AMC-238(N).

It represents work on amorphous polystyrene, polymethyl methacrylate, polycarbonate, polyamide, polyacrylonitrile and other polymers under various uniaxial, biaxial, and triaxial stress conditions (notched). This has resulted in yield and fracture criteria and theoretical proposals for the mechanisms involved in yielding.

The U. S. Army Natick Laboratories Project Officer was Mr. Roy C. Laible and the Alternate Project Officer was Mr. Anthony L. Alesi, Materials Research Branch, Clothing and Organic Materials Division.

                                        S. J. KENNEDY
                                        Director
                                        Clothing & Organic Materials Division

APPROVED:

DALE H. SIELING, Ph.D.
Scientific Director

W. M. MANTZ
Brigadier General, USA
Commanding

CONTENTS

LIST OF FIGURES

ABSTRACT

A fundamental study of the phenomenon of cold-drawing
(plastic yield) in polymers has been carried out, through
which a better understanding of several of the features of
this process has been achieved. The effects of temperature,
thermal history, stress-field, chemical structure and pre-
orientation on the stress-strain behavior of both glassy and
crystalline polymers have been explored. The behavior of
several polymers, particularly polystyrene and polymethyl
methacrylate, in stress relaxation, relaxation-recovery
cycling and creep, especially with respect to delayed draw-
ing, was investigated in detail. The geometry of neck
formation has been quantitatively investigated by photo-
graphic techniques, and volume changes during compression
have been measured using a mercury dilatometer. Micro-
scopic modes of yielding, particularly the formation of
deformation bands, are described. Birefringence changes
during deformation of polyacrylonitrile under various
conditions and during hot and cold extension of polystyrene
and polymethyl methacrylate are presented and related to
the molecular processes believed to be occurring. The
development of a molecular theory of drawing is attempted
through three different paths of approach: (1) a defect
model analogous to dislocations, (2) a mathematical model of
the "fiber bundle" type, and (3) a description in terms of
the breakdown of secondary intermolecular cohesive bonding.
General conclusions and recommendations for future studies
in these areas are presented.

x

RESEARCH STUDY ON COLD DRAWING PHENOMENA
IN HIGH POLYMERS

I. INTRODUCTION

This Final Report covers the work carried out during
the period of a two-year contract with the U. S. Army
Natick Laboratories, having as its aim a fundamental study
of the phenomenon of cold drawing (or plastic yield) in
solid polymers. This was a continuation of the work begun
under a previous six-month contract [DA 19-129-AMC-100(N),
covering the period 5/1/63 to 10/31/63] with the Army
Natick Laboratories, which involved an exploratory study of
this area, using glassy amorphous polymers (polystyrene
and polymethyl methacrylate) exclusively.[1] The use of
glassy amorphous polymers avoids the complications asso-
ciated with crystalline morphology and structure which are
encountered in crystalline polymers; also, since the yield
and drawing behavior of amorphous and crystalline polymers
seems to be remarkably similar, there is considerable
advantage in first studying the yield phenomenon in amor-
phous polymers. We have continued to employ this strategy
of attack on the problem during the present two-year
contract, confining our attention primarily to amorphous
glassy polymers; however, we have also carried out detailed
measurements on polyacrylonitrile, a polymer with ill-
defined crystallinity, as well as preliminary investigation
of some polymers with well-characterized crystallinity.

The phenomenon of plastic yield in polymers is of
considerable importance both from a practical and from a
theoretical standpoint. From the practical standpoint
this process has been of major importance in the textile
industry for several years, since synthetic fibers are
routinely subjected to a "drawing" process after spinning
in order to orient them and increase their tensile strength
(or "tenacity"). Processes of "cold-forming" are also under
consideration in the plastics industry at the present time;
these would utilize the yield property of the polymers,
just as "cold-stamping" or "wire drawing" utilizes the
same property of metals to give a rapid method of shaping
and fabricating metal parts. The yield phenomenon is also
of importance in connection with the problem of impact
strength and impact response, since the common classifica-
tion of materials into the brittle vs. ductile categories

is based entirely on whether the material will show plastic
yield prior to fracture. Consideration of the role of
plastic yield in the ballistic response of polymers, where
very high speed impact is involved, is of obvious impor-
tance. The effects of complex stress fields must also be
taken into account in order to give a satisfactory des-
cription of ballistic response. Delayed yield under creep
conditions (constant dead load), which we have observed in
our studies and investigated in some detail, may also be
a significant failure mechanism in cases where dimensional
stability is a critical factor.

From the theoretical standpoint, an understanding of
the plastic yield effect is clearly necessary in achieving
any sort of adequate understanding of the mechanical
properties (or stress response) of solid polymers. Yield
and fracture are the two phenomena which are of greatest
interest in the stress response of a polymer in the high
stress range. It may seem surprising that the nature of
these processes is not better understood at the present
time, considering their fundamental importance. Most
studies of stress response have been concerned with the
linear viscoelastic type of behavior observed at low
stresses, and this range of behavior is now fairly well
understood (at least from the phenomenological standpoint;
the molecular theory is by no means completely established).
The non-linear viscoelasticity which is observed in the
intermediate ranges of stress is also not well understood,
and is only now beginning to receive careful study. An
adequate elucidation of the nature of the yield process
could very well aid in achieving an understanding of
both non-linear viscoelasticity and the fracture process.

Because of the broad and fundamental nature of the
yield phenomenon, it has many aspects which can be studied,
and it is of interest from many different points of view.
An understanding which will be adequate for one purpose--
because it emphasizes certain features which are relevant
in that specific case--may be inadequate for another. This
means that a study such as this cannot take an approach in
which yield is regarded as a problem to be "solved" by
some obvious, direct line of attack; rather, it must be
examined in a broad way, using several exploratory lines
of approach, with the aim of achieving an understanding
of as many facets of the phenomenon as possible. This is
particularly necessary when the phenomenon as a whole is
so poorly understood. Experimental knowledge is particu-
larly needed at the present time, but the theoretical

2

aspects of the problem cannot be neglected. The ultimate
aim of this research would be to achieve a comprehensive
understanding of the various aspects of the phenomenon
which would include an understanding of the relation between
the yield process and the chemical and molecular structure
of the polymer, and additionally the relation to the
crystalline and morphological structure in the case of
crystalline polymers.

In the study which is being reported here, we have
pursued several different lines of investigation. These
have included a study of the time effects associated with
drawing (e.g., effects of interrupted drawing and drawing
with a delay time under dead load). Since the phenomenon
of neck formation and propagation is one of the most strik-
ing features associated with drawing, we have investigated
this aspect of the process by the use of sequence photo-
graphy. Some general idea was obtained of the effects of
stress fields other than simple tension, and attention was
paid to the different deformation modes encountered
(including the localization of deformation in shear bands--
a frequently observed effect analogous to the "Luder's
bands", or "slip bands", observed in metals). Effects of
molecular orientation, temperature, stress level, thermal
history (annealing) and absorbed moisture (acting as a
plasticizer) were also investigated. Birefringence effects
associated with drawing were studied, particularly in
connection with the drawing of polyacrylonitrile; this
polymer also provided a useful bridge between amorphous
and crystalline polymers. The phenomenological theory of
drawing has been treated through a consideration of yield
criteria and the possible applicability of an equation of
state approach. The development of a "molecular" theory
of drawing has also been attempted through three different
paths of approach: (1) a description in terms of a defect
model analogous to the dislocation mechanism operative in
metals and other crystalline non-polymeric solids, (2)
the development of a mathematical model of the "fiber
bundle" type, in which the yield deformation is assumed to
result from a microscopic breaking and re-forming process
similar to that involved in the rupture of a yarn, and
(3) a description in terms of the breakdown of secondary
intermolecular cohesive bonding in the glassy state.

The results mentioned above are presented in some de-
tail in the body of this report. However, because of the
extent of the work carried out during the two-year period,
it is not feasible to attempt to present all of the

3

detailed results obtained. Rather, an attempt has been
made to give an overall picture of the various types of
studies which were carried out, and the most significant
results obtained. Where details could not be presented,
we have in some cases referred the reader to other sources
where further details may be found. This report, there-
fore, has the essential character of a summary report,
despite its size. It is planned to publish much of this
material in journal articles during the next year or two,
and these articles will allow more detail to be presented
and more complete literature references to be given.
There has been a general increase of research interest in
the plastic yield of solid polymers recently. References
are given in some cases to related recent work by other
investigators, but no attempt has been made to give
exhaustive or complete references of this type; it is
planned to do this in the final publications.

A. INTRODUCTION

A general description of the type of yielding of concern here is most easily understood in terms of stress-strain behavior. A typical stress-strain curve contains at least five distinct portions. Upon initial loading, the stress-strain curve rises in an almost linear way up to relatively high stresses. Gradually, as the stress continues to rise, the material "strain-softens" and the local slope of the stress-strain curve decreases towards zero at the upper yield point. Whether the slope ever goes to zero, or the curve has a maximum depends on sample geometry and stress field, but there is, in general, a true strain-softening of the material in all stress fields. In some stress fields, after the upper yield point, the deformation mode is formed, such as a neck in the tensile case, or a kink in uniaxial compression. In the former case, the stress-strain curve drops as the instability is formed, then levels out at a constant stress as steady state propagation of the local mode over the entire sample takes place by a process of sequential local strain softening and hardening. Finally, when all the material in a sample has been yielded or drawn to a certain extent, further deformation of the yielded material occurs only at increasing stresses. The two significant material properties for this yielding process are, therefore, those that produce strain softening and strain hardening. The details of the exact shape of the stress-strain curve and local deformation mode are more dependent on experimental variables.

There are a large number of material and experimental variables that determine the nature of the observed deformation and yielding, or conversely, that can be used to characterize the nature of the yielding process. Polymer or material variables can be grouped in several categories: chemical structure variables (which determine the nature of the intra- and inter-molecular forces); polymerization variables (molecular weight, cross-linking, branching, stereo-regularity); pre-treatment variables (orientation); thermodynamic properties (T_g, secondary transitions, T_m); and crystallinity variables (amount, crystal type, morphology). Some of the important experimental variables are: temperature, strain rate, environment, adiabaticity, pressure, stress-field, and stress-

5

strain-temperature history. (These categories are of course overlapping to some extent.)

This review of some of the pertinent variables serves to put our work in a better perspective. By necessity we were restricted to an exploration of only a limited number of these variables. We chose those experimental variables which were both experimentally accessible and which showed promise of contributing to our understanding of the yield process. The materials which we used were those which, in general, were readily available in convenient form. In particular, polystyrene and polymethyl methacrylate, which we investigated in detail, are high molecular weight, glassy, amorphous polymers with quite different chemical structure, yet very nearly equal glass transition temperatures. The pre-treatment variable, orientation, was used extensively. Almost all of the experimental variables were utilized, the only restriction being that strain rates be kept low enough so that isothermal conditions could be assumed during deformation. For characterization of the material response to these experimental variables, the range of deformation behavior around the upper yield point was most closely analyzed, using parameters of stress, strain and time.

B. EFFECT OF TEMPERATURE AND POLYMER TYPE

Compressive tests have been used in this part of the study to determine the temperature and material dependence of both elastic and yielding behavior. Tensile behavior, as a function of these variables, has not been studied, but appropriate comparison tensile data can be found in a report previously issued by this Laboratory, and by the U. S. Army Natick Laboratories. The polymers that were most thoroughly studied were polystyrene (PS), polymethyl methacrylate (PMMA) and Lexan polycarbonate (PC). These were chosen as being representative of the range of glassy behavior from brittle to ductile.

The following quantities, which have been defined in the above-mentioned report, are redefined here because of their frequency of use in the discussion which follows. Modulus (E) was calculated from the slope of the initial straight-line portion of the load-elongation curve; proportional limit stress ($\sigma_{P.L.}$) and strain ($\epsilon_{P.L.}$) were calculated from the point on the load-elongation curve where the curve begins to deviate from a straight line; the upper yield stress (σ_y) and total strain at yield (ϵ_y^T)

6

were calculated from the point of maximum load on the load-elongation curve (peak point); the "plastic" strain at yield (ϵ_y^p) was calculated as the difference between the total and elastic strains (extrapolation of elastic part of curve to the yield load). All stresses were calculated using the original cross-sectional area where this had the smallest value, and all strains were calculated by using the original approximate length of the gauge section (the section with constant cross-sectional area).

Extensive investigation of the compressive stress-strain properties of the three glassy polymers mentioned above was undertaken for several reasons. First, the compressive properties could be compared to the available tensile data[2] to determine the effect of these opposite stress fields. Second (and most important), compression tests allow the study of yielding behavior without the complications of the crazing, cracking, and fracture that accompany tensile tests. Also, there are no problems of gripping the specimen, although there still are end effects of greater or lesser severity depending on the end geometry. A special compression apparatus was built for use on the Instron tensile tester.

The stress-strain properties of the three polymers (polystyrene, polymethyl methacrylate, and Lexan poly-carbonate) are shown in figures 1 and 2. The specimens used for PS and PMMA were of two types: cylindrical spec-imens with end fillets; and rectangular columns with end fillets and with a small cross notch in one side. For the latter specimen, the minimum cross sectional area (at the notch) was used in calculating stress values.

The results for the two types of specimen were similar, except that for PMMA the cylindrical specimens showed similar moduli and yield stresses, but much larger total and plastic strains at the yield point than the notched rectangular specimens. Since this difference may well be connected with initiation of localized deformation modes, only the results with notched PMMA specimens are presented in figures 1 and 2, so that material comparisons can be made. All specimens were about one inch long, in the gauge section, and the machine crosshead rate was 0.02"/min, unless indicated otherwise.

The most striking difference between the stress and modulus porperties of the three polymers in figure 1 is

7

that the polycarbonate is much less temperature dependent
and has lower values of all properties than the other two
polymers. The polymers are consistent, though, in the
way that the proportional limit and yield stresses are
approximately linear functions of temperature and extra-
polate to zero somewhere near the glass points of the
respective polymers (see arrows in figure 1). Compared to
the tensile data for PMMA and PS, the slope of the yield
stress vs. temperature curve for PMMA in compression is
about twice that for tension, whereas for PS in compression,
this slope is only slightly larger than in tension.

This difference between polymers could be a reflec-
tion of the different effect that hydrostatic stress has
on the yielding behavior of the two polymers. It might
also be due to the fact that the PMMA tensile data were
being limited to a small temperature range just under the
glass point and thus were not truly representative.

The strain parameters for these three polymers are
shown in figure 2 as functions of temperature. Looking at
the proportional limit strain first, we see that it
decreases in a regular way for PS and PMMA, indicating
relatively more decrease of proportional limit stress than
modulus with increasing temperature. For PC, on the other
hand, it goes through a slight maximum, indicating quite
a different relative temperature dependence of the
modulus and proportional limit stress for this polymer.
Even though PS has the highest proportional limit strain
(and stress) in the temperature range below 70°C, it is
seen to have the lowest strains at yield (total and
plastic). As mentioned above, this is characteristic of
polystyrene and is reflected in the sharpness of the upper
yield peak. It will be shown that the extreme localiza-
tion of the plastic deformation mode for PS also reflects
this sharp upper yield point.

The total strain at the yield peak decreases with
increasing temperature for all the polymers in about the
same way, thus showing that the upper yield point is not
determined by a constant strain criterion. Rather, it
seems that the shape of the stress-strain curves remains
about the same and just the limits, both elastic and
plastic, become less in magnitude as the temperature
increases. The one exception to this is the plastic strain
at the yield point (ϵ_y^P), shown in figure 2. It is seen
that for PMMA, the plastic strain is low at low tempera-

tures and increases as the temperature is raised. The behavior is opposite for PC. Furthermore, the plastic strain for PS is very low and appears to be independent of temperature.

A variety of other polymers was tested in compression at room temperature using rectangular cross-section samples with small side notches. The objective here was to investigate a range of materials and stress-strain properties and to see which materials would deform in a localized way with the notch as a stress concentrator. None of the materials (with the exception of the styrene derivatives) showed as extreme a local yield as polystyrene, even though some of the plastic strain at yield values were as low as in polystyrene (less than 1%). Both PVC and Formvar showed relatively local yielding in the form of kink bands, as seen in polarized light, but no deformation bands were seen. However, isotactic polystyrene, poly α-methyl styrene, and styrene-acrylonitrile (75/25) copolymer all showed at least some very distinct deformation bands.

C. LOSS MEASUREMENTS

A dynamic property, specifically dynamic loss, was obtained on pieces of the polystyrene, polymethyl methacrylate, and polycarbonate sheets from which the previously reported stress-strain specimens had been cut. The dynamic loss was obtained over the same temperature range as the stress-strain tests. Because one of the projected applications of these data was correlation with deformation band propagation (see Section IV.C.1 below) which occurs with internal strain rates of up to 100 sec^{-1}, a dynamic test in the corresponding frequency range was designed.

We are indebted to T. J. Hammack (Fibers and Polymers Division, M.I.T.) for the design and construction of the apparatus used--a bouncing-ball rebound tester. Essentially, the apparatus consisted of a 1/2" diameter steel ball which was released mechanically to drop onto a sheet of plastic. The height of the rebound was read by eye on an adjacent meter stick. The tester was calibrated by selecting polystyrene, known to have a low loss at room temperature, as the standard material. Several bounces were made at each temperature and the rebound readings averaged to the nearest millimeter. The yield point of the materials

9

was not exceeded (no indentations remained on the surfaces), and the elastic strain rate was estimated to be of the order of 10-100 sec^{-1} (frequency, 10-100 cps). The equation used for calculating damping, expressed as log decrement, (Δ), was:

$$\Delta = \frac{\pi G''}{G'} = \frac{\pi(60-B)}{60} \tag{1}$$

where:

B = bounce height in cm.
G',G" = real and imaginary parts of shear modulus.

The results of these dynamic loss measurements for PS, PMMA, and PC (Lexan) (relative to PS at room temperature) are plotted vs. temperature (in figure 3). It is clear that both PC and PMMA have values of dynamic loss that are an order of magnitude higher than PS at room temperature and that, while the value for PC goes through a definite minimum as the temperature rises, the values for PMMA and PS rise sharply with temperature. At temperatures above 50°C, the loss for all three polymers is rising with temperature, with PMMA having the most and PC the least amount of loss at any given temperature.

D. EFFECT OF PREORIENTATION

Briefly, preorientation entails heating a sample to a temperature above the glass point, stretching it a pre-scribed amount, and then cooling it back into the glassy state, whereby most of the stretch and molecular chain orientation put into the sample in the rubbery state is retained in the glassy state. Results and discussions of the effects of preorientation in tensile tests of PS can be found in reference (2). Some PS samples were cut from preoriented sheets, so that the preorientation direc-tion was at various angles to the long dimension of the column, i.e., the compressive stress direction. These were tested in compression, as described above, and the results (for notched samples) are presented in figure 4. There is very little dependence of the yield stress on the orienta-tion angle, just a slight (5%) increase at higher angles, where the compression axis is almost normal to the preorientation direction.

Also shown in figure 4 are a series of results at a higher temperature and a series at higher strain rate. There seems to be less of a dependence on angle for the former and more for the latter, but the differences are

10

still very small. The strain rate and temperature
coefficients of these yield stress data are about 1000
psi/log cycle of strain rate, and 180 psi/°C, respectively.
Un-notched samples were also tested at several of the
birefringence levels and gave similar but slightly lower
and less consistent yield stress results. It is felt that
the chief effect of the notch, which is across the narrowest
(thickness) direction, is to initiate a consistent deform-
ation mode across the sample. Otherwise, in un-notched
samples, a variety of deformation modes--banding, kinking
and buckling--take place, usually across the narrow
direction.

Some of the other stress-strain properties were not
quite as insensitive to angle as were the yield and pro-
portional limit stresses. As seen in figure 5, where
data obtained on the samples of intermediate orientation
at 21°C and 0.02"/min are plotted, the total strain at
yield increases and the modulus decreases as the pre-
orientation angle is increased. The plastic strain at
yield also seems to show a slight dependence on the angle.

E. EFFECT OF THERMAL HISTORY

The effect on stress-strain properties of varying
quenching rates through T_g was investigated because,
theoretically, it should be possible in this way to vary
the "free volume" in the glassy state and to relate
this "free volume" change to mechanical properties.
Furthermore, this information would be useful in separa-
ting the effects of quenching from those of hot stretch
(preorientation) in the preorientation experiments
mentioned above. The thermal histories investigated for
PS and PMMA were: as received; annealed just under T_g for
10 hours; heated 20°C above T_g and quenched into ice water
and into liquid nitrogen. All samples were equilibrated
at 70°C, 65% R.H. for at least 24 hours before being
tested. A hydrostatic weighing method was devised for
the measurement of sample density and this seemed to work
reasonably well, with an apparent accuracy of $+0.0002$
gms/cc. Because the density changes produced in the
samples were small (PS varied from 1.050 - 1.052 gms/cc,
PMMA varied from 1.194 - 1.197 gms/cc) and because of the
possibility of incomplete wetting of the sample, the
absolute values of the densities were not precise enough
to be used as parameters in the presentation of the data
below.

11

The effect of thermal pretreatment on stress-strain properties in compression at 21°C is as follows. For PMMA the yield stress decreased by 8% and the modulus by 6.5% after a water quench, and decreased by 13.2 and 16%, respectively, after a liquid nitrogen quench. For PS, the yield stress decreased by 13% and the modulus by 8.4% after the water quench. Since these modulus and stress values decreased by about the same proportion, it is not surprising to find very little overall change in any of the strain values.

The changes in the stress-strain data are roughly similar for increasing test temperature and for decreasing (initial) sample density (i.e., faster quenching from above T_g, giving more frozen-in free volume). Calculations, using the glassy thermal expansion coefficient (α_g) to define an equivalence of density changes ($\Delta\rho$) produced by quench and changes that would be produced by temperature change (ΔT), indicate that the extremes of density produced by these quench pretreatments should have been equivalent to about an 8°C change in test temperature, ($1/\Delta\rho = \Delta V/V = \alpha_g \Delta T$), where α_g is the coefficient of thermal expansion in the glassy state.

F. EFFECT OF STRESS FIELD

Yielding seems to be a very general phenomenon in glassy polymers, provided that fracture does not take place first. This can be illustrated for polystyrene in tension by using molecular preorientation to raise the tensile strength to values above the yield stress, in which case the mode of failure changes from brittle fracture to yielding. Under compressive stress, PS normally shows yield rather than fracture. Thus, glassy polymers such as PS are not brittle materials in the classic sense described by the Griffith criterion, even though they are ordinarily regarded as "brittle" materials under practical use conditions.

1. Effect of the Hydrostatic Component of t.   Stress Tensor

Glassy polymers actually behave more like classic plastic materials at high strains and stresses, and we have carried out a preliminary exploration of this plastic behavior as a function of the nature of the stress field. Experiments have been run on PS at room temperature (22°C)

12

at a strain rate of about 10^{-4} sec^{-1} in the following
stress fields: (1) uniaxial tension, (2) uniaxial com-
pression, (3) torsional shear, (4) plane strain compress-
ion, and (5) biaxial tension. There were slight differences
in sample geometry, presence or degree of preorientation,
and sample material in these experiments, but since other
observations have indicated that none of these variables
has a very significant effect on the value of the yield
stress, we have disregarded these minor differences and
have collected these values in the plot of figure 6.
Values of yield stress were calculated from the load peak
in the stress strain curve. The principal stresses are
denoted as σ_1 and σ_2 on the two axes in the usual way
($\sigma_3 = 0$). The relationship between principal stress axis
and sample axis depends, of course, on the type of experi-
ment. A line has been drawn to connect the yield stress
data, and the resulting figure, which is symmetrical around
the $\sigma_1 = \sigma_2$ diagonal, is commonly referred to as a "yield
locus". The numbers in circles refer to the different
types of experiment listed above. The "fracture locus"
for unoriented PS is also sketched in the figure for
comparison, and since it lies within the yield locus
in parts of the tensile and shear quadrants, it is clear
that fracture will take place before yield in unoriented
PS in these stress fields.

The most important conclusion to be drawn from figure
6 is that there is a significant effect of the mean stress
(hydrostatic component of the stress tensor) in the yield-
ing of PS. This dependence on the mean stress is seen in
a simple way in the significant difference between the
values of the yield stress for uniaxial tension and
compression (10,000 psi vs. 14,000 psi, respectively).
The yield locus corresponding to the Tresca yield criterion,
which applies to plastic yielding in metals, is also
sketched in figure 6 as a dashed line and is represented
by the equation

$$\tau_{max} = \frac{\sigma_1 - \sigma_3}{2} = \frac{y}{2} \tag{2}$$

where τ_{max} is the maximum shear stress, σ_1 and σ_3 are the
principal stresses and y is the yield stress in uniaxial
tension. The predominant role of the shear stress, with no
dependence on mean stress, is clear from the Tresca criterion.
One advantage of setting up such a yield criterion is that
is allows the prediction of yield stresses in more complex
types of stress field from a knowledge of basic material
constants, such as the value of the yield stress, y, in a

13

simple uniaxial stress field.

The yield behavior shown by PS, where dilatation
(or mean stress) effects are prominent, seems more analo-
gous to the behavior of soils than to the behavior of such
solids as metals and ceramics. It is best represented by
the Mohr yield criterion which contains a term with the
mean hydrostatic stress, $\sigma_m = (\sigma_1 + \sigma_2 + \sigma_3)/3$ combined with
a material parameter $(\tan \phi)$, which relates to the direction
of the yielding mode.

$$\tau_{max} = \frac{\sigma_1 - \sigma_3}{2} = \frac{y}{2} + \sigma_m \tan \phi \qquad (3)$$

One reason for the greater importance of volume effects
in glassy polymers may be the fact that the ratio of yield
stress to bulk modulus, a quantity which is proportional
to volume change at the yield point, is orders of magnitude
higher for the glassy polymers than for metals, even though
the absolute magnitude of the yield stresses is similar
for the two classes of materials. These experiments have
been further discussed recently[3].

2. Behavior in Torsion under Hydrostatic Pressure

The following experiments were initiated as a more
ideal method of studying the effects of pressure and
stress field on yielding. With this method, (torsion of
thin wall tubes) the basic shear stress field is of a
particularly simple nature, and it is possible to vary the
superposed pressure independently of the shear stress.
Thus, a more complete exploration of three-dimensional
stress space is possible. Although the results of tests
with PS were incomplete, it seems useful to summarize the
technique and method of analysis.

A sketch of the device constructed to perform these
torsion experiments under pressure is shown in figure 7.
The specimen (1) is held firmly by two torque rods (2)
and (3), which are attached to a hand-driven torsion device
(not shown in the sketch). When a torque is applied to
the specimen, the fluted section (4) of low torsional
stiffness enables the end of rod (2) to undergo a small
but measurable amount of elastic twist with respect to the
fixed frame of the machine without any complications which
could have been produced by friction from the Bridgman-
type high pressure seals. Pressurized water is introduced
into the pressure chamber (7) through the pressure line (6).

14

The water is pressurized around the specimen by means of a hand pump to about 5000-6000 psi.

A number of experiments were performed on both solid and thin-walled tubular specimens under superposed pressures of up to 10,000 psi. In these experiments the pressurizing fluid was tap water which was contaminated with hydraulic oil. In all experiments fracture preceded plastic deformation. Examination of the fractured specimens showed that fracture was always helicoidal with its origin lying inside the gauge section.

The specimens which fractured at low superposed pressures showed many crazing cracks on the surface while those fracturing at high superposed pressures did not show any crazing cracks. The results of four selected experiments are reported in Table I.

The results given in the table indicate a reduction of the tensile strength of the polystyrene specimens in the pressurized environment. If the Griffith theory of brittle fracture under multi-axial stress conditions is assumed to be valid in these experiments, the fracture should obey the Griffith equation[4],

$$(S_1 - S_2)^2 + 8 S_o (S_1 + S_2) = 0 \qquad (4)$$

where the symbols have the meanings indicated in Table I.

Experiment #4 which is typical for the case of uniaxial compression gives the propagation stress for deformation bands through the specimen instead of the fracture stress. The value S_o entered for experiment #4, therefore, is a lower limit for the tensile strength as calculated from the Griffith equation--the actual value, in all probability, being much higher. On the other hand, the tensile strength S_o calculated from the Griffith equation for the first three experiments listed in Table I is only around 650 psi. This indicates that the pressurizing medium made up of tap water contaminated with hydraulic oil has had an embrittling effect on the polystyrene specimens. Protection of the surfaces of solid specimens with hydraulic sealing tape or with a tightly fitting rubber tube was evidently not effective in preventing contact of the pressurizing medium with the surface, as the results indicate. These results suggest that the experiments should be repeated with another pressurizing medium free of embrittling effects such as, perhaps, dry silicone oil.

15

Table I
Results of Torsion Experiments on Polystyrene

Experiment No.	S_s psi.	p psi.	S_1 psi.	S_2 psi.	S_o psi.	Remarks
1	3,900	8,500	-4,600	-12,400	620	Spec. surface unprotected
2	4,700	10,000	-5,300	-14,700	700	Spec. surface covered with pressure sealing tape
3	5,100	10,000	-4,900	-15,100	650	Spec. surface covered with tight fitting rubber tube
4		0	0	-12,000	1,500	Spec. tested in uniaxial compression without pressure, undergoing plastic deformation

S_s = applied shear stress at time of fracture.

p = hydrostatic confining pressure.

S_1 = maximum principal stress.

S_2 = minimum principal stress.

S_o = uniaxial tensile strength as it is used in the Griffith theory of brittle fracture under multi-axial stress.

III. TIME EFFECTS

A. INTRODUCTION

Important rate effects are noticed in the yielding
and drawing processes in glassy amorphous polymers. In
connection with the practical problem of the high-speed
"strength" of polymers, these rate effects are usually
characterized by stress-strain tests run over a range of
strain rates.[5] Although much data of this sort have
been accumulated[5], there are inherent limitations to this
approach. Practically, the range of strain rates usually
available on the conventional testing machines is not large,
though the use of time-temperature superposition can be
used to extend the effective range of testing rates[6].
Furthermore, stress-strain data are not the simplest type
to analyze and interpret because of the continual change
of stress and strain (also true and plastic strain rate)
during the test. The only quantity held constant during
the test is strain rate.

Stress relaxation (at constant strain), creep
recovery (at zero stress), and creep (under constant load)
are simpler types of experiments which are frequently used
at low stresses, where linear viscoelastic theory is
applicable.

One of our objectives in the work here was to use
these methods of stress relaxation, creep under dead load,
and creep recovery in the high stress range of yielding,
where non-linear viscoelastic and plastic effects are
observed and the deformation may not be homogeneous. We
have also studied the more complicated time effects
associated with drawing by experiments that interrupt the
yielding process; in this way, it is also possible to
more closely associate the time effects with particular
modes of yield deformation.

B. STRESS RELAXATION AND STRAIN RECOVERY[2]

These experiments were carried out by straining at a
constant rate to (a) stress levels up to the range of
the upper yield stress, and to (b) strains beyond the
upper yield point and into the drawing range. The strain-
ing was then interrupted in various ways to create differ-
ent types of histories. When the sample was then restrained
at a constant rate, the change of properties ("hardening"

17

or "softening") could be clearly observed. The histories employed during the interruption period included stress relaxation at constant strain, creep recovery at zero stress, and various combinations of the two, and the basic experimental variables were stress field, stress level, and time.

1. Stress Relaxation as a Function of Stress Level.

Stress relaxation behavior before the upper yield point was studied as a function of the stress level for both tension and compression.

Polystyrene (Compression)--The most complete stress relaxation data were obtained for a compression sample and the schematic stepwise loading history is shown in figure 8. The sample was strained at a relatively rapid rate to each successive load level at 100-pound increments, allowed to relax for thirty minutes, then strained to the next level, and this process repeated. The extrapolation of each relaxation curve is shown as a dotted line. By keeping track of the displacement of the machine cross-head and making appropriate corrections, a load(stress)-strain curve was calculated. As shown in figure 8, this curve was linear with an elastic modulus of 3.4×10^5 psi in the entire load range studied.

Because of the linearity of the load-strain curve, it seemed that the stress relaxation curves might obey the Boltzmann superposition principle (i.e., be independently and linearly additive). Thus, the difference between any one stress relaxation curve, say at 400 pounds, and the extrapolation (dotted line) of the previous curve should represent the stress relaxation behavior of that increment alone. In this way, the stress relaxation behavior of successive load increments could be determined independently.

Several of the curves of stress-difference vs. time for this sample are shown in figure 9, where the curves are designated by their initial or highest stress for each cycle and normalized according to this stress (σ_0). The relaxation curves for low initial stresses are very flat, as ordinarily observed in the viscoelastic relaxation of glassy polymers. As the stress level is increased, the relaxation becomes more rapid and the curves shift to shorter times and become more sigmoidal. The relaxation curves at high stress levels show almost complete decay in about three cycles of log time, indicating that they

18

are approaching the Maxwellian shape corresponding to a single relaxation time. If a relaxation time for the other curves is defined as the time where the stress (difference) falls to 0.36 of its original value, then a curve of relaxation time vs. stress level can be constructed as shown in figure 10. If, from stress-strain experiments, the yield stress and the time of loading to the upper yield stress are included in the same plot, the data from the two different types of experiments seem to fall on the same curve. It would appear, then, that this curve might well represent the strain rate dependence of the upper yield point over quite a range of rates.

In an attempt to identify the beginning of yielding in stress-strain data, the proportional limit stress (where the stress-strain curve starts to deviate from linearity) vs. the corresponding time values is also plotted in figure 10. In terms of the stress relaxation curves of figure 9, these time and stress combinations correspond to relaxation of only 5-15% of the original stress.

Polystyrene (Tension)--A number of samples of oriented 0.0017" polystyrene film (Δn_o = 20 x 10^{-4} measured in the plane of the film) were tested in stress relaxation at various stress levels. Data given in figure 11 show that the behavior was similar to that discussed above for the bulk compression sample, even though equal stress increments were not used for the film. The significant deviations corresponding to the onset of yield occur at stress values which are low compared to the stress values in compression and even compared with the upper yield stress in tension (10,800 psi at 0.5 minute loading time).

2. Stress Relaxation in the Upper Yield Stress Range

a. Relaxation Rate and Deformation Modes

Since the stress relaxation rate has been seen to increase progressively as the stress level is raised towards the upper yield stress, we will now consider the question of what happens right around the upper yield stress, where the nature of the deformation mode begins to become complicated. In the present section, emphasis will be placed on the stress-strain-time behavior; the details of the various deformation modes are discussed below and thus will be mentioned here only where necessary for understanding of the relaxation data. Some definitions of terms are important at this point, however. In the film samples, a

19

neck is defined as any area on the film which has yielded through the whole thickness direction. These areas are of two types. A micro neck is defined as a small yielded area (usually less than 1/16 inch in the tensile direction) not extending across the whole width of the sample; this usually starts at one edge and grows across the width to the other edge like a crack or tear. A macro neck, on the other hand, is defined as a neck which already extends across the whole width of the sample, and therefore grows by increasing its length in the tensile direction.

In the experiments discussed in the preceding section, a step-by-step increase in load level was employed in order to study incremental relaxation behavior at different stress levels. In the present experiments, the sample was immediately loaded into the stress range where yielding is observed, and incremental relaxation behavior was studied by applying strain increments which maintained the sample in this stress range. The computation of the incremental relaxation behavior was done as before, i.e., as the difference between the experimental relaxation curve and the extrapolated preceding relaxation curve.

In general, it was found that the propagation of different deformation modes could be associated with different rates of stress relaxation. For example, during the slow, pseudo-stable propagation of deformation bands or micro-necks across the width of the film, the relaxation rate was relatively slow, although it had a concave downward shape vs. log time. When the plastic yielding zone (whether a micro neck or more diffuse form of yielding) reached the other side of the sample, thus forming a macro neck, an abrupt increase in the relaxation rate occurred. This higher relaxation rate is generally associated with the propagation of a macro neck--an observation which is further explored below during relaxation after drawing.

Experiments on PS film strips at slightly higher stresses showed similar yielding effects during their initial relaxation period. For example, some samples, loaded to just under the yield point, underwent what may be defined as "spontaneous necking"--a process whereby a sample undergoes a delayed necking at a constant strain which is less than the usual yield strain. This is behavior complementary to that observed in a dead load creep experiment in which a sample undergoes a delayed necking at a

20

constant load which is less than the usual yield load. In the case of these film samples, it was possible to observe the details of the deformation modes during the "delay time", which is the elapsed period of time prior to macroscopic necking, and to relate the stress relaxation curves to the growth of micro necks. Generally, as the micro necks spread across the sample width, they become unstable and their rate of growth constantly increases (even against linear time), and consequently the stress relaxation rate increases.

b. Effect of Stress Relaxation Before Upper Yield on Subsequent Stress-Strain Behavior

The influence of relaxation on stress-strain behavior was also studied by running stress relaxations and load-unload histories on samples before they had reached the upper yield stress. The stress-strain properties of the samples upon restraining after these histories can then be compared with the properties of a virgin sample. Because the stress-strain behavior of these materials had been extensively studied, most of these histories were studied on Formvar and Lexan films.

The general result obtained is that stress-relaxation at a high stress but before necking, results in a reloading curve to the upper yield stress which has a greater slope (higher modulus) and a higher and sharper upper yield peak(relative to its subsequent steady-state drawing stress). These increases in slope and height of upper yield peak appear to be greater the longer the relaxation time and the higher the stress level during the relaxation. This hardening and strengthening effect of stress relaxation when carried out before the upper yield point, was also found for PMMA samples in tension at 75°C and in compression at 22°C, although the magnitude of increase of the upper yield stress is not as large in PMMA as in PS.

It is probably this hardening effect of stress relaxation that causes the stress-strain behavior of the compression sample illustrated in figure 8 to be apparently linear up to such high stress levels. In other words, each period of stress relaxation hardens the sample so that upon application of the subsequent load increment, a constant high modulus is shown, even up to very high stresses.

21

3. Stress Relaxation and Strain Recovery during Drawing

Some very significant and revealing experiments on time effects can be performed during the course of steady-state drawing, which help to clarify the nature of the "plastic" state of glassy polymers. These experiments, in which drawing or yielding is interrupted and resumed, were first reported by Vincent[7]. The interruption of yielding can be carried out in two ways: (1) the straining can be simply stopped, and the sample allowed to undergo stress relaxation at constant strain, or (2) the straining can be reversed so as to remove all stress from the sample during the interruption period. The effects of these two types of interruption are quite different. Figure 12 illustrates this schematically, in the form of a load-elongation history of a tensile specimen strained at constant machine crosshead rate. The first loading takes the specimen through the yield point (L_y^1), formation of a neck, and into steady-state drawing at L_D^1. If the crosshead of the machine is then stopped, the sample undergoes stress relaxation at constant strain. Upon reloading, the slope (S^2) of the load vs. elongation curve is much steeper than the original slope (S^1), and a new value of the upper yield point (L_y^2) is obtained, the level of which is dependent on the time of stress relaxation.

If the load on the sample is completely released at a rapid rate by reversing the crosshead, and the sample is allowed to retract freely, as in the second sequence of figure 12, the slope (S^3) of the load-elongation curve on reloading (measured at an arbitrarily selected load value less than the drawing load) is much lower than the original (S^1) and no upper yield point (yield peak) is observed. In all the steps of this sequence, the steady-state drawing load remains about constant ($L_D^1 = L_D^2 = L_D^3$). Variations and combinations of these two basic histories, such as: retraction/partial reloading/relaxation/ reloading, were also investigated and the results will be discussed below.

a. Stress Relaxation Followed by Reloading

The type of experiment to be discussed here has been illustrated in figure 12. Since a large number of experiments were carried out, the results will be discussed for the different polymers individually in the sections which follow. All the results are expressed in terms of

loads or load ratios. Stresses are not calculated because of the lack of precision in defining the actual cross-sectional area undergoing deformation. Due to minor thickness variations and other experimental variables, such as multiple neck formation, the yield and drawing loads were not always constant from sample to sample, so the yield drop is expressed as a relative yield drop, $\Delta L_{yD}/L_D = (L_y - L_D)/L_D$. The load decay during stress relaxation from the original (L_O) to the final load (L_F) is similarly expressed as a relative relaxation, $\Delta L_{OF}/L_O = (L_O - L_F)/L_O$.

The data are presented below as relative yield drop ($\Delta L_{yD}/L_D$) vs. the log of stress relaxation time. This quantity could equally well have been plotted vs. relative stress decay ($\Delta L_{OF}/L_O$), because, for the three materials most extensively investigated (Formvar, Lexan and Nylon 6-10), there is a linear relationship between relative stress decay and log stress relaxation time. In these polymers, there is about a 12% stress reduction for each cycle of log time, independent of the original stress or material.

Formvar

The increase of the upper yield peak with increasing time of stress relaxation is shown in figure 13 for Formvar film at 22°C. Most of this increase occurs over only three cycles of log time, and from this curve it is possible to define a "relaxation time" of about three minutes for whatever process is involved here. It should be noted that the final limiting value of relative yield drop (.15) after very long times of stress relaxation is only about half the initial relative yield drop (.30) when necking first took place. This is probably related to the fact that the neck already exists: this may be important either because of the nature of the stress concentration in the neck shoulder, or the reduced cross-sectional area of the neck, which is almost exactly one-half of the original cross-sectional area.

For Formvar the slopes of the loading curves after stress relaxation (measured at an arbitrarily fixed load level) were all about the same as the original loading slope, independent of the stress-relaxation time or height of the upper yield point. The sharpness of the upper yield point and its position, i.e., amount of

23

plastic strain at yield (ϵ_y^P), also were about the same.
Although the upper yield points were slightly more rounded
and occurred at higher strains in the experiments at very
short relaxation times, where the yield drops were low,
the shape of the loading curve for Formvar was nearly
constant--only the height changed appreciably.

The increase in height of the upper yield peak is a
function not only of the time of stress relaxation, but
also of the stress range in which the relaxation took
place. The effect of this stress range will be described
in more detail below, but essentially the data show that,
for a given stress relaxation time, when the relaxation
takes place below a certain minimum load level, no upper
yield point is seen upon reloading.

Nylon

The increase of the upper yield peak with increasing
time of stress relaxation is shown in figure 14 for Nylon
film at 22°C. The increase is seen to be more abrupt than
for Formvar. Most of the increase occurs over less than
two cycles of log time, for which a "relaxation time" of
about five minutes can be defined. The final limiting
value of the relative yield drop (0.17) reached at long
times of relaxation is again about half the original (0.34).
The scatter in the data is much less than in the case of
Formvar. This is probably due to the more uniform thick-
ness of the Nylon. Multiple neck formation was frequently
seen in Nylon and as many as five separate necks were
observed to form in a sample with an original gauge
length of 2". This strong tendency to multiple necking in
Nylon was also commented on by Williams and Bender[8,9].

For Nylon, the slopes of the reloading curves after
stress relaxation (again measured at an arbitrary fixed
load level) were a function of the stress relaxation time.
From a low of 0.13 (arbitrary units) at the shortest time
of relaxation, the slopes increased to about 0.30 (at
four minutes of relaxation) and then remained constant
for longer times. The initial loading slopes before
necking were closer to 0.50. There was some slight varia-
tion in the sharpness of the upper yield peak and in the
amount of plastic strain at the yield point (ϵ_y^P) as a
result of the relaxation. This may be connected with
the details of the micro deformation modes, described
elsewhere.

Lexan

The increase of the upper yield peak with increasing time of stress relaxation is shown in figure 15 for strips of Lexan film. These samples were stretched at 22°C at two Instron crosshead speeds, 1.0"/min and 0.2"/min. Just as for the two polymers previously discussed, the curve obtained from the 0.2"/min tests has the same sigmoidal shape, about the same relaxation time of three minutes, and a limiting, long-time value of the yield drop (0.042) about half the original (0.085). Thus, the yielding behavior is similar to that of the other polymers even though the yield drop has a very much smaller magnitude (less than 10% of drawing load).

In the 1"/min tests, the drawing loads observed were almost exactly the same as for the slower speed. Yet, it is observed that the upper yield point undergoes an increase in magnitude in the usual way as a result of stress relaxation, but has a shorter relaxation time associated with it. The ratio of "relaxation times" (for the yield peak increase) for the two crosshead speeds is larger than the factor of 5 in crosshead speed.

Saran

The increase of the upper yield peak with increasing stress relaxation time for Saran at two crosshead speeds, is shown in figure 16, and contrasts greatly with the Lexan results. The curves for Saran at the two crosshead speeds have the same shape and are displaced along the log time axis approximately by the same factor of 5 as the ratio of crosshead speeds.

Two significant observations concerning this polymer should be noted. First, no evidence of inhomogeneous deformation (band formation) could be seen by viewing, either normally or between crossed polarizers, even when a definite upper yield point and yield drop appeared on the load-elongation curve after periods of stress relaxation. Second, there is no upper yield point or yield drop upon initial loading and the drawing curve has a definite upward slope to it rather than remaining level (see figure 17). This phenomenon is seen often for drawn fibers, and in the metals and ceramics field, and has been designated as a "constant rate of strain hardening". Upon reloading after stress relaxation, however, a

25

definite yield peak appears, as shown in figure 17. This is followed by drawing, which continues along the same strain hardening line of upward slope, but displaced in time as a result of the relaxation interval. If the yield peak is disregarded, the drawing load appears to begin to increase again only after the load exceeds the previous load maximum.

b. Stress Relaxation Behavior during Interrupted Drawing.

Some comments can be made regarding the detailed nature of the stress relaxation curves obtained during interrupted drawing. One general observation is that the relaxation rate following interrupted drawing is initially higher than the rate for undrawn material at the same stress level. However, at longer times of relaxation (10^2 - 10^3 minutes), the relaxation rates for drawn and undrawn material are similar. Another general result is that many of the differences and similarities between the history dependent stress-strain properties of the different polymers, described above, are reflected by analogous differences and similarities in the relaxation curves. The more exact relationships between relaxation behavior during interrupted drawing and the stress-strain properties obtained on subsequent reloading can only be established by further investigation.

c. Retraction at Zero Load Followed by Reloading.

This type of experiment is illustrated in figure 12. Here, the Instron crosshead is reversed while the sample is undergoing drawing. After a given period at zero load, during which the sample retracts freely, the sample is reloaded at the original crosshead rate. Almost all the materials investigated showed no evidence of an upper yield point after this history--rather, the load gradually and asymptotically increased to the drawing level when elongation was resumed. (The upper yield peak is recovered at long times of unloading, however.) The slope of the reloading curve at a specified load value, usually taken as 70-80% of the drawing load, was used as an index of the change of material behavior after this history, in the usual way. The retraction of strain at zero load was measured for some of the materials as a function of time.

26

This softening effect of unloading is very similar to the "Bauschinger effect" which has been studied extensively for many metals. The Bauschinger effect, originally defined as the lowered deformation resistance in one direction after prestraining in the opposite direction, can be regarded in a more general sense as referring to any unloading-loading cycle[10]. This softening effect in glassy polymers is illustrated for Formvar film samples in tension in figure 18, where the unloading and loading were all done at the same crosshead rate. The load-elongation plot shows a hysteresis effect, a low proportional limit stress (linear elastic limit) on reloading, and a rounding of the "corner" of the reloading curve. These are all characteristic of the Bauschinger effect. The solid reloading line in figure 18 represents a sample immediately reloaded just after the unloading reached zero stress; the dotted line is for a sample left at zero load for 20 minutes before reloading. The 'Bauschinger strain", equivalent to the plastic strain of the reloading curve (the difference between the reloading curve and the extrapolation of the original elastic modulus) is also shown in figure 18 as a function of the reloading load.

Figure 19 presents the reloading slopes (as defined above) of Formvar, Nylon and Lexan as a function of time at zero load. The values of the slopes as presented are in arbitrary units, but the change of these slopes is proportional to the change in modulus of the respective polymers. Even though there is quite a bit of experimental scatter, it can be seen that, in general, the results are more complicated than for the relaxation histories described previously. The slope values first decrease, then rise again towards the original value as the time at zero load increases. Using the arbitrary units of figure 19, the slopes of these polymers on initial loading (before necking) were: Formvar = 4.5 to 5.5, Nylon = 5.0, Lexan = 1.3 to 2.5.

The appearance of a minimum in these curves of reloading slope vs. recovery time suggests that two processes are operative, one which "softens", and another which "hardens" the material with increasing time. The "softening" process, illustrated as an increased Bauchinger effect with increased time in figure 18, is most evident after short times at zero load. The "hardening" process seems to become operative only after the "softening" process slows down. The "hardening" process is no doubt related to the increase of upper yield peak after relaxation,

27

as described above, but, in the relaxation case, the "hardening" process is shifted to shorter times as the relaxation takes place at higher stress levels. The rate of the "softening" process appears to be related to the rate of strain retraction at zero load, measurements of which are discussed in the following section.

d. Retraction of Strain after Drawing

The sample retraction observed after the load is reduced from the drawing value to zero is shown for several samples in figure 20, where retraction in inches is plotted vs. log time. The data show, at least for the PMMA samples, that the retraction occurs at ever decreasing rates, even against log time, and would undoubtedly level out at long times. This is the type of curve obtained in normal viscoelastic retraction experiments. The decreasing part of the curves of reloading slope vs. time at zero load (figure 19) could perhaps be associated with this effect.

To get an idea of the magnitude of total retraction, a Nylon strip sample was loaded through the yield point to a steady drawing load, unloaded and then allowed to retract for 1200 minutes. The total strain attained under load was 34%. The total retraction after 1200 minutes was about 18%, of which 16% would be viscoelastic or time dependent retraction, and 2% immediate elastic retraction on unloading. Thus, about one-half of the total "plastic" strain was actually recoverable on standing, in contract to the usual definition of plastic strain. (The plastic strain would be totally recoverable if the sample were heated above the melting point.)

e. Other Stress-Time Histories

The following results indicate that the processes of retraction and relaxation during interrupted drawing have distinct and opposite effects on subsequent stress-strain behavior. Hardening can be associated with relaxation and softening can be associated with retraction, at least at short times. Relative proportions of these two effects can be obtained by suitable combinations of these two types of history.

Drawing/Retraction/Stress Relaxation

This history is schematically illustrated in figure

28

21, where typical differences in stress-strain behavior
upon sequential loading are shown. In the histories
illustrated, the free relaxation periods were both of one
minute duration, but the stress level of the relaxation
period is varied.

The results in figure 21 indicate that stress relaxa-
tion for one minute does not modify the effect of a
previous free retraction of equal duration unless the
stress level for the relaxation is above 10 lbs. (above
50% of upper yield load or 60% of drawing load).
However, at initial 1 ds for relaxation higher than 10
lbs. both the slope of the reloading curve and the rela-
tive yield drop increase towards their upper limits.

Quite similar results were obtained for Lexan film
samples subjected to a 0.4 minute free retraction period
followed by a one-minute stress relaxation period. As
above, the slope of the reloading curve and the relative
yield drop increased to their upper limits provided stress
relaxation was carried out at load levels above 60% of the
drawing load. The effect of stress relaxation time at
constant initial load was also investigated. As the
stress relaxation time increased, the relative yield drop
got closer to what had been obtained before (figure 15)
as a result of stress relaxation without a preceding free
retraction period. In other words, the effect of a free
retraction period on stress-strain behavior becomes less
important as either the stress level or relaxation time
of an intervening stress relaxation period becomes
greater.

Drawing/Stress Relaxation/Retraction

This history is, in a way, the reverse of the
preceding one. Here, we ask what is the residual effect
of a stress relaxation period starting from the drawing
load, if it is followed by a period of free retraction at
zero load. This type of history is illustrated in figure
22, along with the results for Formvar. The systematic
decrease to zero of the relative yield drop with increased
free retraction time suggests that all that is needed to
erase a previous stress relaxation effect is about an
equal time of free retraction at zero load.

C. DELAYED DRAWING UNDER DEAD LOAD.

1. Introduction

29

In the previous report mentioned above[2], some experiments on PS were described in which cold-drawing was initiated with a constant load attached to the polymer specimen. This type of experiment has also been described previously in the literature[8,11]. In drawing experiments carried out at constant strain rate, the formation and propagation of a neck after some degree of uniform extension is the phenomenon typically observed. This formation and propagation of a neck is also observed in many cases for the constant load experiments, but other, seemingly uniform modes of extension also occur. Drawing initiates some time after load application; the time required has been termed the "delay time". This delay time may vary from seconds to many hours, depending on material properties and experimental conditions. At sufficiently low stress levels the polymer deforms uniformly (no localized necking) and at a decreasing rate under a constant load, due to viscoelastic creep. Drawing takes place when the stress is sufficiently high. In the studies reported here, we have attempted to establish the conditions under which one or the other mode of deformation occurs, and to study quantitatively the effects of the most important experimental variables.

It was established previously[12] that temperature, stress level and molecular preorientation are important variables affecting the dead load drawing behavior. This information was used to plan the present experiments. In the course of the present work it was found that thermal history, and in the case of PMMA, moisture absorption, are also experimental variables of considerable importance.

2. Experimental Procedure

Specimens of both PS and PMMA were milled from cast sheet, 1/16th inch thick. The parallel gauge section of the test specimen was 1.8 by 0.25 in, with a fillet radius of 7/16th in. The thickness of the preoriented specimens varied according to the degree of preorientation; the starting thickness was always 1/16th in.

A special preorienting device (see figure 23) was built, consisting of two heated aluminum plates, the temperature of which could be held constant at any desired value. The plates were arranged in such a way as to provide a vertical air space between them, into which strips of polymer were inserted. Convection of outside air into the heated slot was prevented by felt strips

30

glued to the edges of the plates. The polymer strips were held by a clamp at each end, the lower clamp being movable by hand. After a heating time of the order of ten minutes, the plates were moved apart and the strip quickly extended to the desired length and allowed to cool in the room temperature air.

The birefringence produced by this hot orientation procedure was used as a measure of the degree of molecular preorientation. Birefringence was measured with wedge compensators having retardation ranges from nearly zero to 25 orders for the mercury green line (5461 A). These wedge compensators were milled from oriented PS or PMMA pieces.

The dead load experiments were carried out in a thermostated chamber with forced air circulation (figure 24) which was specially designed and built for the purpose. The temperature variations at any specimen position were smaller than +0.5°C. The chamber allowed three specimens to be run at the same time. The length changes were either measured with a cathetometer or were recorded on drums wrapped with chart paper and driven at a constant rotation rate by synchronous motors. Ballpoint pens were attached to the connecting rods carrying the weights and these gave a continuous trace of the specimen length on the drums.

The temperature chamber contained windows to permit observation of the samples, including visual or photographic monitoring of their shape changes and modes of deformation and approximate measurement of changes in their optical anisotropy.

3. Results: Polystyrene

In order to obtain drawing in PS, some preorientation had to be introduced in the direction of the stress. The preorientation serves to raise the fracture stress to values above the yield stress. The glass transition temperature of the polymer used was 90°C, and it was preoriented at 115°C. The higher the orientation, the more cautiously the specimens had to be machined, as there was a tendency for them to split in the orientation direction.

Temperature, stress and preorientation were varied

31

in such a way that the experimental points could be regarded as being the lattice points of a three-dimensional lattice. Temperature was varied in steps of 5° or 10°C, stress in increments of 400 or 800 psi, and three preorientation levels were used ($\Delta n = 1$, 5 and 10×10^{-3}).

Three different types of elongation-time curve (figure 25) were observed in these experiments. When the specimen drew with a neck (curve a), deformation first took place homogeneously for some time and at a slow rate. The rate then increased until a constant rate, several times higher than the initial one, was again reached. Simultaneous with this acceleration of deformation rate, the appearance of a constriction somewhere along the specimen was observed. This developed into a neck; when the steeper slope was reached, the neck had formed and the specimen was drawing by propagation of the neck. When the neck had reached the ends of the specimen, elongation became slow and homogeneous again. The intersection of the first and second straight line regions of the drawing curve (figure 26) was taken as defining the delay time, t_d, and the delay strain, ε_d. These two quantities were tabulated from the experiments.

Sometimes deformation remained homogeneous. In this case, high strains were sometimes reached after sufficiently long times (figure 25b); however, in other cases deformation rate decreased progressively with time and only comparatively small strains were attained even after very long times (see figure 25c).

Figures 27 and 28 are representative results for delay times and delay elongations for the polymer samples with preorientation $\Delta n = 10 \times 10^{-3}$. These results are in the form of a combination table and graph. A complete presentation of the results obtained for all three preorientations has been given in a recent publication[13]. At any fixed value of preorientation, the delay times (figure 27) increase with decreasing stress and decreasing temperature, as would be intuitively expected. Below a certain critical stress, which decreases with increasing temperature, extension is homogeneous. The stress-temperature plane is thus divided into two distinct regions--one in which cold-drawing takes place by the formation and propagation of a neck, and another in which the deformation is homogeneous and consists merely of viscoelastic creep. In the region above the boundary line, type "a" deformation (figure 25) is obtained; below the boundary line, type "c"

32

deformation takes place. The third type of deformation, "homogeneous drawing" (figure 25b),was observed in the vicinity of the boundary line, particularly at higher temperatures. At the lowest degree of preorientation ($\Delta n = 1 \times 10^{-3}$), drawing occurred only in a limited region at high temperatures and low stresses. At higher stresses specimens failed by fracture, either immediately or after some time, before cold drawing had started[13].

The change in deformation mode is also reflected in the delay elongations (figure 28). The elongation at which necking initiates is usually of the order of 5 to 10%. In the region of "homogeneous deformation", much higher strains than this can be reached after sufficient time, without the occurrence of necking. These specimens apparently reached the stress necessary for necking only after some reduction in cross-section had taken place by homogeneous creep. This borderline case could perhaps be avoided by carrying out the experiments at a strictly constant stress rather than at constant load. This was not done for the sake of experimental simplicity.

At the onset of necking, localized areas of high strain were always seen in the samples. These "deformation bands"[1,14] ran across the specimen at an angle of approximately 50° to the stress axis. The bands usually formed to some degree along the entire gauge length. The neck would form either where the band density was highest, or where some of the individual bands were particularly pronounced. Sometimes a great number of bands formed simultaneously and so densely that no single neck was formed, and drawing took place entirely by proliferation of the band structure. On superficial observation, the specimen appeared to be drawing homogeneously, but closer inspection revealed a great number of these shear deformation bands.

When the deformation remained truly homogeneous (type "c" extension, figure 25), no bands could be observed during the experiment, nor could they be detected by microscopic inspection afterwards. The origin points of the deformation bands were often imperfections at the edges of the specimen. In all specimens crazes and internal cracks developed to some degree after load application and these became sources of deformation bands. Figure 29 shows an example of this. The row of cracks which can be seen in this photograph developed in the interior of the specimen in the center of the specimen

33

gauge area when the specimen was stressed. Band structures
could be observed particularly in the neck of the PS
specimens and in the undrawn material close to the neck.
In the drawn region of the specimens, over which the neck
had passed, the bands had disappeared. Figure 30 shows
part of a neck in a flat specimen with a dense pattern of
intersecting deformation bands.

4.   Results: Polymethyl Methacrylate

Commercial PMMA cast sheet produced by Rohm and
Haas Company (Plexiglas II UVA) was used in this study.
The polymer had a glass transition temperature of approx-
imately 106°C. The experiments were all carried out on
samples without preorientation, since PMMA will draw with-
out preorientation (unlike PS). In many of the measure-
ments on PMMA the windows of the chamber were used to
project an image of the specimen on a ground glass screen
by means of a point light source. A carbon arc, focus d
by a condenser lens on a pin hole in a thin brass sheet,
served as the point light source. With this simple
arrangement, optical inhomogeneities developing during
deformation were easily observed as dark areas in the
projected image (Schlieren" patterns).

The time allowed for thermal equilibration of the
specimen in the test chamber before load application was
kept constant to reduce variations due to thermal history
effects. Initially, all specimens were kept for three or
more weeks in air of 65% RH and 22°C. These conditions
result in 0.6% absorbed moisture in PMMA. When it was
found that moisture is one of the important variables in
the yielding of PMMA, further experiments were made with
dried specimens. Three days' exposure in 80°C dry air was
chosen as the drying procedure. No further water loss was
observed on more prolonged heating, as indicated by ample
weight.

The behavior of the PMMA in dead load experiments was
very similar to that of polystyrene. At low stress the
specimens deformed by creep, but above a certain charac-
teristic stress an instability in the elongation vs. time
curve appeared of the nature shown in figure 26. The
occurrence of the instability was first indicated by
optical inhomogeneities (bands) growing from the specimen
edges, oblique to the stress direction, towards the center
of the sample. These bands were detectable by Schlieren
observations before the rapid part of the cold drawing

34

curve had occurred and they continued to persist in the neck or in the homogeneously drawing sample. The typical phases of their appearance and their relation to the specimen behavior were, in fact, the same as described above for polystyrene. Varying density of their formation indicated that necking would occur (where their density was greatest); uniform denisty indicated that macroscopically homogeneous deformation would take place ("homogeneous drawing"). For both modes of drawing the curve of figure 26 is typical. When only viscoelastic creep was observed, there was no indication of band formation. The use of the Schlieren technique to observe the deformation bands in PMMA was necessary because they are difficult to see clearly by visual observation, unlike the bands in PS. In some of our early studies, in fact, it was concluded incorrectly from visual observations that deformation bands did not form in PMMA.

Figures 31 and 32 present the delay time and delay elongation values determined from tests at various combinations of stress and temperature. At each temperature there is a critical stress, lying on the boundary drawn as a solid line, below which the deformation remains homogeneous in a microscopical sense (i.e., no bands are observed and the deformation consists merely of viscoelastic creep), and above which delayed drawing occurs. This stress decreases with increasing temperature, just as in the case of polystyrene. Also, as for polystyrene, a large scatter of experimental delay times at the boundary between homogeneous and inhomogeneous extension is observed which is believed to be the consequence of doing a constant load rather than a constant true stress experiment--the specimen reduces its cross-section by creep until the stress becomes high enough for yielding to occur.

Polymethyl methacrylate is known to absorb water. To obtain some knowledge of the magnitude of the effect of water absorption on the yielding behavior, several samples were exposed at room temperature to 0%, 65%, and 100% RH, respectively. After three weeks, the weight did not change further and the specimens had 0, 0.6 and 2.0% equilibrium moisture content.

Figure 33 presents the delay time data of the samples described above measured at 80°C. The delay time is strongly reduced by increased moisture; 2% moisture is equivalent to a temperature increase of nearly 25°C.

35

Measurements of the stress relaxation of PMMA by McLoughlin and Tobolsky[15] showed that, at least at small strains, the mechanical properties depend greatly on the rate at which the polymer was cooled through the glass transition region. Figures 34 and 35 give elongation vs. time curves of specimens which have been thermally pre-treated under the conditions indicated. The specimens quenched from 150° to 0°C (figure 34, bottom) deform much more rapidly than the original polymer under the same stress (figure 34, top). The tendency to neck was also much reduced in the quenched specimens; drawing occurred rather uniformly, without a pronounced neck.

The curves of figure 35, from specimens with a variety of thermal histories, all tested at the same temperature and the same stress, also show large differences in behavior. The annealed material shows greater rigidity (a reduced ease of deformation). The specimens were permitted to reach equilibrium with 65% RH air before the test.

An attempt was made to correlate the change in drawing behavior with density changes produced by the thermal treatments. The weight change upon immersion in water due to buoyancy of the sample was measured. It was possible to make the measurements rapidly enough so that water absorption remained negligible. The density found was 1.187 g/cm^3, and did not seem to show any systematic change due to thermal treatments. Changes might be detectable by use of a more sensitive method.

5. Discussion of Results

a. Effects of Stress and Temperature

The behavior of PS and PMMA in these tests is so similar that many of their characteristics can be discussed together.

The delayed drawing of both polymers appears to occur in three steps:

1. Appearance and growth of oblique deformation bands (pre-drawing phenomenon).

2. Increase of band density and frequently the simultaneous formation of a neck (initiation of drawing).

36

3. Either neck propagation or drawing by shear
   band proliferation (completion of drawing).

The same phenomena have been observed in tests at constant
strain rate, and with other polymers. The ultimate sample
strain (draw ratio) attained when the drawing took place
by shear band multiplication was the same as in the
experiments where necking took place. In a test at constant
strain rate, the load drop after yielding causes a drop in
stress in the regions still undrawn, and thus reduces the
probability of formation of further shear bands in the
sections of the specimen outside the neck, or the further
growth of the bands already initiated in those regions.
The "homogeneous" shear band drawing is, therefore, not
ordinarily observable in drawing tests at constant strain
rate. The reason that neck formation initiates at a
particular point on the sample in the constant load draw-
ing is undoubtedly a result of either a mechanical
imperfection in the sample (such as a slight local narrow-
ing of cross-section) or a small temperature gradient,
since there would otherwise be no tendency for localization
of strain at any particular point.

When the logarithm of the delay time is plotted vs.
initial applied stress at different temperatures, straight
lines are obtained which also seem approximately uniformly
spaced vs. temperature (see figures 36 and 37).

For PS, the effect of temperature and stress on log
t_d is the same at different degrees of preorientation.
The delay time does, however, increase slightly with in-
creasing preorientation, in agreement with previous
observations[12].

The experimental points drawn above the upper border
of the graph in figures 36 and 37 correspond to experi-
ments where only viscoelastic creep occurred. These points,
therefore, indicate merely the duration time of the
experiment rather than a delay time; but it is clear that
these points no longer fall on the straight lines for the
samples which showed delayed necking and drawing. These
specimens showed neither deformation bands nor necks. The
strains reached by the samples which deformed by creep in
the region just below the boundary line in figures 28 and
32 were, after a sufficient length of time, much higher
than the delay strains of the samples which drew
inhomogeneously, again indicating a major, qualitative

37

change in the nature of the deformation.

The fact that deformation bands are always present in the case of delayed drawing and consistently absent in viscoelastic creep, taken together with the existence of two distinct regions in the temperature-stress plane where these two modes of deformation take place, leads us to conclude that the boundary line between the two regions represents a critical stress required for the formation and propagation of deformation bands. Below the boundary line in figures 27 and 31, the stress is too low either to form or to propagate shear bands. Whether the formation or the propagation of the bands is the controlling process, and what role the strain plays in the initial appearance of bands, will require further and more quantitative observations to decide.

We conclude further that the delay time is the time necessary for the initiation and the growth of deformation bands over a certain distance which is probably related to the specimen dimensions transverse to the stress axis. To understand how the delay time is divided between initiation and propagation time again will require a more quantitative study of the band behavior.

It is interesting to note that delayed yielding is also observed in metals[16,17]. Only metals with an upper yield point (peak in the load-elongation curve) show the effect. One finds also in metals (as we did for polystyrene) a critical stress below which yielding does not occur in finite time. The delay time is observed to be a function of the grain diameter in this case. It is believed to be the time necessary for the slip band density within grains to increase to a critical value so that macroscopic yielding can take place. This occurs by thermally activated release of dislocations from pinning points. Although it is difficult to visualize an exact analogy with the above dislocation mechanism for the case of an amorphous polymer, an analogy could perhaps be drawn between crystallographic slip planes and shear deformation bands. The viscoelastic process at the propagating tip of the band would then be equivalent to the production of slip bands in neighboring grains through the grain boundaries. The time scale of these processes is presumably governed by viscoelasticity in the case of the polymer, and in the case of the metal by the thermally activated freeing and generation of dislocations within grains.

38

b. Effect of Moisture on PMMA

The data of figures 31, 32, and 37 were obtained
from specimens with a moisture content of 0.6%, correspond-
ing to 65% RH. Under testing conditions at elevated temp-
erature these specimens will have lost water during heating
up and testing. The moisture content was thus no longer
constant or uniform, to an extent depending on temperature
and time. After having found the large influence of ab-
sorbed water on drawing (figure 33) we measured the delay
times of some thoroughly dried specimens. In a plot of log
(t_d) vs. stress, the lines of constant temperature were
displaced in the direction of increased delay time equi-
valent to a 10°C temperature drop. A change of slope due
to drying, which was observed when moisture content was
increased to 2%, was not found.

Drying had an effect on the crazing behavior of the
polymer (see also section IV.C.3). The dried specimens
did not show large crazes, which had been observed regularly
in the samples containing moisture, but only microcrazes
of the order of 10 microns in length. These microcrazes
disturbed the deformation bands less, thus making their
observation much easier. We assume that drying the outside
of the specimens during the test introduces tensile stresses
in a thin surface layer, which add to the applied test load
and increase the tendency to crazing in this surface layer.
The drying treatment, consisting of an exposure to 80°C dry
air for three days, also anneals the polymer and this may
influence the crazing behavior also.

c. Effect of Thermal History on PMMA

Measurements of stress relaxation of glassy PMMA by
McLoughlin and Tobolsky[12] cited earlier showed a profound
influence of the cooling rate through the glass transition
on subsequent relaxation rate. The more rapid the cooling,
the faster the stress relaxes. They explained this by the
freezing-in of empty space (free volume) during a rapid
quench. The result of similar pretreatments in our own
experiments (figures 34 and 35) affects the deformation
behavior at high stresses in the expected manner. The
rapidly cooled specimens, which are expected to have the
most frozen-in free volume, deform faster than the slowly
cooled ones. In addition, in the more severely quenched
specimens yielding did not set in as abruptly and with
such a clearly definable delay time, and necking was not so
clearly observable, as in well-annealed or original material.

39

By introducing additional free volume, the polymer started to show behavior intermediate between that of the original glassy polymer and the behavior of a viscous liquid.

d. Relation Between Constant Strain Rate and Constant Load Drawing

The question arises as to how the two experiments by which yielding is produced--the constant rate of extension and the constant load experiment--are related. The existence of an equation of state for the material would allow a direct answer to this question. Such an equation of state specifies a unique relation between the force, F, the sample length L, and the velocity v, with which the ends of the tensile specimen move apart; that is,

$$F = F(L,v) \tag{5}$$

This equation requires that the three quantities a e uniquely related, independently of the path by which a momentary state was reached. There is evidence that such a relation does not exist in a strict sense. Keeping this in mind, we will proceed to use equation (5) as a first approximation. A useful way to describe the properties of the real polymer might be in terms of deviations from this type of relationship. By forming the total differential of (5), setting $dF = 0$, and dividing by dL we obtain the relation

$$\left(\frac{\partial F}{\partial L}\right)_v + \left(\frac{\partial F}{\partial v}\right)_L \left(\frac{\partial v}{\partial L}\right)_F = 0. \tag{6}$$

From tensile tests at various strain rates it is known that for polymers, the load increases with strain rate[18,19]; that is,

$$\left(\frac{\partial F}{\partial v}\right)_L > 0. \tag{7}$$

Since this discussion is in terms of force and length, the yielding criterion for the constant rate of extension test is

$$\left(\frac{\partial F}{\partial L}\right)_v = 0. \tag{8}$$

For yielding in the constant load test, we therefore

obtain

$$\left(\frac{\partial v}{\partial L}\right)_F = 0. \tag{9}$$

This criterion will be valid at an inflection point in the
L vs. time curve. Beyond the yield elongation, $(\partial F/\partial L)_v < 0$
so from (6) and (7), $(\partial v/\partial L)_F > 0$.

We consider the relation $F(L, v)$ only prior to yielding
because of the complications in specimen geometry afterwards.
Figure 38 shows engineering stress-strain curves of PMMA
measured at 100°C at a number of strain rates. The data have
been obtained from the same type of specimen as was used in
the delayed drawing experiments. To facilitate mathematical
representation, the experimental curves have been smoothed
out by the following procedure. The upper yield points of
the measured curve were plotted vs. log v. They followed
the linear relation

$$\sigma_{uy} = 3600 + 725 \log v, \tag{10}$$

where σ_{uy} is expressed in psi and v is expressed in minutes.
The yield maximum for each strain rate was then calculated
from equation (10) and each curve was redrawn by multiplying
all stress values by the ratio of extrapolated to experimental
yield maximum. The yield maxima fell experimentally on a
straight line, parallel to the initial slope of the load-
elongation curves.

We now consider the curves of figure 38 to be the
relations $F(L, v = const)$. From these we calculate the time
for a specimen to yield in a constant load experiment. This
is easily done by integration of the time intervals dt = dL/v
along a line of constant stress between zero elongation and
the elongation where it is tangent to a constant strain rate
curve. The contribution of the elastic deformation to the
time integral is negligible, compared to the times involved
in our experiments. The integration is therefore only over
ΔL_p (see figure 38). The result of the graphical integration
for a number of stresses can be represented by the equation

$$\log (t_d) = 3.2 - \sigma/725 \tag{11}$$

where $\log (t_d)$ is expressed in min., for the range of strain
rates shown in figure 38.

41

A comparison of the predicted values of delay time with those experimentally observed for the same temperature is shown in figure 39. The experimental delay times appear to be about four times larger than the values predicted. The slopes of both experimental and predicted straight lines are in good agreement, however. This discrepancy is believed to be due to our experimental definition of delay time (figure 26). This graphical definition allows easy evaluation of the delay time from the experimental elongation vs. time curves, but actually does not conform with the criterion of equation (9). When we made precise creep measurements which established more accurately the initial part of the elongation vs. time curve, it was found that the inflection point where creep rate acceleration begins, which corresponds to the upper yield point, occurs at time values 3.5 to 5 times shorter than the delay time as defined graphically by the intersection point. This brings the curves of figure 39 into close agreement.

It is known that polymers which cold draw at normal strain rates will in many cases not cold draw (yield) when strained very slowly[7]. Our studies on PMMA and PS under constant load show that below a certain stress level, yielding does not occur. This is precisely what the above treatment would predict. If the upper yield point disappears from the stress-strain curve at constant strain rate, then one of the necessary requirements for delayed yielding has also disappeared and equation (6) predicts uniform deformation under constant load for all strains; that is, $(\partial v/\partial L)_F$ is always negative.

<div align="center">

IV. MODES OF DEFORMATION

</div>

A. INTRODUCTION

Some indication of the various deformation modes shown by glassy amorphous polymers during yielding has been discussed above in the appropriate experimental context. In summary, it has been demonstrated that these materials can deform homogeneously or inhomogeneously, the latter occurring on scales of magnitude from that commensurate with sample dimensions to beyond the limits of optical microscopy. The particular active mode is very dependent upon sample history (thermal and strain) and especially on experimental conditions.

In this section, the emphasis is placed on discussion

of the detailed nature of some of these deformation modes, rather than the circumstances of their occurrence. Both shear and hydrostatic modes and effects are discussed, and an arbitrary distinction between macroscopic or bulk phenomena and microscopic or local modes (not traversing the sample cross section) is made.

B. MACROSCOPIC YIELDING MODES

   1. Geometry of Neck Formation[20]

      a. Introduction

      Up to the present time, very little emphasis has been placed on the most common and most striking characteristic of cold drawing--that is, the formation and propagation of the neck. As early as 1947, Miklowitz[21] pointed out that in a series of six or seven experiments, which he carried out on Nylon, the neck which formed during cold drawing decreased in length (or increased in sharpness) as the rate of stretching was increased. In the course of this study Miklowitz prepared strain profiles of the necked regions of samples tested under differing conditions of strain rate but he made no attempt to generalize upon his results or to extend his experiments to include the effects of other variables such as temperature and orientation on the neck shapes.

      Miklowitz performed his experiments nearly twenty years ago, but since then there has been published no further detailed study of neck formation and propagation. Despite the lack of experimental data on the subject certain assumptions have been made about neck geometry and the effects of testing variables on it. It has been widely believed that: (1) the neck shoulder becomes increasingly steeper as the material is stretched at higher rates, and (2) the neck becomes more diffuse as the temperature of stretching is increased. The first of these assumptions, of course, is based upon the limited experiments of Miklowitz.

      On the basis of the results presented below, it appears that neither of these assumptions is entirely valid. In fact, these assumed necking characteristics are correct only over a limited range of strain rate and temperature.

      b. Experimental Procedure

Cylindrical samples (for which a single profile view completely characterizes the geometry) were strained in the Instron at various extension rates and temperatures (using an air thermostat especially constructed for the purpose). The sample profile was observed during the test by taking sequence photographs at roughly uniform time intervals during the deformation. Reference marks were scribed on the unstrained samples (using India ink) to allow diameter measurements to be made at fixed points along the sample using photographs taken at different sample extensions.

An example of the typical results of a neck geometry experiment is shown in figure 40. The reference marks mentioned above can be seen in the photograph which is one of a series taken during a stress-strain test at the conditions indicated.

The plot below the photograph shows the detailed neck geometry of this sample. The circles represent diameter values read by projecting the original photograph and measuring the diameter at various points with dividers. These distances have then been converted to fraction of original diameter (D/D_O), where D_O represents the original machined diameter before the test. This is plotted vs. axial distance along the sample, in inches.

c. Results

Experiments were first carried out on PMMA samples milled from cast Plexiglas II UVA sheet to a 0.2 in. diameter and one inch gauge length. It was found, however, in such samples, that the neck did not attain a final steady-state shape, despite the fact that the load-elongation curve soon reached a constant and apparently steady-state drawing load. Consequently, samples of the same diameter (0.200 in.) but with double the gauge length (2 in.) were machined from the same cast sheet and photographs taken as these samples were strained at a constant rate on the Instron machine. In these samples, the neck seemed to initiate at a strain between the upper and lower yield strains. The load-elongation curve settled down to a final, apparently steady-state drawing stress (after the yield peak) at an overall sample extension of about 15%. The neck did not stabilize, however, until about 60% overall strain (based on the gauge length) was reached. Thus, the stabilization of neck geometry between 15 and 60% overall strain takes place at constant external

44

load. Note that this behavior is somewhat contrary to the usual assumptions that the neck has completely formed at the upper yield point and has stabilized in shape by the time the lower yield point is reached.

The progressive development of a neck profile with increasing overall strain is illustrated in figure 41 for an experiment at 75°C and 0.2 in/min. crosshead rate using a sample with 2 in. gauge length. The profiles were read from photographs taken at different values of overall strain (or crosshead displacement) designated as $\Delta \ell$ and expressed simply in inches. The sample diameter is plotted as D/D_o vs. distance along the strained sample in inches as above. For values of $\Delta \ell$ above 1.0, the neck shape seems stabilized. The sharpness of the neck can be expressed in a quantitative way by its slope at the steepest point (inflection point of the profile curve). This is shown as a dotted line for the curve at $\Delta \ell = 1.3"$; the slope of the neck at this point was computed as 0.978 inches per inch distance along the sample axis.

The variation of neck sharpness (of the stabilized steady-state neck) with extension rate and temperature was investigated and the results are presented in figures 42 and 43. The important result obtained is that neck sharpness goes through a maximum vs. both (log) strain rate and temperature. The effect of strain rate was investigated at two temperatures (75°C and 95°C) and this same behavior of going through a maximum was observed at both temperatures. Duplicate experiments were run in a few cases, as shown, to indicate the general precision of the data. An adequate theory of the necking and drawing mechanics must succeed in explaining this pattern of behavior.

In order to determine the effect of preorientation on the geometry of the neck, several sheets of PMMA (Plexiglas II UVA) were stretched at temperatures above T_g and then rapidly cooled to prevent relaxation. Cylindrical samples with gauge lengths of 2 inches were prepared from regions of uniform birefringence following the same procedure as was used in the production of unoriented samples. A series of four specimens with progressively higher amounts of preorientation as measured by birefringence was then tested on the Instron at a temperature of 75°C, and an extension rate of 0.5 in/min.

An analysis of the sequence photographs and a comparison of the profile plots obtained from them indicated that

45

as the amount of preorientation in the gauge section of the samples increased, the degree of strain localization decreased. In other words, as the preorientation was increased, the neck became more diffuse. The slope of the steady-state neck was calculated for each sample and plotted against the initir birefringence of the sample, giving the results shown in figure 44. The neck slope is seen to decrease very rapidly as the preorientation increases from zero, but then levels off at a value of about 0.2 in^{-1}.

The effect of the test temperature on the neck geometry of samples having a fixed amount of preorientation was also investigated. Three samples were prepared, each with an initial birefringence of 2.8-2.9 x 10^{-4}. Each sample was stretched at a rate of 0.5 in/min. Testing temperatures of 65°, 75°, and 95°C were used. Profile plots derived from these experiments indicated a general decrease in the neck slope as the temperature increased. In fact, at the highest temperature no neck was observed to form, although a gradient in the diameter was observed from one end of the sample to the other. Apparently, the length of the neck under these experimental conditions was greater than the gauge length of the sample.

d. Discussion of Results

The mechanics of neck formation and propagation are not yet clear. The general principle can be enunciated that neck formation and propagation take place because the sample can deform more easily in this way than by homogeneous extension. This is a principle of minimum work, and it must then be explained why the inhomogeneous deformation constitutes such a minimum work path. One approach to such an explanation involves the assumption of a strain-softening and strain-hardening process occurring in the material in sequence. Any such approach requires a knowledge of material properties as a function of strain. The load vs. elongation curve measured in a drawing experiment does not correspond to the stress-strain properties of a microscopic volume element of the material, because of the inhomogeneous nature of the strain. However, by combination of the load-elongation curve with sequence photographs, something approaching the true tensile stress-strain curve of the material (for homogeneous deformation) can be obtained from measurements on one point of the specimen-- the point where the neck initiates--which remains a point of minimum diameter. The local strain at this point can be calculated from the diameter, assuming that strain

46

produces no volume (density) change in the material.
The local stress at this point is calculated by dividing
the external load by the cross-sectional area at this point.
The stress field at this point will be essentially one of
pure tension, unlike the situation in the neck itself, since
the sides of the specimen are parallel to the sample axis
here.

Examples of the true stress-strain curves derived in
this way are shown at different strain rates at 75°C, and
at different temperatures at a fixed strain rate ($\Delta \ell$ = 0.5
in./min., gauge length = 2 in.) in figures 45 and 46.
Since photographs were not available for the smallest
strains, this part of the curve has been sketched in by
dashed lines. After the abrupt onset of yield, at a stress
value which is clearly rate- and temperature-dependent,
there seems to be ordinarily a slight decrease of stress
with increasing strain, followed by a pronounced increase
of stress with further strain. It is interesting that
the general stress level of these curves seems to vary
linearly with the logarithm of strain rate, but linearly
with linear temperature; this type of dependence has been
observed in other experiments.

True stress-strain curves have also been calculated
for oriented PMMA. A series of these curves for various
amounts of preorientation is given in figure 47. Each of
these curves corresponds to a testing temperature of 75°C
and an extension rate of 0.5 in./min. One can observe
an increase in the tendency to strain-harden as the amount
of preorientation is increased (the stress-strain curve
for unoriented PMMA is also indicated in figure 47 for
comparison purposes). Such an increase is expected on
the basis of the classical assumption that strain-hardening
is due to the lining up of polymer chains.

It has been reported previously[2] that the draw ratio
of polystyrene is a strong function of the amount of
preorientation in both dead load creep tests and tensile
stress-strain experiments. These experiments on PMMA
indicate that a similar relationship between the amount
of preorientation and the draw ratio holds for this material
as well.

2. Volume Changes During Yielding

In order to establish more clearly the role of bulk
and local volume changes in the yielding process, direct

47

measurements of volume changes of compression samples
undergoing deformation were carried out[2]. The sample
was strained in a dilatometer, filled with mercury and
provided with a capillary tube open to the atmosphere.
The mercury level therefore moves in response to changes
of sample volume in the dilatometer. The dilatometer it-
self was made of stainless steel. The design was of a
simple piston and cylinder type (clearance, less than
0.0005") in which the sample was subjected to a uniaxial
compression between the flat parallel surfaces of the end
of the piston and the cylinder base. The dilatometer and
capillary tube were carefully calibrated. Volume changes
of less than 0.0005 cc could be determined.

Experiments were run on samples of polystyrene, poly-
methyl methacrylate, polycarbonate (Lexan), and polyvinyl
formal (Formvar) at 22°C. These were run through the upper
yield peak, most frequently at constant strain rate.
Experiments of other, more complicated, types were also
run, such as: stress relaxation from various points on the
load-elongation curve, creep at constant load, and types
of interrupted yielding histories.

Typical results of a simple loading cycle at constant
strain rate are illustrated in figure 48 for Formvar at
22°C. Figure 48a is the load-contraction curve for the
sample with the yield point indicated by an arrow and an
extrapolation of the initial linear elastic region shown.
(The slope of this line is, of course, Young's Modulus.)
Figures 48b and 48c, in which the volume change of the
sample is plotted vs. load and contraction respectively,
show several interesting points. We consider the "plastic"
volume change as the difference between the actual sample
volume and the linear extrapolation of the elastic volume
decrease (which is due to the Poisson's ratio effect). For
the experiment shown, it is seen that even though the total
sample volume decreases as the yield point is approached,
the plastic volume increases. The magnitude of the plastic
volume change at the yield point, v_y^p, is indicated in
figure 48b. We see from figure 48c that after yielding,
the sample deforms plastically at constant volume (Poisson's
ratio = 0.5) which is the usual assumption. It should be
noted also that the slope of the linear elastic region in
figure 48b is the reciprocal of the bulk modulus of the
material.

The magnitude of plastic volume change at the yield
point was different for the different polymers. It was

48

greatest for PMMA, which yielded in a homogeneous way, and least for PS, for which the yielding mode is one of very localized deformation bands, described in previous reports. The detailed nature of the curve of plastic volume vs. load around and after the yield point was quite variable, and is probably dependent on complicated experimental variables.

During the periods of stress relaxation at constant strain, the total volume increased, whereas the plastic volume decreased as functions of time. In a compression creep test on PS, both total and plastic volume decreased during the delay time before yielding, but they increased again once yielding began at significant rates.

This general volume-change behavior is compatible with a representation of a glassy polymer as essentially a close-packed structure. This structure responds elastically to hydrostatic stresses, whereas a portion of the sample has to expand, if only in a local sense, to allow yielding and the movement of molecules past one another under the influence of shear stresses. This plastic volume component would be expected to be always positive, even though the total volume change will change sign with different stress fields (tension vs. compression).

C. MICROSCOPIC YIELDING MODES

1. Deformation Bands in Compression

a. Introduction

The first experiments on deformation bands in PS were mostly descriptive and have been previously reported[14]. These experiments were carried out in compressive stress fields so that the competing tensile processes of crazing, cracking, and fracture would be minimized.

The principal conclusions of these studies can be summarized. Deformation band initiation and growth are associated with permanent plastic shear deformation. The bands as seen edge on are thin (10^{-2} to 10^{-3}m m.) plate-like regions of intense shear and follow the theoretical maximum shear stress plane of the particular geometry considered. They thus are easily differentiated from crazes and cracks which are more nearly parallel to the principal stress directions. As plastic deformation proceeds, the individual bands do not appear to widen;

instead, more bands form beside the original ones.
Macroscopic, homogeneous shear can also occur at high
plastic strains. More detailed experiments involving
cleavage of deformed specimens demonstrated the extent and
character of these bands through the interior of the spec-
imens and ending at the surfaces. The strain inside of
these bands was consistently of the order of unity.

Several interesting aspects of the nature of these
deformation bands has been further investigated. The
consistency of the band propagation angle, the temperature
and preorientation effects on band propagation, and the
relationship of band propagation to the load-elongation
curve will be briefly discussed.

b. The Band Propagation Angle

The fact that the band propagation angle is always
at about 35° to the compressive stress axis is not limited
to the specific geometry of the sample. Whether initiated
at a fillet, at a notch, or at a surface flaw in an
unnotched sample, the propagation angle is the same.
Godrick[22] has suggested that this propagation angle
results from a propagation mechanism involving pure shear
plus a rotation due to a kinking effect. This is the type
of kinking observed in metals, and it requires the
assumption that a sufficient amount of strain softening
occurs in initial shear planes to promote the continuation
of shear on these planes rather than on more favorably
oriented planes after rotation occurs. For this mechanism
the amount of rotation depends on the shear strain in
a band.

An alternate suggestion for explaining the constancy
of the 35° propagation angle is based on the nature of
the stress field and, thus, would not depend on strain
parameters. It was shown above in Section II.F.1 that the
yield stress for PS depended on the mean (hydrostatic)
stress. Following the reasoning of the Mohr yield criter-
ion[4] yielding occurs first on the plane where the resolved
shear stress first reaches the shear resistance in the same
direction. This shear direction (θ) varies from 0° to
45° from the compressive axis, because, while the shear
component is a maximum at 45°, the hydrostatic component
varies from zero at 0° to a maximum at 90°. From the data
on the pressure dependence of yield stress for PS, the
direction of propagation of the yielding mode is cal-
culated to be near 35° to the compressive axis. This

50

propagation angle is also exhibited in preoriented samples
(see below), where the amount of band strain would be
expected to be much less than in the unoriented samples[23].
Thus, a stress field, rather than a strain criterion appears
to govern the band propagation.

c. Temperature and Preorientation Effects in PS

The temperature dependence of band formation has
been studied fr ~ near T_g down to -196°C[22]. As the
temperature is lowered, less homogeneous or diffuse shear
strain takes place and the bands become more distinct and
better defined. At temperatures far below T_g essentially
all the plastic strain before the upper yield point can
be accounted for by the bands. As the temperature is
raised to near T_g, the deformation bands become less
distinct with slightly greater width/length ratios and more
homogeneous shear occurs. In experiments run at a strain
rate of 0.02 min^{-1}, only a very few distinct bands could
be observed in samples tested at 75°C. The temperature
dependence of the mechanical properties (stresses and
strains) for these samples has been discussed in Section
II.B.

Experiments on PS samples that had been preoriented
by various amounts and tested with the angle between the
compression and preorientation directions as an additional
variable were described previously and their compressive
stress-strain behavior was discussed (see Section II.D).

The observations on the effect of these variables
on deformation band formation and propagation can be
summarized. Neither the amount nor direction of pre-
orientation had a large effect on the bands. The two
chief effects of the amount of preorientation, within the
range investigated (i.e., birefringence from 6 to 70 x
10^{-4}), were that at high preorientation, cracking in
planes containing the preorientation axis became very
prevalent and that the variations in behavior seen with
change of preorientation angle were accentuated. It
seems that band propagation is easiest in the direction of
the preorientation axis, and hardest across the pre-
orientation axis. Furthermore, if certain shear directions
become less favorable, deformation can shift to other
planes containing the orientation axis. The fact that
the direction and amount of preorientation has such a slight
effect on the band propagation directions helps to confirm
the hypothesis, mentioned above, that this band propagation

direction is primarily governed by a stress criterion.

   d. Deformation Band Propagation and the Load Drop
       after Yielding

       The preliminary observations of band formation
during compression stress-strain tests indicated that the
bands initiated (first became visible) at the proportional
limit (end of the linear elastic region) and that the
yield load occurred when the bands extended across an entire
cross-section. Several questions remained though; what
effect did sample size (ratio of band length to cross-
section) have on the yield load and what mechanism could
explain the drop in load after the bands extended across a
cross-section.

       Although the size effect was not extensively investi-
gated, it appears that in larger samples single bands have
a finite length; that is, they do not extend across the
cross-section. Thus, the deformation in the larger samples
was accommodated by a sequential array of bands across the
section or by a combination of bands and homogeneous shear
deformation.

       The explanation of the load drops after the yield
load has not been satisfactorily resolved in terms of
deformation band propagation. Since there is severe strain
hardening within the bands themselves (shown by the almost
constant limiting strain in them) and since they do not
appreciably widen in the stress direction, the load drops
which reflect macroscopic strain softening, cannot be
explained by the nature of the bands. A possibility is
that the inhomogeneous deformation resulting from the bands
provides stress concentrations and initiation sites for
further, easier deformation. But it is observed that the
deformation during and after the yield drop is generally
macroscopic and diffuse and thus not necessarily related
to band initiation or propagation.

       Another possibility is that load drops arise from
shape changes. In most experiments the specimen contains
a single transverse notch in its gauge section, and the
bands grow out of this region, apparently when the local
concentrated stress reaches a critical value. Since the
shape change resulting from the partial penetration of two
43° bands into the specimen can be approximated by an edge
dislocation with Burgers vector parallel to the compression
axis, the problem of the climb of an edge dislocation across

a speciman under a critical local compressive stress was
studied. It was reasoned that the shape change resulting
from the presence of the dislocation would be a concave
curvature of the sample toward the notch. This would then
require the application of a bending moment at the parallel
compression faces which would give rise to a tensile stress
component at the site of the dislocation, requiring an
increase in the compressive load to keep the compressive
climb stress a constant. The results of the analysis
showed that the major component of the load drop could
indeed be attributable to such a shape change during
deformation when the specimen is singly notched or when
deformation preferentially starts from one surface in an
unnotched specimen.

However, load drops have also been observed in doubly
notched specimens (i.e., with notches on opposite sides
of the gauge section) and in specimens with a central hole
to initiate banded deformation[22]. This behavior is very
difficult to understand in terms of the above mechanism.
Such complications in the compression experiment provided
the incentive to perform the torsion experiments using
notched thin-wall tubes which have been described above
(section II.F.2).

2. Deformation Bands in Tension

a. Constant Strain Rate and Stress Relaxation
Experiments

Localized deformation bands have been observed in
bulk tensile specimens of PS tested at 25°C and they appear
to be similar, but not identical to the bands in PS
compression samples. The tensile bands are of the order
of microns in thickness, and form conjugated sets near, but
not in, the directions of 45° to the principal stress axis.
The bands were identified as light streaks when viewed
edge-on between crossed polarizers and as characteristic
waves of colors, when viewed through the plane of the bands.

The close relationship between these bands, craze
marks, and macro necking modes is discussed below for the
case of dead load creep experiments, but a description of
a particular PS sample in stress relaxation will serve as
a further example. This sample was 0.038 x 0.295 inch in
cross-section, 1-5/8-inch gauge length, and had a pre-
orientation birefringence of 51 x 10^{-4}. The deformation
modes to be described developed at very slow rates during

53

stress relaxation at constant strain at 25°C, in the stress range of 8000-9000 psi. One gross neck grew from one side of the sample to the other at an angle of 57° from the tensile direction. From the contraction in thickness, an approximate drawing extension in the middle of the neck was estimated to be 30%. Many surface crazes, normal to the tensile direction, were evident in the undrawn material above and below this macro neck. Interspersed between, and connecting, the ends of the crazes were light streaks identified as deformation band sets, which made angles of about 55° with the tensile axis. Conjugate sets of deformation bands were also observed along the edges of the sample in the vicinity of the macro neck. It is presumed that both the crazes and deformation bands were formed just before or during the propagation of the macro neck, because the deformation bands that are observed in the neck itself are rotated towards the tensile axis due to the extension taking place in the neck, and are rotated to one side, in addition, due to the angular direction of neck propagation. A similar sample with three times the preorientation birefringence (150×10^{-4}) had a much more diffuse macro neck and many fewer crazes and deformation bands.

Closer observation of the relationship between micro and macro deformation modes was accomplished during studies of tensile necking phenomena in thin film strips of polystyrene, Formvar, and Nylon 6-10. In these thin films it was possible to observe (using a microscope) deformation bands, micro necking and macro necking in the plane of the film during and after yielding and drawing, and to relate qualitatively the occurrence of, and transitions between, these modes as a function of the stress-strain history. The relation to stress-strain behavior is covered in more detail in Section IIIB. A particularly significant result of this study was that Formvar, a glassy polymer, and Nylon 6-10, a partially crystalline polymer, showed remarkably similar types and behavior of the various deformation modes, as well as stress-strain behavior.

A picture of a typical Formvar film (0.004" thick) during drawing is shown in figure 49, where the different deformation modes are all seen. This picture was taken with parallel polarizer and analyzer set at 45° to the tensile axis. The macro neck is at the bottom of the picture, short micro necks project from the neck shoulder into the undrawn material in the middle of the picture and thin dark streaks are seen throughout the undrawn material.

54

These streaks are at about 55° to the tensile axis and are
a first retardation order brown color in this parallel
polarized light. They develop during the first loading,
but continue to grow at points other than at the neck, even
during steady state drawing at constant load. Occasionally,
several were noticed to get darker, then develop high order
retardation colors while transforming into a micro neck.
Actually, on closer examination, the region of the micro
neck was seen to acquire a greater density of streaks
before necking, rather than one streak growing larger.

Samples of PS film with a slight preorientation were
studied for deformation mode under stress relaxation
and slow stress-strain conditions. Crazing, micro necking
and macro necking were the deformation modes observed
and the particular deformation mode and/or propagation
behavior was very dependent on stress level and strain
rate. The pre-yield streaks discussed above for Formvar
were not observed in these tests on PS. Crazing occurred
generally at lower stresses and at shorter times than any
sort of yielding phenomenon.

Birefringence measurements were made on the interior
of several well developed micro necks. The angle that the
principal optic axis makes with the tensile axis was in
the range of 5°-8°, which matched the offset angle at the
edge of the sample. Retardation in the neck was of the
order of 1.75 fringes, which corresponds to a birefringence
of between 0.03-0.04 for drawing extensions of 50%-100%.
This corresponds very well with the values of the birefrin-
gence in the necks of cold drawn bulk tensile samples[23]
and monofilaments[24].

b. Creep Experiments

In our studies of the microscopic deformation
phenomena which occur during delayed drawing under dead
load, we have been mainly concerned with the detection and
observation of shear or deformation bands. Among all of
the phenomena which have been discussed above, they are
the ones that can most easily escape detection. This is
primarily because only the optical anisotropy of the polymer
and not its light absorption changes within such a band.
In PMMA, deformation bands are particularly hard to detect.
This is apparently due both to the small transverse
dimensions of the bands and also to their small optical
anisotropy, which, for equal strains, is only one-tenth
that of PS.

Several methods were tried in an attempt to improve the visibility of deformation bands. For macroscopic observation, the Schlieren method mentioned previously was found to be very useful. Though more sophisticated Schlieren systems were tried, it turned out that a simple method, observation of the shadow of the specimen cast on a ground glass plate by a point light source, gave the best results. The method, as practiced, did not permit single bands to be resolved, but showed areas of optical inhomogeneity as dark and light streaks on the ground glass screen. These inhomogeneities are believed to consist of shear bands and the method therefore was useful to observe their growth and intersection.

For the detection of details of the shear bands, another method was developed. Before deformation the specimen was coated in vacuum with a thin metal film. By choosing the right metal and layer thickness, the film could be made to adhere to the polymer even during deformation. We have used platinum, chromium and aluminum in layer thicknesses which, judged by their light absorption, ranged from semi-transparent to nearly completely transparent. Under the light microscope the shear bands appeared as cracks in the metal film. The complementary experiment of coating the polymer with metal after drawing was also performed. After coating, the polymer was allowed to retract at a temperature above the glass transition temperature. The metal film cracked in a similar fashion as during drawing, showing that the polymer also recovers along the shear bands.

In light-microscopical observation of uncoated surfaces in transmitted light it was found that band structures as well as other surface features are observable by phase contrast microscopy even though in many instances normal or polarizing microscopy does not show such details. An alternative route chosen for the study of the surface topography was by electron microscopy. A replicating technique[25] of high resolution was adapted to our purpose.

Below we discuss some of the deformation phenomena we have observed, using these methods, in PS and PMMA samples during dead load deformation (creep) experiments.

Polystyrene

The more typical surface structures of polystyrene in various stages of deformation are shown in figures 50

to 53. Crazes (figure 50) have been observed in all specimens. They form perpendicular to the stress direction and, at the high stresses necessary for cold drawing, shortly after stress application. An impression of the differences in size and spacing of crazes can be obtained by comparing figures 50 and 52. Their number remains the same when plastic yielding occurs. Crazing is a common observation in amorphous polymers[26] and has been studied extensively. One of the findings is that the craze walls are still connected by oriented polymer molecules. This internal cohesion can however break down. This is shown in figure 51, where one of the crazes has opened up under stress, forming a diamond shaped hole. Such opening up usually leads to fracture. Cracks of this sort have been observed previously by Curran and Andrews in their study of the dead-load creep rupture of PMMA[27]. At the specimen edges crazes open resulting in a serrated edge. In intermediate stages of drawing crazes in PS sometimes assume a zig-zag shape due to the displacement of one section of a craze with respect to another by localized shear. When drawing is complete, they assume a straight configuration again.

An example of internal cracks has been mentioned before (figure 29). They are also perpendicular to the stress direction and frequently occur in nearly linear columns. Figure 52 is characteristic of a neck region when observed with polarized light. The two sets of intersecting lines are due to localized shear strain. It is not possible to focus on these bands. The light and dark streaks are caused by refractive index differences extending through the thickness of the specimen. Focussing on the surface sometimes reveals the traces of the bands where they intersect the surface (figure 30). The bands form at an angle of 50° to 60° to the stress, the angle decreasing as the specimen draws.

On the drawn surface one frequently sees a much more irregular line pattern than that of the crazes. Figure 53 is an example. The oblique lines seen in the figure come about during plastic deformation, after the crazes have formed. In many cases they appear to be made up of very small micro-crazes which are aligned, sometimes preferentially in the direction of the shear bands, but with each individual micro-craze remaining perpendicular to the stress direction.

Soon after drawing the drawn part of the specimen

turns opaque if the load is not removed. This is often
an indication of incipient fracture, which occurs at the
place where the specimen had first started to draw. The
opaqueness occurs only in a thin surface layer, while
the specimen center remains transparent. The structure of
the opaque polymer has not been determined.

Polymethyl Methacrylate

Localized modes of yielding were not observed
for PMMA samples in compression[1]. A close examination
of PMMA specimens drawn under tensile load has, however,
revealed the existence of shear bands for this polymer as
well as for PS. We were able to obtain clear evidence of
their presence from specimens with craze-free surfaces.
In the presence of crazes, regions of high shear strain,
which appear to be associated mostly with the tips of
crazes, are also seen. Surfaces of PMMA samples show a
much more uniform appearance than those of PS. This is,
at least in part, a consequence of the higher uniformity
of the PMMA sheets from which we made our samples.
Cracks, crazes and aligned or random microcrazes are also
common in PMMA, figures 50 and 51 being typical for PMMA
as well as for PS. Opaqueness caused by prolonged stress-
ing of the drawn polymer has not been seen in PMMA. It
should be noted also that the crazing of PMMA was reduced
or even eliminated when the specimens were dried before
drawing.

3. General Discussion

It is now well established that macroscopic deforma-
tion of a polymer sample, whether in tension or compression,
and whether at constant strain rate, constant elongation
or constant load, is accompanied by a variety of deformation
phenomena on a microscopic level. These include shear or
deformation bands, cracks, crazes and various surface
fissures. Deformation bands are the phenomenon most
clearly related to yielding. Some aspects of this
relationship have been explored in the preceding sections.
It is still not completely clear which other phenomena
have an effect on the yielding behavior of the polymer.
Crazes, for example, which develop before yielding begins,
are known to act as stress concentrations from which
yielding originates. The drawing behavior, however,
seems quantitatively the same with or without them.

It is known that these micromodes of deformation

58

are influenced in their details by the conditions under which the deformation is carried out. This relationship is a very complicated one, which we have investigated only briefly. A particular problem lies in the necessity for differentiating among features which are associated directly with yielding and those which were originally in the sample, or which were produced by a pretreatment such as preorientation.

Further detailed investigation of these phenomena, their interrelationships, their dependence on experimental parameters and their influence on the drawing process is obviously indicated.

V. BIREFRINGENCE STUDIES

A. INTRODUCTION

One of the objectives of this project was to explore the use of birefringence measurements as a method of obtaining valuable information concerning the mechanism of the drawing process and the nature of the oriented states produced by extension under various conditions. Some previous results using birefringence as a measure of chain orientation for hot stretched and cold drawn polystyrene were reported in our previous report on drawing[2] where the results implied that drawn PS attained a constant orientation state independent of preorientation (from hot stretching) prior to drawing. One phase of our birefringence studies reported below has explored these results further for both PS and PMMA.

Another of the objectives of the present investigation was to extend our studies of cold-drawing to include crystalline as well as amorphous polymers. As a means of combining the birefringence studies with the investigation of a crystalline polymer, we decided to study the drawing of polyacrylonitrile (PAN) by extension at constant strain rate, at different temperatures, and to measure the birefringence changes of the sample during the course of such an experiment. We had already obtained a great deal of birefringence data on this polymer, some of which have been published[28]; and we also have a considerable background of experience in interpreting its birefringence behavior. It seemed also that PAN would be a good polymer to serve as a bridge between the glassy amorphous polymers (polystyrene and PMMA) which we have used extensively and the more usual crystalline polymers, since it seems to show

a particularly simple sort of crystallinity and remains a transparent, single-phase material even when it "crystallizes". This simplifies the interpretation of birefringence effects, as compared to the usual crystalline polymers which are two-phase materials and consequently show the complicating phenomenon of "form birefringence".

B. POLYACRYLONITRILE STUDIES[29]

1. Introduction

Polyacrylonitrile (PAN) is a polymer of great practical importance in the synthetic textile field, since it is the basic constituent of the acrylic (e.g., Acrilan and Orlon) and modacrylic (e.g., Dynel) fibers. We used solvent-cast film samples rather than fibers, however, for experimental convenience (particularly as regards the birefringence measurements).

PAN appears to have two glass transitions--one near 95°C and the other at about 140°C. Some preliminary investigations have shown that these glass transition temperatures define regions of different kinds of mechanical behavior. Below 95° the polymer behaves in a brittle, glassy manner. Above 140° the polymer is very weak, and when strained, fails in some sort of "plastic" mode. Between 95° and 140°, the polymer necks and draws. In thin films such as we employ (1-2 mils), very high true strains (as high as 13) can be attained in this region.

Based on our previous birefringence studies of PAN, and a thorough study of the literature on its physical and chemical properties, we have recently proposed[30,31] a theory of the solid state structure of this polymer, and the nature of its glass transitions. We have described the structure as a "hetero-bonded" single phase, in which the secondary intermolecular forces are of two types: dipole-dipole associations and some weaker type of van der Waals bonding. Since the two types of bonding are of different strengths, they will dissociate at different temperatures, and we assume that the two glass transitions are due to the dissociation of these two types of bonding. The 140° transition seems to be due to the dissociation of the dipole-dipole bonding between nitrile sidegroups, and this also produces large birefringence effects (such as can be seen in temperature cycling of a sample under dead load).

60

2. Experimental Procedure

Since we had a large Instron testing machine available, we designed and constructed equipment which could be used in conjunction with this machine. An oven with temperature control had already been constructed for use with the Instron as described above, in connection with the studies of neck geometry as a function of temperature and strain rate, but was very suitable for use in the present studies as well. Birefringence measurements were made by the usual Sénarmont compensator method, and an optical bench in two pieces was constructed which could be mounted on the vertical support beams of the Instron (one section in front of the sample and temperature box, and one section behind). One-half inch diameter aluminum and stainless steel rods form the supports of the bench. The optical equipment can be removed or mounted quite rapidly (in about 15 minutes, including adjustments for proper alignment). In order to allow convenient access to the inside of the oven, part of the front half of the optical bench can slide forward on its support rods, so that the oven door can be opened.

3. Birefringence Changes During Stress-Strain Curves

Stress-strain-birefringence measurements were performed on strips of polyacrylonitrile film at eight different temperatures between room temperature and 183°C. The measurements were all made at a constant elongation rate of 1% per minute. The PAN samples used for these experiments were solvent-cast films 0.0017 in. (1.7 mils) thick, cut into strips 1/2 in. wide and about 3 in. long. The films were cast from 15% solution in dimethyl formamide (DMF) and were subsequently dried in a vacuum oven for 17 hours at 90°C. The DMF was not completely removed by this treatment and there is some discussion below as to how this retained solvent is influencing the observed behavior.

Figure 54 shows curves of engineering stress (stress on original cross-section) vs. per cent elongation for samples stretched at the eight test temperatures. At 110°C and 135°C, the samples formed stable necks and drew to large extensions. At 85°C and below, the samples reached high stresses at comparatively low elongations and broke in a brittle manner. Above 140°C the samples seemed to form "unstable necks" and broke in some sort

61

of "plastic" or "ductile fracture" mode at low stresses
and elongations. The apparent breaking elongation thus
goes through a maximum somewhere close to 140°C and the
apparent yield stress decreases with increasing tempera-
ture, though not in a linear manner as was found for poly-
styrene and polymethyl methacrylate.

Figure 55 shows the birefringence changes (vs.
elongation) accompanying the stress-strain curves of
figure 54. The insert shows the birefringence-elongation
curves at low temperatures plotted on an expanded scale.
Note that the results are plotted in terms of the
"corrected extinction angle"--an experimental quantity
which includes a correction for the thickness change of
the sample during the experiment and which is therefore
directly proportional to the birefringence of the sample.
(Actual birefringence values can be calculated by
multiplying the corrected extinction angle values by
6.0×10^{-5}.)

Between room temperature and 85°C, the birefringence-
elongation curves show a combination of two types of
behavior: a glassy-type response giving positive birefrin-
gence effects with increasing elongation, and a rubbery-
type response giving negative birefringence effects with
increasing elongation. The transition between these two
types of behavior can apparently be brought about either
by higher temperatures or by higher elongations (or
stresses).

At 60°C the initial slope of the birefringence-
elongation curve is zero (apparently due to a balance of
the two effects of opposite sign), but at higher elonga-
tions the slope becomes negative. At 85°C the transition
to a totally negative response is complete.

We have generally interpreted the positive bire-
fringence response of a glassy monosubstituted vinyl
polymer as indicating that the sidegroups (from which the
birefringence effect primarily arises) are tilting in the
direction of the strain, little or no long-range chain
backbone motion being possible. In the region of the
glass transition the chain backbones become more free to
move and they themselves orient in the stretching direc-
tion. This forces the sidegroups to move in a direction
perpendicular to the stretching direction, producing a
negative birefringence effect. We might note here that
it seems possible that we are inducing the same sort of

62

transition by higher elongations (or stresses) as by temperature. Such a concept of a stress-induced transition (discussed further in Section VI below) might have important implications for yielding phenomena.

Between 85°C and 140°C, relatively large negative birefringence effects can be produced. Since we were watching the undrawn region of the sample in these experiments, the birefringence becomes essentially constant as the sample starts drawing, indicating that the increase of total sample deformation is taking place almost entirely by neck propagation. At temperatures above 140°C, the birefringence effects become progressively smaller in magnitude, reflecting a decrease in the effectiveness of sidegroup orientation.

Of interest also are the initial slopes of the birefringence-elongation curves in figure 55, i.e., the ratio of birefringence to strain or the "strain-optical coefficient (St.-O.C.)". The temperature dependence of this quantity is shown in figure 56. The St.-O.C. is positive around room temperature. It drops to negative values around the lower glass transition and seems to level off in the temperature region between the two glass transitions. It then drops again to larger negative values around the 140°C transition before rising to much smaller negative values as the temperature is increased further.

Thus, several different orientation states, or alternatively, different forms and degrees of sidegroup orientation, can be seen from these data. We see a glassy (positive) form of orientation at low temperatures, which gradually changes to a more rubbery (negative) form as the 90°C transition is approached. Even more sidegroup orientation is possible around the 140°C transition, but at higher temperatures, the side groups progressively lose their ability to orient with strain in such a way as to produce negative birefringence effects. This last effect is a very curious one, which requires further investigation.

The chain backbone mobility is probably reflected most clearly in the plot of log modulus vs. temperature in figure 57. These values represent the initial slopes of the stress-strain curves in figure 54. The polymer has a typical glassy modulus value around room temperature. As the 90°C transition is approached, the modulus falls by about a factor of 20. At higher temperatures it remains

63

about constant, although a slight upward trend is evident.

We usually expect a drop in the modulus of an amorphous polymer by about a factor of 1000 at the glass transition temperature. The behavior of PAN is therefore anomalous in this respect. We would also normally expect a sharper drop in the modulus-temperature curve at the transition. In this connection, it seems likely that the retained solvent in our samples is producing this more gradual drop by acting as a plasticizer, which makes the polymer softer at lower temperatures. That there is little change in the modulus at high temperatures suggests that, although the ability of the sidegroups to orient is changing drastically, the chain backbone responds to strain in a roughly constant manner.

The data presented here indicate how critically the two transitions in PAN affect its behavior at the molecular level. It is apparent that the 140°C transition is closely associated with the nitrile groups because of the large birefringence effects associated with this transition. The 90°C transition seems to be involved with larger sections of the chain backbones. Since drawing only occurs at temperatures between the two transitions, the birefringence effects associated with drawing should be an important key to the interpretation of the detailed molecular mechanism of drawing of this polymer.

We found that it is possible to make some estimates of the width changes of the drawn region during the drawing of a sample at a constant extension rate. Since we can also measure the initial and final thickness of the polymer sample, we can construct approximate curves for the changes in width and thickness during drawing, assuming that the thickness changes in roughly the same way as the width. (The validity of this assumption for our thin films has yet to be completely verified.) Thus, having the actual width and thickness at any time, it is possible to calculate true stress, true strain, and the corrected extinction angle or the birefringence (birefringence = (6.0 x 10^{-5}) x corrected extinction angle).

The true stress-true elongation curve for a strip of polyacrylonitrile film being extended at 1%/min. at 135°C is shown in figure 58. (The load-elongation curve for this sample is similar to that shown in figure 54.)

64

The curve seems to consist of two straight-line regions, one small region at very low elongations (less than 5%) and another of lower slope extending from 25% elongation to 1200% elongation. It is very unusual for a polymer to reach such a high elongation, let alone show this kind of linear relation between stress and strain.

The birefringence changes during drawing also show unusual and unexpected results. Observations of polystyrene and polymethyl methacrylate which we have described above indicate that the birefringence along a polymer specimen during the various stages of a drawing experiment is a simple function of the local strain at that point, and yielding is not accompanied by any discontinuous change of the birefringence. Data for polyacrylonitrile is shown in figure 59. Here we see the birefringence at the center of the drawn region plotted vs. the true strain at that point. Before necking occurs, the birefringence decreases with increasing elongation and as the sample necks and draws, the material outside of the neck remains at the birefringence value reached just before necking. This behavior is consistent with a proportionality between birefringence and local strain. As the polymer yields; however, the birefringence in the neck changes very abruptly from a moderately large negative value to a positive value. As the drawing continues, the birefringence decreases gradually, eventually passing to negative values. At the high strains, the birefringence levels off at a moderate negative value of birefringence (about -0.002). This final value of birefringence, at extremely high strains, is consistent with our previous observations, that very large values of birefringence cannot be obtained in even the most highly drawn PAN filaments.

4. Effects of Environment

Additional information that would be extremely useful in interpreting the behavior during drawing could be provided by the birefringence changes during retraction of a drawn sample. Previous experience[28] has shown us that retraction does not seem to occur on heating a drawn sample to high temperatures. This is probably due to the intermolecular cross-linking reaction which takes place at temperatures at which retraction would be expected. However, the stress-strain behavior of polyacrylonitrile has been shown[32] to be quite sensitive to various solvents and plasticizers. One interesting aspect of this solvent sensitivity is a sudden dissolving of the polymer sample in certain solvents on reaching the yield point.

In view of these effects of solvents on polyacrylonitrile, we designed and built equipment to allow stress-strain-birefringence and retraction measurements to be conducted on polyacrylonitrile films in various solvents at elevated temperatures. The structure was compact enough to be placed in the air thermostat for the Instron which we had previously used in our experiments. In effect, this solvent-testing device replaced the clamps of the Instron. A liquid-containing cell was placed around the sample, the sides and bottom of which were stainless steel, with the front and back being well-annealed parallel optical glass plates (1/4" thick). The seal between the parts of the cell was a soft epoxy resin. Thus, the cell could be used to contain almost any liquid and simultaneously allow measurements of an optical nature, such as birefringence and length change, to be made.

Measurements of the birefringence changes of samples of polyacrylonitrile during straining at 2% per minute at 60°C were carried out in mixtures of water and DMF (dimethyl formamide) with DMF concentrations from 0% to 100% in 25% intervals. The changes in sample appearance proved more interesting than the actual birefringence changes. The former are summarized below.

sample environment	sample appearance after test
100% H_2O	white and opaque
25% DMF - 75% H_2O	white and lightly crazed
50% DMF - 50% H_2O	white, lightly crazed, fine band structure at 45-50°
75% DMF - 25% H_2O	clear, large crazes horizontally across entire sample
100% DMF	(sample dissolves as soon as stress is applied).

The whitening or blushing of the sample is apparently due to void formation caused by the extraction by the water of the DMF initially present in the solvent-cast (from DMF) films. When this effect is suppressed by lowering the water concentration, the effects of the DMF are clearly seen and very striking crazes are produced. We were not able to reproduce the experiments of Rosenbaum[31] in 100% DMF. Apparently his drawn fibers did not dissolve in the solvent as did our undrawn films.

66

An attempt was made to measure the retraction behavior
of a PAN film partially drawn at 125°C, by heating it in
air (under no load) to about 170°C. The drawn region showed
completely reversible behavior both in length and bire-
fringence changes. The undrawn region however retracted
(in length) with an accompanying decrease in its birefrin-
gence of about 24%. This evidence, combined with the
birefringence results, indicates the special nature of the
drawn PAN. These retraction effects require more detailed
investigation.

C. HOT vs. COLD EXTENSION OF POLYSTYRENE AND POLYMETHYL METHACRYLATE

We have observed that the birefringence produced by a
given extension (in both polystyrene and PMMA) is very
different depending on whether the polymer was extended by
hot stretching (above T_g), or by cold drawing. The
birefringence is significantly larger in the case of cold
drawing for equal extensions. If it is assumed that
birefringence gives a direct measurement of the degree of
molecular orientation, this indicates that the relation
between molecular orientation and gross external extension
of the sample is different in cold drawing and hot stretch-
ing, and that the nature of the molecular orientation may
even be different in the two cases. This is certainly the
case for the polyacrylonitrile samples discussed above.
It may be assumed that in the case of hot stretching the
relationship between birefringence and sample strain is
given by the rubber elasticity theory of birefringence
developed by Kuhn and Grün, provided that no molecular
flow takes place (since the theory describes the behavior
of a crosslinked rubber network).

It has been found that PMMA and polystyrene seem to
respond differently to stretching when they are being
oriented by hot stretching above T_g. The PMMA seems to
behave in a fairly rubbery way well above the glass transi-
tion. An explanation of this is suggested in a recent
Russian publication by Shishkin and Milagin[33]. They assume
that PMMA above its glass transition is actually in a
crosslinked state, where the cross links are not chemical
linkages between the molecules, but association bonds
between the dipoles of the ester sidegroups. This
association bonding persists even to 200°C and above, and
the temperature dependence of the concentration of these
association bonds allows an explanation of the dependence

67

of birefringence on strain at different temperatures on the basis of the rubber elasticity theory. This same conclusion was arrived at independently in our own laboratory by another line of thinking before we discovered the above publication. There should be no such association network in polystyrene above its glass transition, because the molecule contains no dipolar groups which could associate in this way. Some molecular flow may therefore take place during the hot stretching of polystyrene, so that complete recovery would not be obtained during shrinkage above T_g.

To investigate some of these birefringence and shrinkage effects, oriented PMMA samples were prepared by three different procedures: by hot stretching alone (above T_g), by a combination of hot stretching followed by cold drawing, and by cold drawing alone (below T_g). Extension and birefringence values for such a set of PMMA samples were as follows:

Elongation (%)			Birefringence x 10^3	
Hot	Cold	Total	Hot	Total
192	--	192	0.62	0.62
115	92	207	0.41	1.30
--	120	120	---	1.25

The elongation values are based on the original length of the sample in all cases.

The elongation possible during cold drawing was set by the natural draw ratio, but the elongation of the hot stretched sample could be matched fairly closely to the total elongation of the sample with the combination extension. The higher birefringence values produced by cold drawing are clearly seen from this table with the combination sample falling in an intermediate position, as expected. When these samples were heated at a temperature well above the glass transition, in an unrestrained state, all of these specimens showed complete shrinkage recovery to their original unoriented length, indicating that no molecular flow took place during the orientation process. The birefringence also went to zero in all cases when shrinkage was complete. A similar series of experiments of PS was not entirely conclusive and requires further verification. It appeared that the hot oriented specimen recovered less than the hot and cold drawn one and both did not recover completely.

A similar set of samples were heated to 105°C and allowed to retract freely. The birefringence and elongation were measured during the shrinkage, and the resulting curves are shown in figure 60. The orientation data for each sample are also indicated on the figure. Elongation values are again based on the original unstretched length of the sample. The complete shrinkage curves are not shown, since shrinkage and birefringence change were too rapid to follow initially, and became very slow as time progressed. The curves shown here were followed out for at least 30 minutes.

Other experiments in which samples with both hot and cold extension were gradually heated in the neighborhood of the glass transition indicated that the strain put in by cold drawing would shrink out at a temperature slightly below that at which shrinkage of the hot orientation took place. This seems to suggest that the orientation put in by cold drawing (or the structure of the oriented state produced by cold drawing) is not identical with that produced by hot stretching. This is in accord with the difference in the magnitude of the birefringence effects produced by hot stretching and cold drawing. The birefringence of a polystyrene sample which had been pre-oriented, then partially cold drawn in a dead-load experiment, was measured after cooling it to room temperature. The birefringence through the necked region was computed from the fringe pattern and the specimen thickness, and it was found that the birefringence increased progressively from the low to the highly drawn part of the neck (figure 61). We also measured the birefringence changes of a sample of PMMA with zero preorientation during the delay period prior to yield. The specimen dimensions were recorded photographically at the same tj e as the retardation measurements were being made. Sinc the specimen became inhomogeneous as the delay time was approached, and the rapid yield and drawing process which then took place could not be followed by the techniques used here, only the birefringence changes in the region of homogeneous deformation prior to yield were obtained (see figure 62). For this polymer also the birefringence is seen to increase progressively with strain, but in a very non-linear way as compared to polystyrene. The first appearance of deformation inhomogeneities (localized bands) which precede neck formation was well within the strain range covered here (0-12% overall sample elongation).

It appears that the birefringence along a polymer

69

specimen during drawing is a function of local strain. In some exploratory tests, however, it as found that the birefringence falls off with time, if the specimen is first strained, then held at constant length. In analogy with stress-relaxation, the rate of birefringence change must be temperature dependent also. The birefringence in cold drawing is therefore expected to be a function of temperature and rate of deformation as well as strain. More thorough investigations of these variables would be of great value in following the chain conformation changes during cold drawing.

VI. THEORETICAL DISCUSSION OF POLYMER YIELDING

A. INTRODUCTION

In conjunction with the experimental investigations carried out in this project, we have also given some consideration to the theoretical aspects of the yield and drawing process. There are several features of the process which require an adequate theoretical understanding. In terms of the continuum properties of the solid polymer itself, an understanding is needed of both the "strain-softening" process which allows yield to initiate, and the "strain-hardening" process which causes the yield to terminate at a certain point, and thus allows a stable drawing process to occur by neck propagation. Such behavior is in contrast to a continuing growth of the initial neck to the point where the material finally pulls apart, as is commonly observed with s. c metals such as copper. The initiation of the yield b. 'structural softening" is probably the first process to attempt to understand. It is this process alone which is being observed in the study of delay times in dead-load drawing experiments.

Also requiring a more detailed understanding is the phenomenon of deformation band formation, in particular, why the material tends to form these bands rather than yielding homogeneously. This seems to be an important part of the initial yield step. The softening and hardening processes must be occurring in sequence in the local yield region, during the initiation and propagation of these bands. The band structure may also be playing an important role in the formation, stabilization and propagation of the neck; some speculations on this point are presented at the end of this section. The "strain hardening" process has generally been assumed to be a result of the molecular orientation produced by the drawing; however, hardening has also been observed to take place as a function of time in interrupted drawing experiments, and a more detailed investigation of this effect is needed. In our studies of neck geometry, we attempted to obtain some information on hardening vs. strain and the role of molecular orientation by deriving the true stress-strain curve as a function of preorientation (introduced by hot-stretching). However, there is some doubt as to whether these curves are actually the true stress-strain curves of the bulk polymer, or whether they may not rather represent

71

the stress-strain relation of a composite structure consisting of a lattice of deformation bands and a matrix of unyielded polymer.

A thorough discussion of the theory of yield and drawing should of course involve a survey of the published literature on this subject, and an indication of the lines of historical development. Space does not permit the presentation of such a background survey here; we will discuss primarily work which was carried out as a direct part of the present study. We would hope to be able to present such a comprehensive survey of the work of other investigators in other publica_ions. A comparison of the mathematical form of the relations between yield stress, strain rate, and temperature proposed by several different investigators is, however, presented in a later part of this section.

We have also given no specific discussion of the behavior of crystalline polymers here. Because of the similarity of the phenomenology of drawing in crystalline and amorphous polymers, it seems likely that the basic theory of drawing is very similar for both. One significant difference, however, is that very high draw ratios are sometimes obtained for crystalline polymers, but not in amorphous polymers; this may be a consequence of a significant difference in the strain-hardening process, and may provide an experimental approach for a more detailed study of the strain-hardening effr t.

B. CONTINUUM (MOLECULAR) THEORIES OF YIELD

Disregarding the question of localized deformation band formation, we have considered three different approaches to the theory of yielding at the molecular level. Each approach is capable of at least a conceptual explanation of the complexities of the yielding process, although the derivation and underlying assumptions of each model are different. These models are designated here as the "defect", "fiber bundle", and "bonding" models.

Some of the distinctions and differences in these models can be summarized as follows. All three are rate theories, based on a summation of localized events and containing a dependence on temperature and polymer history (variable structure). Whereas the defect model treats the "movement" of defects in a stressed continuum as the deformation-producing event, the fiber bundle and bonding

72

models treat the stress-supporting elements themselves. The fiber bundle model, like the bonding model, assumes a rate of both breaking and reforming of the stress-supporting elements, but the elements involved are not precisely defined, and a variable distribution in stress and time, but not in total number, is essential to the proper functioning of the model. The defect and bonding models, on the other hand, depend on a variable number of elements, the elements themselves having a characteristic size or strength in their contribution to the plastic strain.

These different models are not necessarily mutually exclusive. They represent different conceptual approaches, but some compromise between, or blend of, these different points of view may eventually provide the most satisfactory model.

1. Defect Model

Many of the aspects of the yielding behavior of glassy polymers appear to have closer analogies with metal and ceramic mechanics than with the classical concepts of polymer mechanics such as viscoelasticity, rubber elasticity, and melt viscosity. The most striking visual similarity is the occurrence, in both metals and glassy polymers, of localized, inhomogeneous deformation regions (bands) during plastic deformation. In stress-strain properties, both metals and glassy polymers demonstrate true strain-softening and yield phenomena in a variety of stress fields, as well as strain-hardening effects. Furthermore, they both are materials which are rigid at low stresses and, therefore, are probably both close packed structures on a molecular scale.

Many aspects of polymer properties and behavior are, of course, quite different from those of metals and ceramics, especially on the molecular or microscopic structural level. Chief among these differences are the presence of non-crystalline regions and the existence of one-dimensional chains in the polymer structure. The lack of crystalline ordering of the structure has important consequences in regard to any defect model of the glass. The defect cannot be defined or described in terms of any regular molecular structure or arrangement, as is done in the case of dislocations in crystalline materials. Furthermore, the glassy structure does not present any unique plane or direction in which deformation by defect movement is preferred, even though there is a high degree of bond

73

anisotropy on the molecular scale due to the chain nature of polymers. Therefore, deformation would be expected to be difficult for polymers, even if defects were plentiful, because of the tangled structure. A further consequence of the chain nature of polymers is the connectivity of atoms along a chain. Thus, when considering elemental slip processes of atoms or molecules past one another, one must take into account that these slip elements are probably not independent of their immediate surroundings. In other words, the movement of one part of a polymer chain by necessity involves at least the parts of the chain immediately on either side of the moving part. Thus, the effective size of a polymer defect would be expected to be somewhat larger than a dislocation in a metal. The chains would also be an integral part of the strain hardening or maximum extension effect in polymers. As extension proceeds, chain orientation occurs and a greater proportion of strong intra-chain bonds resists further deformation. This sets a limit to the extent of yield.

In the development of a defect model of the material and its deformation behavior, a basic assumption is that the plastic deformation of a polymer can be described as the result of the "movement" of a number of individual defects. Thus, each defect contributes a displacement to the total plastic strain (ϵ^P) by an amount equal to its characteristic dimension (b) in the time $1/v$ (where v is velocity) and that there are a number (n) of these contributions. It may be assumed that there is an initial number (n_o) of defects present in an unstrained material, this number not being determined by thermal equilibrium, but by the previous thermal and mechanical history of the sample. It is further assumed that the velocity of "movement", or equivalently the rate of plastic strain producing contributions of these defects has a very high stress dependence and the usual exponential dependence on temperature, characteristic of thermally activated processes. Finally, the number of active defects is considered to be a function of the current history, that is, of plastic strain or time of deformation. Experimental support for these assumptions is of varying degress. The nature of possible defects has been discussed, but proof of their size, number, and behavior is lacking. The time, temperature and pressure dependence can be correlated with published yield stress data, and the nature of the structure term has been confirmed by consideration of the details of the complete stress-strain-time curves for glassy polymers.

74

From these assumptions, it is possible to write down an Eyring type rate equation for plastic strain rate ($\dot{\varepsilon}^P$) as a function of stress (σ), activation energy (E_{act}), size of defect ($\mathfrak{b}$), and number of defects (n).

$$\dot{\varepsilon}^P = \mathfrak{b}nv = \mathfrak{b}n\left[\mathfrak{b} \frac{kT}{h} \exp -\left(\frac{E_{act}}{kT}\right)\sinh\left(\frac{\mathfrak{b}^3\sigma}{2kT}\right)\right] \qquad (12)$$

where kT/h is a frequency factor and the expression in the brackets can be designated as a velocity. The $\sinh(x)$ term can be replaced by $1/2 \exp(x)$ if it is kept in mind that this substitution is only valid in the high stress range where x is large (i.e., $\dot{\varepsilon}^P$ should go to zero as σ goes to zero, which is not true for the exp expression).

$$\dot{\varepsilon}^P = \mathfrak{b}^2n \frac{kT}{h} \exp\left(\frac{\frac{\mathfrak{b}^3\sigma}{2} - E_{act}}{kT}\right) \qquad (13)$$

This basic rate equation (neglecting such things as pressure dependence, etc., can be further simplified by combining constants, so that

$$\dot{\varepsilon}^P = GTN \exp\left(\frac{H\sigma - A}{T}\right) \qquad (14)$$

where $A = E_{act}/k$, $H = \mathfrak{b}^3/2k$, $G = \mathfrak{b}^2k/h$, $N = n$, and $T =$ temperature.

While A, H, and G are constants, characteristic of the defects, the structure term N is assumed to be a function of the deformation during constant strain rate experiments and thus must be expanded. In previous work[2], both strain-softening and strain-hardening were included in the structure term

$$N = \frac{n_o + \alpha\varepsilon^P}{\hat{\gamma}f(\lambda)} \qquad (15)$$

where n_o is the original number of defects, α and γ are constants, and $f(\lambda)$ is a function of extension ratio ($\lambda = 1 + \varepsilon^P$) not unlike the non-Gaussian correction for rubber networks at high extensions.

75

It is useful to speculate on how some of the
complicated time effects during yielding, discussed above
in Section III, could be explained by this defect model of
deformation. Assuming that deformation is slow enough so
that temperature fluctuations are not significant, it
seems reasonable that the marked changes in stress-strain
behavior or delay time in creep arise from changes in the
structure of the material, specifically the population of
defects. It is known from the theory of yielding based on
dislocation generation and movement that the two parameters
that most affect the height and sharpness of the upper
yield point are the number of original dislocations (n_o)
and the stress dependence of the dislocation velocity.
Since it is assumed that for an isothermal experiment,
T, E_{act}, and $\bar{b}$ all remain constant in the rate equation,
then n, the number of defects, must be the only time-
dependent quantity in the glassy structure. The functional
form would probably include a decay term whereby the defect
population would decrease with time in a relatively simple
way if other variables, such as strain, were held constant.
The decay rate would depend on the number present. During
a stress-strain experiment, though, this decay would be
only one of the components determining defect population;
there would also be the multiplication terms related to
increasing strain, for example. It is conceivable that a
balance of these effects could lead to the attainment of a
steady-state number of defects during yielding, or even
to a decrease of defect population in such a way that the
strain-hardening behavior can be expressed as a time
function. This sort of time function would differ from
that suggested by the "fiber bundle" concept, in that the
latter treats a constant number of elements that have a
distribution in stress and time, whereas this defect model
treats a model of constant (homogeneous) stress with the
number of elements variable in time. But both concepts
contain positive (hardening) and negative (decay or
softening) terms, allowing for attainment of a steady state.

Two additional concepts are needed before the time
effects (Section III) can be adequately discussed. The
first is that, since the time effect experiments were done
on tensile film samples where neck formation and propaga-
tion were prominent, one has to assume not only that the
defect model applies to this macro, inhomogeneous tensile
yielding mode, but also that the volume of the deforming
material remains constant, once steady state drawing has
started. We have, in fact, confirmed this in our studies

76

of PMMA neck shape; neck shapes are nearly constant during drawing, as well as during stress relaxation and reloading history sequences. If this is so, the defect model of yielding has to contain a strain-hardening term, as discussed above. Then, a constant average defect population, designated as n_D, can be assumed to exist in the deformation zone of the sample at the beginning of the stress relaxation period.

The second important concept concerning the time-dependent defect population, expressed as the relative population during drawing (n_D) compared to the original (n_O) is that there might be a thermodynamic equilibrium population (n_T) still smaller than n_O. By allowing that the defect population, during stress relaxation, can decrease to less than the original number, allowance for hardening over and above the rigidity on original loading has been made. But, because the attainment of n_T is no doubt precluded by kinetic effects below T_g, this effect would probably only be important in a polymer sample quenched rapidly through the glass transition.

Assuming, for simplicity, that under any given conditions of T, P, $\dot{\varepsilon}$, etc., there is a maximum number, n_D, and a minimum number, n_O, of defects, then it should be possible to formulate the change of stress-strain properties after various histories in terms of the time-dependence of the number of defects present at the beginning of reloading. As an illustration, the history described in Section III.B.3, consisting of: (a) drawing, (b) stress relaxation at constant strain, (c) reloading with an increased apparent modulus through another yield point, can be discussed with the following simple picture. During stress relaxation, even though the defects are still moving and multiplying because of the finite stress, there is a net decrease in defect population as the effect of defect decay with time overcomes the effect of defect increase due to multiplication. With long enough time, the defect population would approach n_O as the stress relaxation rate approached the normal glassy rate at low stress. Then, at the start of reloading, the stress has a finite value at which value on the first loading there were more defects. Therefore, the stress has to rise rapidly so that the velocity increase will compensate for the small defect population. An upper yield point, then, occurs as multiplication brings the defect population back up to n_D. In this way, it is seen how the height of the second upper yield point and the reloading modulus could depend on the

defect population at the beginning of the reloading. This defect population would probably be a function of both time and stress level during stress relaxation, as suggested by the experimental results (figures 13 and 21, for example). Fitting of the experimental results to a time-dependent function for n with a characteristic "relaxation time" for defect disappearance looks promising from preliminary attempts. It has been observed that the "plastic volume", which was suggested above to be a measure of the defect population, and the load during stress relaxation at high stresses both decrease and appear to be linearly related.

These effects of hardening and associated regain of upper yield point in glassy polymers are similar to what has been called "strain-aging" effects in steels and several other metals, whereby after initial yielding the metal is unloaded, aged for a time at a temperature usually higher than the test temperature, then reloaded. The fact that another upper yield point is observed in steels on reloading has been explained by saying that during aging the number of active dislocations is reduced by a pinning mechanism so that they have to be unpinned again upon reloading. For other metals, such as copper, it is known from other experiments that the number of vacancies, dislocations, and other defects decreases during aging or annealing processes. Thus, the analogy with the defect model of glassy polymers presented here is at least plausible, except that the effect of aging for these polymers at room temperature for a short time depends on stress level. Effects exactly similar to those in metals could be obtained with glassy polymers by aging or annealing them in the unloaded stage just below their glass-transition temperature, or for longer times at room temperature.

Stress-strain tests at constant strain rate are probably not the easiest way to look at the relationship between time effects and yielding parameters. It would seem that creep tests at constant load or "spontaneous necking" tests at constant strain would be simpler cases to explore. J. J. Gilman[34] has applied the formulation of the dislocation model to dead load creep tests on LiF and found that delay times before the onset of high rate creep were accurately predicted. In fact, the discussion of an equation of state for yield in Section III.C.5.d above is the first simplified stage in the use of rate equations in analysis of delay times for polymers.

2. Fiber Bundle Model

78

An alternate approach to the dislocation analogy treated above which can be found in the literature[35] involves the explanation of plastic yield by use of the high-stress form of the Eyring viscosity equation:

$$\dot{\varepsilon} = C \exp\left(-\frac{E_a}{kT}\right) \sinh\left(\frac{\bar{s}v}{kT}\right) = A \sinh\left(\frac{\bar{s}v}{kT}\right) \qquad (16)$$

where $\dot{\varepsilon}$ is strain rate, C is a constant with dimensions of a reciprocal time, E_a is the energy of activation for viscous flow, v is a quantity with the dimensions of a volume, and s is the mean stress per molecular group. This equation, though it gives a reasonable account of the influence of stress level and temperature on deformation rate, fails badly to describe all of the phenomena observed in the yielding of glassy polymers, such as a well-defined yield at constant strain rate, a delay time to yield under dead load, and hardening effects during stress relaxation at constant strain (when drawing is interrupted).

A model has therefore been constructed here, using the Eyring equation as a starting point, but incorporating an additional assumption, which seems to be a logically necessary one; that is, that the stress on a molecular group, rather than being taken equal to the mean stress $\bar{s}$, is taken as dependent on the prior history of this group. If it has just rearranged or "jumped" under the influence of the applied stress, the stress, s, acting on this group is assumed to be zero. As other groups subsequently yield or jump, the value of s acting on this group rises until the element "jumps" again. The jump probability per unit time is taken to be A sinh(sv/kT). The total stress applied to the system must, of course, be supported by the individual elements in any cros   action of the specimen, but the jumps that relieve s   ,s at some sites lead to a higher stress at the other: This re-distribution of stress from "broken" to still-re   .ring elements is a characteristic of statistical theories of fracture of fiber bundles. However, a process of re-formation of "broken" elements is assumed here.

These considerations lead to a description of the time behavior of the system in terms of a distribution function n(s;t) giving the number of elements supporting stress s at time t. The function n(s,t) is subject to the following conditions:

$$\int n(s,t) \, ds = N_o \quad \text{(The number of molecular groups per unit cross-sectional area)} \tag{17}$$

$$\int s \, n \, ds = \Sigma \quad \text{(The applied stress)} \tag{18}$$

$$\dot{\varepsilon} = g \int n \, A \, \sinh \frac{sv}{kT} \, ds \quad \text{(where g is a dimensionless constant)}. \tag{19}$$

The equation which governs the change of $n(s,t)$ with time is non-linear, and a complete solution has not yet been obtained. However, a solution for steady state conditions, combined with certain qualitative considerations based on the form the solution must take, lead to the conclusion that a fair description of the influence of stress history on the material, and hence of the existence of phenomenological plasticity, can be provided in these terms. A somewhat more complete discussion of this model has been presented in a recent publication[36].

3. Intermolecular Bonding and Stress-Induced Transitions

Theories of cold-drawing have been proposed previously which were related to the glass transition phenomenon. One, proposed many years ago by Müller, assumes that the work of drawing heats the polymer locally (at the neck) to the glass temperature (T_g). A second assumes that enough free volume is introduced into the glass by straining (e.g., by the Poisson's ratio effect) to produce the glass transition. However, both of these theories are open to criticism on the basis of known experimental facts, even though it would seem that something like a glass transition effect is needed to allow the magnitude of straining and the molecular slippage and orientation which are observed during the cold-drawing process.

It would seem possible to propose still another "glass transition" theory of cold-drawing, in which it is assumed that the glass transition is "stress-induced", in a way other than through free volume change--perhaps by the elastic strain energy. Let us further assume that the essential nature of the glass transition phenomenon consists in the breaking or loosening of cohesive bonds between the chains (which are frozen and rigid in the glassy state).

80

This is something of a departure from the usual theories of the glass transition, but is the approach used in Section V.B.1 to explain the glass transition behavior of polyacrylonitrile. It has also been utilized in a recent publication[37] in connection with the interpretation of dynamic mechanical loss spectra. The detailed nature of the cohesive bonding will depend on the chemical structure of the polymer, and the existence of more than one type of cohesive bonding could explain the existence of more than one glass transition in some glassy polymers (in such a case, all but one would customarily be referred to as "secondary transitions"). Within this framework, a cohesive bond in the glassy state would be regarded as the analog of a "fiber" in the fiber bundle model and a broken bond, the analog of a crystal dislocation in the defect model. The advantage of the bonding model is the specification of the nature and strength of the elementary unit involved in the deformation process.

It seems likely that only a "partial" glass transition would be necessary for cold-drawing, and not a complete transition to a rubbery state. In addition, such a transition might be anisotropic, allowing the molecules to slip preferentially in a certain direction, in contrast to the usual thermal type of glass transition. One of the important by-products of an understanding of the molecular or microscopic mechanism of yield and drawing in glassy polymers might therefore be an improved theoretical understanding of the nature of the glass transition.

In the development of a microscopic mechanism of the yield process, the initiation of the yield would seem to be the feature capable of the simplest treatment, as noted previously. This can be observed particularly well in experiments of drawing under dead load, which have been described in a previous section. These display the time effects involved in the initiation of yield in a particularly helpful way, as a "delay time" in neck formation.

If it is assumed that the initiation of yield is the result of a stress-induced glass transition (probably a partial rather than complete transition) the sudden initiation of a neck must be the final catastrophic result of a gradual breakdown of cohesive bonding between the molecules, and is a consequence of the kinetics of the bond-breakdown process. The fact that time effects are connected with the glass transition is well known. A useful analogy for the yield initiation might be that of a

branching chain reaction (such as nuclear fission) where a
critical boundary (e.g., of temperature and pressure or
concentration) exists, above which the reaction "runs away"
and becomes explosive--i.e., becomes catastrophic in a
rate sense. This would seem to be analogous to the boundary
observed in dead load drawing, above which necking and
drawing takes place, but below which only creep is observed.
Another feature which seems evident is that the nature of
the microscopic processes involved should not be different
above and below such a boundary; the boundary represents
merely the critical kinetic conditions for explosive popu-
lation growth. Consequently, if a bonding breakdown is
responsible for necking and drawing, it should similarly
be responsible for the viscoelastic behavior observed
below the critical stress level required for yield.

C.   COMPARISON OF MATHEMATICAL FORMULATIONS

Because of the wide use and inherent reasonableness of
theories based, either directly or indirectly, upon an
Eyring type stress-biased thermally activated rate process,
it seems useful to examine these various treatments for
points of similarity and difference. Many of these
formulations were derived from experimental curve fitting
and only afterwards justified theoretically, and thus a
useful comparison of experimental data can be made here also.

The most basic point of departure for all these
formulations is that a characteristic stress (the yield
stress) varies linearly with the log of the strain rate, at
least for reasonable rates well below sonic velocities.
This general experimental fact appear' in all the formula-
tions. Temperature is the other most important and well-
investigated experimental variable, but the representation
of temperature dependence in these formulations varies
somewhat. Other experimental variables such as pressure
and complicated loading histories have not been extensively
investigated. Polymer variables are usually included as
the empirical constants of the equations. But there is no
allowance for variability of polymer structure (crystalline
morphology, density of glass), except for molecular
orientation, and there is little correlation attempted
with other polymer properties.

The most general form of these theories is shown in
equation 20 where $\dot{\epsilon}$ is a strain rate, σ is a stress and

A, B, C are constants.

$$\dot{\epsilon} = \frac{1}{C} \exp \left[\frac{\sigma - A}{B} \right] \qquad (20a)$$

$$\sigma = A + B \ln(C\dot{\epsilon}) \qquad (20b)$$

The discussion of the range of validity (in σ and $\dot{\epsilon}$) of these equations will be deferred until later, as will the derivation from more basic principles. Although there are assumptions and simplifications involved, if $\dot{\epsilon}$ is taken to be the overall strain rate (derived from crosshead rate) and σ is taken to be the yield stress (σ_y) (either offset or maximum load point), the following formulae can be compared with the data on polymers.

Robertson[35] has studied the stress-strain properties of Lexan polycarbonate as a function of temperature, strain rate, and orientation (strain). He presents a constitutive equation of the following form

$$\dot{\epsilon} = C_1 \exp \left[\frac{C_2\, \sigma_y}{(\theta - T)(1 + a\Omega^\alpha)} \right] \qquad (21)$$

where T is temperature, Ω is an orientation function, and C_1 and C_2 are constants. Since the yield point occurs at low enough strain levels, the Ω function can be ignored. Transforming equation (21) into form (20b) we get:

$$\sigma_y = \frac{\theta}{C_2} + \frac{T}{-C_2} \ln \left(\frac{\dot{\epsilon}}{C_1} \right) \qquad (22)$$

$$A = \frac{\theta}{C_2}, \quad B = -\frac{T}{C_2}, \quad C = \frac{1}{C_1} \qquad (23)$$

Thus, all the temperature dependence is contained in the parameter B.

Lohr[38], in two recent articles, has reported studies of the yield stress of both glassy and crystalline polymers as functions of temperature and strain rate. His data can be represented by an equation of the form

83

$$\sigma_y = K_1 + K_2 \; \ln(\dot{\epsilon} \; a_T) \tag{24}$$

with the simple correspondence between (20b) and (24) being

$$A = K_1, \quad B = K_2, \quad C = a_T \tag{25}$$

where K_1 and K_2 are constants depending on the polymer and choice of reference temperature and a_T is a temperature dependent shift factor used for shifting data along the $\ln \dot{\epsilon}$ axis. Here, then, all of the temperature dependence is contained in parameter C.

Roething[39] has investigated PMMA and PEMA over a range of strain rates and temperatures, including the T_g range. Because his data, when plotted against log $\dot{\epsilon}$, shows two linear portions, he represents the behavior as Eyring type viscosity with two species of flow units, corresponding to the behavior above and below the glass transition. The basic equation is

$$\frac{\sigma_y}{T} = \sum_i \; (\frac{1}{A_i}) \; \sinh^{-1} \left[(C_i \; \frac{\dot{\epsilon}}{T}) \; \exp \; (\frac{\Delta H_i}{RT}) \right] \tag{26}$$

where A_i and C_i are constants and the ΔH_i are the activation energies for the two processes denoted by the index i. Taking the usual high-stress limit of the Eyring type equation where

$$\sinh x \approx \frac{1}{2} \exp x \quad \text{if } x \geq 3.5 \tag{27}$$

equation (26) is put into the form of equation (20b)

$$\sigma_y = \frac{\Delta H_i}{RA_i} + \frac{T}{A_i} \; \ln(\frac{2\dot{\epsilon}C_i}{T}) \tag{28}$$

and

$$A = \frac{\Delta H_i}{RA_i}, \quad B = \frac{T}{A_i}, \quad C = \frac{2C_j}{T} \tag{29}$$

The temperature dependence, then, is here directly included

84

in the parameters B and C, and indirectly in A through the choice of processes involved. Polymer variables are also included in all three parameters. In the data of Lohr on semicrystalline polymers, two straight line regions of behavior are also evident, but he arbitrarily picks one or the other to fit to his equation (24).

Kaelble[40] has developed a theory of yielding based directly on the WLF equation, which applies not only to yielding but also to large strain and rupture behavior as well, using the analysis of T. Smith of rupture of rubbery networks[41]. Although the basis of Kaelble's theory of yielding is the idea of T_g being lowered by the hydrostatic component of the tensile stress, which has limited validity, the constitutive equation is still of interest.

$$\dot{\epsilon} \propto \frac{\epsilon}{a_T} \exp\left[\frac{C_3\sigma - C_4\Delta T}{T}\right] \qquad (30)$$

where

$$C_3 = T_g, \quad C_4 = T_g\left(\frac{\partial\sigma}{\partial T}\right)_{f_g},$$

$$f_g = \text{free volume at } T_g, \quad \Delta T = \left[T - T_g\right]$$

$$a_T = \exp\frac{-C_1\ \Delta T}{C_2 + \Delta T} \cong \text{WLF shift factor.}$$

Rearranged into the form of equation (20b), at σ_y it becomes

$$\sigma_y \propto \frac{C_4\ \Delta T}{C_3} + \frac{T}{C_3}\ \ell n\left(\frac{\dot{\epsilon}}{\epsilon}\ a_T\right) \qquad (31)$$

and

$$A = \frac{C_4\ \Delta T}{C_3}, \quad B = \frac{T}{C_3}, \quad C = \frac{\dot{\epsilon}T}{\epsilon} \qquad (32)$$

Beside the fact that the temperature dependence is included in all three parameters, though in different ways, this formulation is interesting in that superposition of the total stress-strain behavior is possible. Thus, even

85

though the strain dependence in parameter C and the T_g temperature dependence (through ΔT) are both derived from mechanical behavior above T_g (rubbery and viscous flow, respectively), they seem to fit correctly the stress-strain behavior below T_g in the glassy state. The inclusion of the "structure factor" $(f(\epsilon))$ is significant here.

It is interesting to compare the basic behavior with the defect theory discussed in Section VI.B.1. Further development of the ideas in that section leads to the general yield stress equation for glassy polymers:

$$\sigma_y = \frac{A^g}{H^g} + \frac{T}{H^g} \ln \left(\frac{S}{G^g F^g_T} \right) \tag{33}$$

Where S is a strain rate, F^g is a structure factor (linear in strain), and A^g and H^g are constants dependent on the polymer, G^g being related to H^g. Compared to equation (20b), the parameters are

$$A = \frac{A^g}{H^g}, \quad B = \frac{T}{H^g}, \quad C = \frac{1}{G^g F^g_T} \tag{34}$$

where both B and C are linear functions of temperature and C contains a strain dependence. The dependence on T_g is contained in the parameter A through A^g.

A comparison of these equations, all of which appear to fit the experimental data reasonably well, reveals many similarities and a few important differences. In this comparison, it must be kept in mind that there might be differences in the definition or characterization of the yield point and in the definition of which strain rate to use, total or non-elastic (plastic) strain rate. But these slight differences, discussed below, are minimized at the yield point.

The parameter A of equation (20b) is represented in all of the treatments except that of Kaelble as temperature

86

independent, and, where specified, includes an activation
energy term characteristic of the polymer. Similarly,
parameter B, in all but Lohr's treatment, is linearly
related to temperature and is a polymer constant. Parameter
C, in all but Robertson's treatment, is a decreasing
function of temperature though not exactly linear in
Kaelble's and Lohr's treatment. Furthermore, in the two
treatments that claim to apply to strains other than the
yield point there is a reciprocal dependence of parameter C
on total strain (Kaelble) or on plastic strain (Whitney).

Since the equations fit their respective yield stress
data fairly well, it is not surprising that the value of
the polymer constants in similar treatments are about the
same for the same polymer. There is little attempt,
however, to investigate how these constants might relate to
other characteristics of the polymer, in the sense of
chemical, conformational, or morphological structure.
The relation to T_g is the only explicit correlation with
polymer properties.

D. NECK FORMATION AND DRAW RATIO

The problem of neck formation is perhaps the most
obvious phenomenon associated with polymer yielding. As
such, it is useful to offer some observations on this
subject, which, although of a speculative nature, might
be helpful in pointing the way to the ultimate resolution
of this problem.

Although most discussions have approached the problem
of neck formation in terms of the stress-strain properties
of the material considered as a homogeneous continuum,
the detailed observations of neck initiation and propagation
in the dead-load (creep) drawing discussed in a preceding
section seem to indicate that the development of a neck may
be connected in a very direct way with the development of
deformation bands in the specimen, although this is not
yet certain. Since the bands which have been observed
start to develop prior to the formation of the neck, it
would seem that they can hardly fail to have an influence on
the mechanics of the neck formation and propagation; in
fact, it seems more likely that they play a key role in the
overall process. The formation of these deformation bands
has been observed in many polymers, both amorphous and
crystalline, and their appearance during the yield process
may be a perfectly general phenomenon for all polymers
(although this point cannot yet be regarded as established).

87

In cases where deformation bands accompanying neck formation have been seen, the typical sequence of behavior observed in neck initiation and propagation is the following:

(a) Growth of deformation bands in the specimen.
(b) Formation of a neck at the point on the specimen where the concentration of deformation bands is greatest.
(c) Tilting of the bands into the axial direction as the undrawn material containing the band structure feeds into the neck.
(d) Disappearance of the bands as the neck moves further along the specimen, leaving a drawn region which appears to be homogeneous, and in which bands can no longer be seen.

Setting aside the question of why such localized deformation bands tend to form in the first place, their propagation through the specimen requires a localized softening and yield (compared to the surrounding bulk material) followed by a hardening which arrests the local yield at a certain point. The band itself may then be regarded as consisting of "strain-hardened" polymer. Since the bands tend to grow in from the various lateral faces of the sample, they will eventually form an intersecting lattice in three dimensions, embedded in a matrix of unyielded material. The details of the structure of this lattice, if it indeed exists, are still open to question. The specimen could thus be regarded as a composite structure somewhat similar to a fiberglass-reinforced plastic, except that the rigid network is made up of some kind of cells rather than filaments. A better analogy would perhaps be a composite with a honeycomb core. The formation of a neck then requires the localized collapse of the rigid lattice, which acts as the primary load-bearing element of the structure, in the axial direction (this would resemble the folding-up of an umbrella). This lattice collapse requires the yield of the undrawn matrix material, and lattice and matrix coalesce into uniformly (homogeneously) yielded and strain-hardened polymer as the neck propagates away from this point.

The fact that a localized neck tends to form in the specimen is not at all surprising from a consideration of this model since such a lattice might be unstable and would tend to collapse when strained; this collapse would take place first at some local point in a sample which is

not perfectly homogeneous, as is observed. The strain hardening when the lattice is fully extended, and the propagation of the neck by a "collapse wave" in the lattice can easily be visualized; the collapse of the lattice at one point will make it easier for the adjoining parts of the lattice to collapse in turn. The gross features of neck formation and propagation when accompanied by deformation bands might thus be understood in terms of this picture of a collapsing lattice composite. However, a full understanding still requires a knowledge of the material properties on the molecular (or bulk homogeneous) level. This will be necessary to understand how deformation bands form initially, and how the matrix material yields as the lattice collapses. (The photograph in figure 30 indicates that the band concentration becomes quite dense in a specimen neck, and this is probably part of the answer as to how the matrix material yields.)

This approach also has important relevance to another basic problem--that of explaining the "draw ratio" of a polymer (the magnitude of extension produced by the drawing process). If the drawing can be visualized as a process of lattice collapse, then the draw ratio should be merely a combination of the strain magnitude in the deformation bands and the geometrical extension factor resulting from the lattice collapse. Since the deformation bands always form at a roughly 45° angle for different polymers, the lattice collapse factor should be about the same for all polymers. Variations in the "natural draw ratio" for different polymers should then be primarily a result of differences in the magnitude of strain in their deformation bands. Data of this type are not now available on a wide enough variety of polymers to allow such a correlation to be verified at the present time. However, the magnitude of the strain in the deformation bands of polystyrene has been estimated (Section IV.D.) to be approximately unity (i.e. 100% extension) and combination of this with a lattice collapse factor where the bands are at an angle of perhaps 50-55° to the sample axis would give a value of the draw ratio which is in good agreement with that experimentally observed for polystyrene (150-200% elongation, for polymer containing only a small amount of preorientation).

VII. CONCLUSIONS

During the period of the present contract, we have had the opportunity to extend our studies of cold-drawing to provide a more satisfactory understanding of several of the important aspects of the phenomenon. Based on the results of our previous six-month exploratory contract, we have followed out some of the lines of investigation indicated there in greater detail, and have done some further exploratory work as well. We have extended our work to a wider range of polymers (including crystalline as well as amorphous types).

The time effects associated with the drawing process have been investigated in different ways and in considerable detail. Measurements of stress relaxation before and after yield, and of interrupted drawing, indicate definite soft-ening and hardening effects taking place as a function of time in both amorphous and crystalline polymers in the ranges of stress level and strain where yield takes place. This must reflect reversible changes in the solid state structure of the polymer. There are large differences in the effect of interrupting drawing during the neck propa-gation stage, depending on whether the sample is held at constant strain or is completely unloaded and allowed to retract during the interruption period; hardening takes place in the first case, softening (initially, followed by re-hardening) in the second.

The phenomenon of delayed drawing under dead-load (creep) conditions has been carefully investigated, for polystyrene and polymethyl methacrylate, as a function of stress level, temperature, and pre-orientation of the polymer. The delay time for initiation of necking under these conditions has been particularly studied. It is found that there is a critical stress level, which decreases with increasing temperature, above which delayed drawing takes place, but below which only viscoelastic creep is observed. Since drawing always seems to be preceded by the formation of localized shear bands, it seems probable that this critical stress represents the stress required for their formation or propagation. The logarithm of the delay time is found to be a linear function of both stress and temperature. The delay time depends only slightly on preorientation.

Sequence photographs of samples of PMMA during stress-

90

strain curves have shown that he usual assumption that the neck stabilizes its shape at the beginning of the lower yield stress region is not correct and that the vie that the neck forms at the yield peak needs to be modified. The neck is not clearly seen until a point well beyond the yield peak, and it does not reach its steady-state shape until a point well along in the level region of the stress-strain curve. The sharpness of the steady-state neck seems to go through a maximum vs. both temperature and strain rate. From these photographic studies, an attempt was also made to derive the "true stress-strain curve" of the material (in the sense of the homogeneous properties of the bulk polymer) from successive measurements of external load and local sample diameter at the point where the neck first formed. The fact that the "strain hardening" of PMMA takes place at progressively lower strains as the degree of pre-orientation increases can be seen from these curves.

There seems some doubt, however, that the above curves represent the true stress-strain properties of the bulk polymer. It was believed from early observations that PMMA did not draw by shear band formation. However, it now appears that the shear bands in PMMA, although difficult to see by eye, are actually present and can be seen by "schlieren" techniques, although it is not clear whether these bands are the same in nature as those in other polymers. If the formation of shear bands precedes necking in a similar fashion for all polymers, then perhaps the formation and propagation of a neck actually represents the initiation and spread of a "collapse wave" in a composite bulk structure consisting of a lattice or network of inter-secting deformation bands embedded in a matrix of undrawn polymer. This picture of the polymer structure during drawing also gives a method of describing the "natural draw ratio" of a polymer; an estimate of the natural draw ratio of polystyrene by this method gives a value in good agreement with the experimental value of 150-200% extension.

Studies of the effects of absorbed moisture and of temperature history (quenching and annealing in various combinations) on the dead-load drawing of PMMA indicate that these treatments produce very important effects, in addition to affecting the value of the delay time. Drying PMMA enhances the visible formation of deformation bands, and rapid quenching produces specimens in which the tendency to localized necking during drawing is greatly reduced, so that the sample shows almost "homogeneous" drawing.

91

Attempts were made to observe directly the volume changes of samples during yield in compression, by use of a mercury dilatometer. The results indicate that a volume expansion accompanies the onset of yield, and in general accompanies any "softening" of the polymer. These results, combined with the results of yield experiments in different stress fields, indicate that the hydrostatic component of the stress tensor (which would be related to volume changes) plays a very important role in the yield criterion of polymers, unlike the case of metals, but resembling the behavior of granular soils. It is not completely clear whether these volume changes should be interpreted in terms of the "free volume" of the polymer.

The possible applicability of an equation of state to the yielding process (in which deformation rate is one of the parameters or state variables) has been checked by attempting to correlate the delay time for drawing of PMMA under dead load with the rate dependence of the stress-strain curve of the same polymer in tests at constant strain rate. The results indicate that such a correlation is possible, and thus that an equation of state can probably be applied, provided the delay time is defined in a way slightly different from that which we have conventionally used.

Some drawing studies have been carried out on poly-acrylonitrile (PAN), which is useful as a bridge between amorphous and crystalline polymers, since it has some of the characteristics of both types of polymer. Birefringence measurements have also been made on this polymer in some detail. The birefringence changes produced by drawing of this polymer are somewhat complex. One interesting phenomenon which has been observed is that a striking birefringence change which is observed when a slightly oriented sample is cooled through the 140°C transition region is completely eliminated when the polymer is drawn. Birefringence measurements on other polymers indicate that the sign of the birefringence produced by cold drawing is the same as that produced by hot-stretching, indicating that molecular chains are being extended in the process. However, the magnitude of birefringence produced by a given strain is greater in cold-drawing than in hot-stretching, indicating that the efficiency of orientation in the cold-drawing process is greater.

In order to explain (or represent) the softening of

92

the solid polymer which is involved in yield, we have
developed three theoretical approaches to this problem.
One involves a treatment of "defects" in the solid structure,
analogous to the theory of dislocations used to explain
yield in metals and other crystalline materials. The
second involves an analogy with the theory of fracture of
a "fiber bundle", in which the Eyring flow theory is modi-
fied to allow for redistribution of stress among flowing
elements which release stress by jumping and then re-form.
The third approach is formulated in terms of a large-scale
breakdown of secondary cohesive bonding between the polymer
molecules, which can be visualized as a stress-induced .
glass transition. No conclusive decision can be made at
present as to the relative merits of these different
approaches; further work is needed to see which fits the
facts most successfully. The "strain-hardening" effect is
probably associated with molecular orientation, but since
hardening is also observed when drawing is interrupted by
a period of stress relaxation at constant strain, further
study of this hardening effect is obviously needed.

VIII. RECOMMENDATIONS FOR FUTURE WORK

Based on the results of the present investigation, some recommendations can be made for future work which will be needed in order to obtain a still more complete understanding of the yield and drawing process in solid polymers.

Continuing evidence of the importance of the formation of localized deformation bands in the normal drawing process, which involves the formation and propagation of a neck in the specimen, indicates that a more detailed study of the nature and formation of these deformation bands would be desirable. Their geometry and the mechanics of their initiation, propagation and termination are not satisfactorily understood at the present time. A knowledge of why they form in preference to homogeneous deformation of the bulk material is needed. It seems likely that such an understanding will be required to achieve a realistic and totally satisfactory understanding of the phemomenon of neck formation and propagation. Measurement of the magnitude of the shear strain in the deformation bands of several polymers, and an attempt to correlate these values with the "natural draw ratio" for the same polymers would be very desirable, for reasons pointed out in the previous section; this could provide at least a partial theory of the draw ratio, which like neck formation is another very obvious and central characteristic of the drawing process.

Another related area requiring further investigation is the nature of pretreatment effects (quenching, annealing, moisture and other plasticizer effects) on the drawing process. Since quenching has been found to suppress neck formation, this may be a way to achieve and study the truly homogeneous bulk drawing process. The true stress-strain curve of the bulk material might be obtained in this way. This would be the type of data needed in an equation of state of the bulk material. These various effects may be related to the free volume in the bulk polymer, and further attempts should be made to correlate the results of these conditioning treatments with the specific volume or free volume of the polymer. High-pressure studies might be useful in this connection, as a means of altering these volume relationships. Solvent swelling might also be a helpful technique. If the yield or drawing could be carried out by a process of homogeneous deformation, this could with some justification be treated as a process of solid-

state "flow". The ability to evaluate an activation energy from the temperature dependence of such a flow process would extend the possibilities of a continuum mechanics treatment of the yield process of the sort implicit in the use of an equation of state.

The time effects associated with drawing should be studied in more detail. The study thus far of the delay times associated with drawing under dead load has given very useful information particularly about the long-time region and the low-stress boundary where delay times become infinite and below which viscoelastic creep rather than yield is obtained. More information about the short-time and high-stress behavior is needed, which could be provided by high-speed testing. It is believed that at high stresses there is a boundary beyond which fracture is observed rather than yield (i.e., a brittle-ductile transition). We have not yet observed this boundary or attempted to map its position. This would have particular relevance to the problem of ballistic response, and would define the limits of applicability of an equation of state describing the yield process. This also has obvious relations to the general problem of what defines or determines the "toughness" of a polymer.

The structural hardening and softening associated with interrupted drawing should also be investigated further. Measurements of the strain changes during interruption periods in which the sample is completely unloaded and allowed to retract would be desirable in completely characterizing the softening and final re-hardening which takes place under these conditions. An attempt to observe the softening which occurs prior to yield (e.g. in a dead-load experiment during the delay period) should be attempted using other physical methods (such as dielectric, NMR, or light scattering). Birefringence measurements have not shown any significant changes during this period.

The role of transition temperatures in the drawing process needs to be clarified. This question is frequently raised, and requires an answer. This is a relevant question, since these transitions are responsible for the softening of polymers under purely thermal conditions (where the polymer is heated with no stress, or negligible stress, applied). One approach to this problem would be to study yield and drawing in the temperature ranges of such transitions, determining for example the yield stress as a function of

temperature in the transition region. It would be particularly helpful to study in this way polymers showing multiple transitions (both amorphous polymers showing primary and secondary glass transitions and crystalline polymers showing both first order and second order transitions). The position of such transitions could be changed in some cases by absorbed moisture or addition of other plasticizers, to provide an additional experimental variable.

Crystalline polymers should receive more study than we have been able to devote to them so far. Our observations in the present project have continued to confirm the surprising similarity in the yield and drawing behavior of crystalline and amorphous polymers, in view of their obviously great differences in solid state structure and morphology. Nevertheless, the yield and drawing behavior of crystalline polymers is of great practical interest and importance, and some study should be devoted specifically to them—preferably in parallel with corresponding measurements on amorphous polymers. The morphological changes accompanying the drawing of crystalline polymers provide an obvious area of investigation, but such changes may be only an incidental effect, and not a controlling feature of the yield mechanism. A significant problem for study which could be carried out even without the specialized equipment (such as an electron microscope) needed for morphological studies, would be to attempt to characterize the relative roles of the crystalline and amorphous regions in the drawing process. The amorphous regions of nylon can be selectively cross-linked, for example, by an exposure to the vapor of toluene di-isocyanate for suitable combinations of temperature and time; this should affect the behavior of the amorphous regions. Irradiation of polyethylene produces interlamellar cross-linking which should affect any process of interlamellar slip. The use of stereospecific structure as a parameter to control degree of crystallization or crystallizability should also be helpful in this connection, since crystalline and glassy amorphous (atactic) polymers of the same chemical type could be studied and compared. Polymers such as polyethylene terephthalate, which can be quenched into an amorphous glassy state, but which will crystallize on drawing, should also provide useful information on the role of crystalline structure in the overall drawing process.

No brief listing such as this can attempt to cover all of the possible areas of research which would cast useful light on the nature of the yield process, and lead to its

96

better understanding. Many approaches are possible, and the suggestions offered here are influenced considerably by the results already obtained. One further area may be mentioned, however, which would seem to have great interest for detailed study and which has important relations to the theory of structural softening which has been described in the preceding section of this report as the "bonding breakdown" theory. This is the study of the mechanical breakdown of gels--an example of the type of behavior generally described as "thixotropy".

This should provide a highly relevant analogy to the structural softening taking place in the solid state. Gels of this type can be made with polymer and plasticizer (or solvent) and the concentration could be varied in suitable systems from dilute gel to swollen polymer to solid polymer. Such gels are often thermally reversible (i.e., they will break down to solutions on heating, and re-form the gel on cooling). In some cases, a "glass transition" has been observed in these gels--a temperature where the thermal expansion coefficient of the gel changes, just as in a glassy polymer. The kinetics of bonding breakdown in dilute gels could probably be deduced quantitative'" using the theory of rubber elasticity and treating the bc ding points as cross-links in a rubbery netwo.k. The combined effects of temperature and stress could thus be studied in a situation where the mechanical breakdown is clearly due to a breakdown of intermolecular bonding; and the progressive change in behavior could be followed over the composition range leading all the way to 100% polymer.

IX. ACKNOWLEDGMENTS

REFERENCES

1. R. D. Andrews, Jr. and W. Whitney, "Study of the Phenomenon of Cold-Drawing (Plastic Yield) in High Polymers." U. S. Army Natick Laboratories, Natick, Massachusetts (August 1964), C & OM-3, also issued by the Textile Division, Dept. of Mechanical Engineering, M.I.T., as Report TD-123-64 (May 1964).

2. This subject has been discussed in greater detail in W. Whitney, Sc.D. Thesis, Dept. of Civil Engineering, M.I.T., (November 1964).

3. W. Whitney and R. D. Andrews, IUPAC Macromolecular Symposium, Prague (September 1965). Preprint 373 (to be published, J. Polymer Sci.).

4. See for instance F. A. McClintock and A. S. Argon, Mechanical Behavior of Materials, Addison Wesley (1966).

5. See for instance A. G. H. Dietz and F. R. Eirich (editors) High Speed Testing, Interscience, New York (yearly).

6. See for instance A. V. Tobolsky, Properties and Structure of Polymers, Wiley, New York (1960). Chapt. IV.

7. P. I. Vincent, Polymer 1, 7 (1960).

8. M. L. Williams and M. F. Bender, J. Appl. Phys. 34, 3329 (1963).

9. M. L. Williams and M. F. Bender, Textile Res. J. 33, 1023 (1963).

10. G. E. Dieter, Mechanical Metallurgy, McGraw-Hill, New York (1961) p. 350 ff.

11. J. W. Kauffman and W. George, J. Colloid Sci. 6, 450 (1951).

12. D. W. Morrison, B.S. Thesis, Dept. of Metallurgy, M.I.T. (May 1964).

13. D. H. Ender and R. D. Andrews, J. Appl. Phys. 36, 3057 (1965).

14. W. Whitney, J. Appl. Phys. $\underline{34}$, 3633 (1963).

15. J. R. McLoughlin and A. V. Tobolsky, J. Polymer Sci. $\underline{7}$, 658 (1951).

16. D. S. Wood and D. S. Clark, Trans. Amer. Soc. Metals $\underline{43}$, 571 (1951).

17. T. L. Russell, D. S. Wood and D. S. Clark, Acta Met. $\underline{9}$, 1054 (1961).

18. R. G. Cheatham and A. G. H. Dietz, Trans. ASME $\underline{74}$, 31 (1952).

19. J. K. Knowles and A. G. H. Dietz, Trans. ASME $\underline{77}$, 177 (1955).

20. For a more detailed presentation of the material in this section see S. W. Allison, M.S. Thesis, Dept. of Civil Engineering, M.I.T. (1964).

21. J. Miklowitz, J. Colloid Sci. $\underline{2}$, 193 (1947).

22. J. A. Godrick, M.S. Thesis, Dept. of Mechanical Engineering, M.I.T. (May, 1964).

23. S. Cooper, B.S. Thesis, Dept. of Chemical Engineering, M.I.T. (May 1964).

24. R. D. Andrews and J. Rudd, J. Appl. Phys. $\underline{28}$, 1091 (1957).

25. W. L. Grube and S. R. Rouze, ASTM Proceedings $\underline{52}$, 573 (1952).

26. O. K. Spurr and W. D. Neigisch, J. Appl. Polymer Sci. $\underline{6}$, 585 (1958).

27. R. J. Curran and R. D. Andrews, M.I.T. Dept. of Civil Engineering Report No. R63-55 (December 1963).

28. R. D. Andrews and R. M. Kimmel, J. Appl. Phys. $\underline{35}$, 3194 (1964).

29. Further discussion of the material in this section can be found in R. M. Kimmel, M.S. Thesis, Dept. of Mechanical Engineering, M.I.T. (May 1965).

30. R. D. Andrews and R. M. Kimmel, J. Polymer Sci. 33, 167 (1965).

31. R. M. Kimmel and R. D. Andrews, J. Appl. Phys. 36, 3063 (1965).

32. S. Rosenbaum, J. Polymer Sci. A9, 2085 (1965).

33. N. I. Shishkin and M. F. Milagin, Sov. Phys.-Solid State 4, 1967 (1963).

34. J. J. Gilman, J. Appl. Phys. 36, 2772 (1965).

35. R. E. Robertson, J. Appl. Polymer Sci 7, 443 (1963).

36. M. Goldstein, J. Polymer Sci. B4, 87 (1966).

37. R. D. Andrews and T. J. Hammack, J. Polymer Sci. B3, 655 (1965).

38. J. J. Lohr, Trans. Soc. Rheology 9, 65 (1965).

39. J. A. Roetling, Polymer 6, 311 (1965).

40. D. H. Kaelble, paper presented before Fourth International Congress on Rheology, Providence, Rhode Island, (1964).

41. T. L. Smith, J. Polymer Sci. 32, 99 (1958).

Stress-Strain Properties vs. Temperature

△ PS - Polystyrene
● PMMA - Polymethyl methacrylate
○ PC - Polycarbonate

FIG. 1

102

Strain Properties vs. Temperature

△ PS - Polystyrene
● PMMA - Polymethyl methacrylate
○ PC - Polycarbonate
ε_y^T Total strain at yield point
ε_y^P Plastic strain at yield point
$\varepsilon_{P.L.}^E$ Proportional limit strain

FIG. 2

103

Mechanical Damping vs.
Temperature Measured by Ball
Rebound Test

Temperature, (° C)

104   FIG. 3
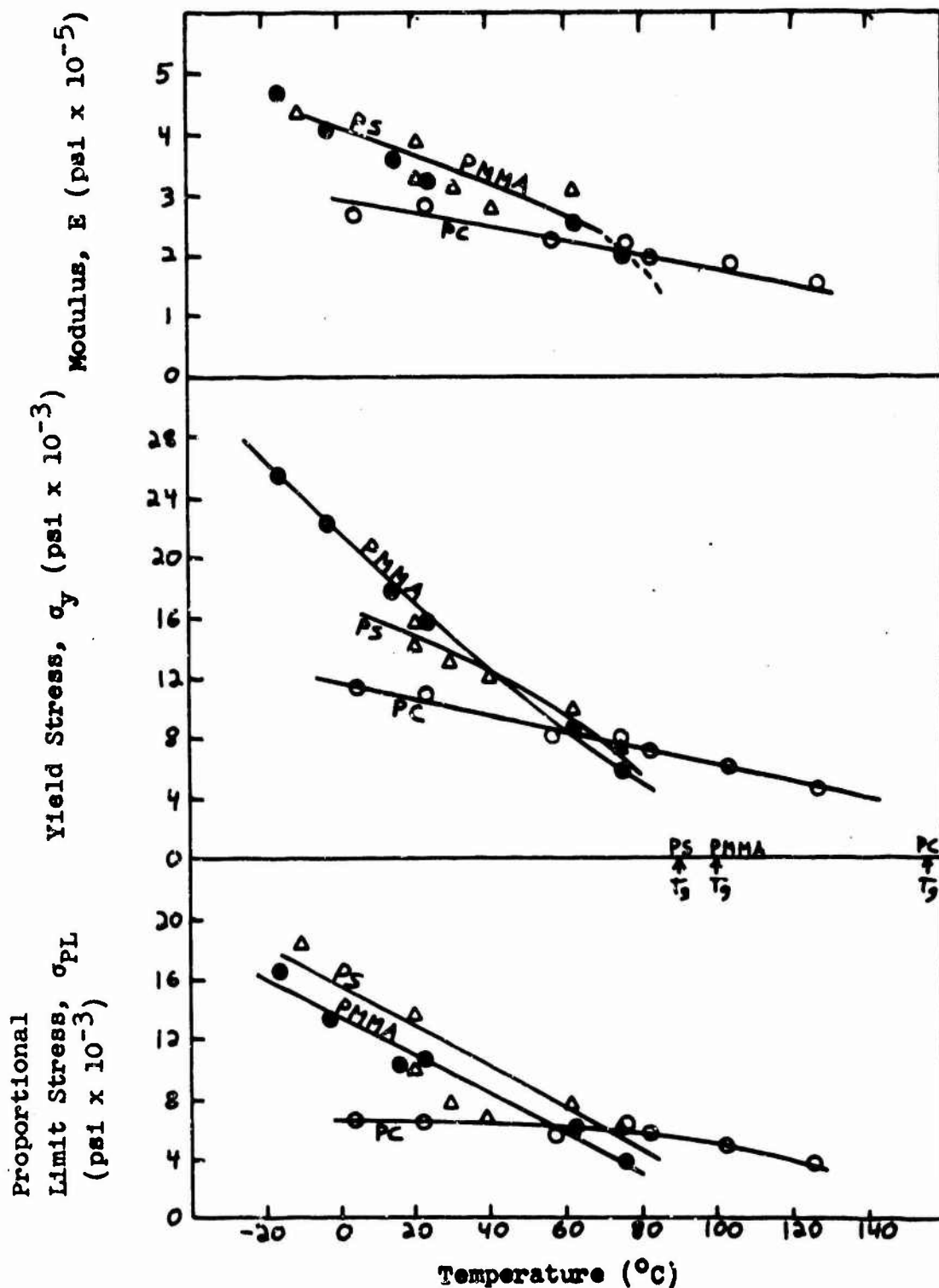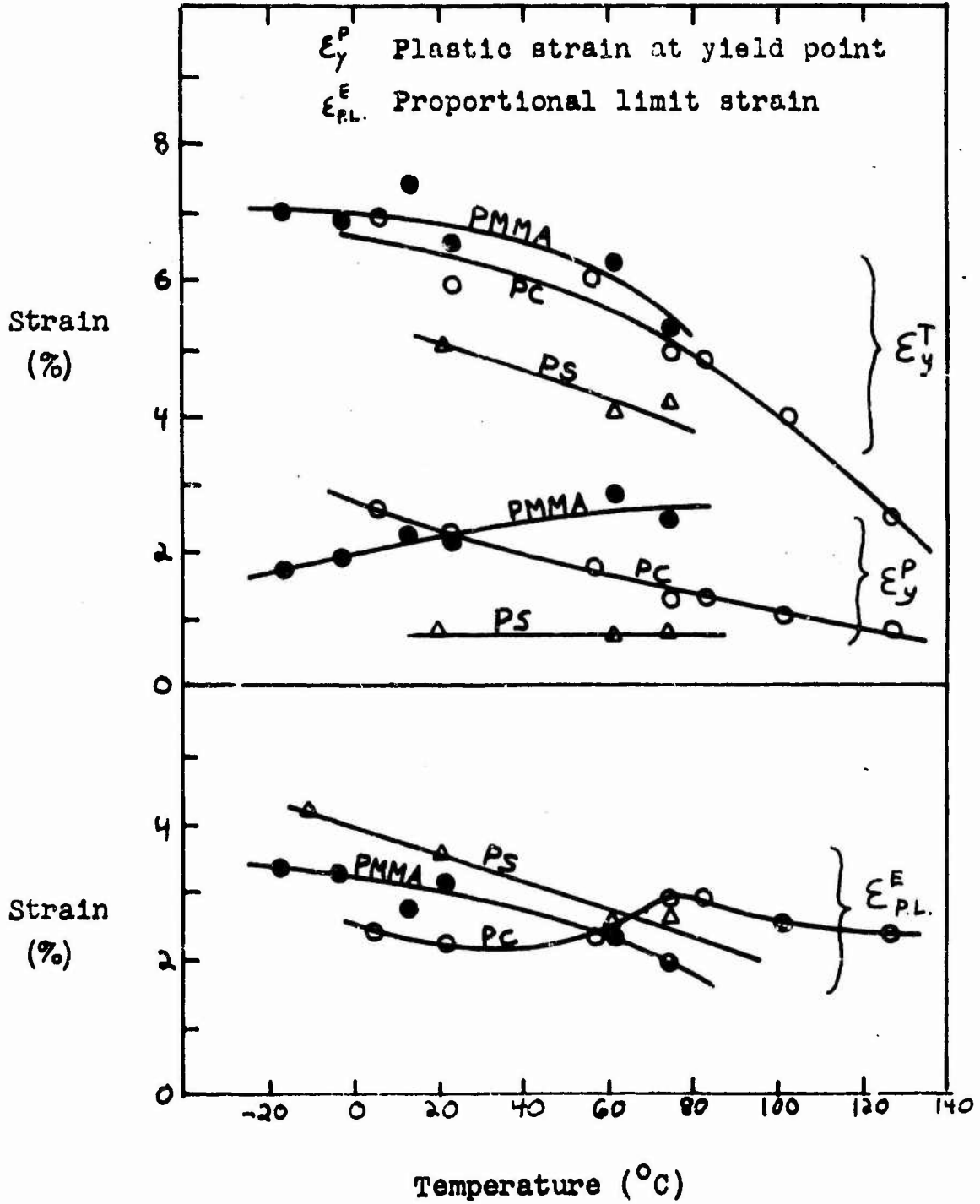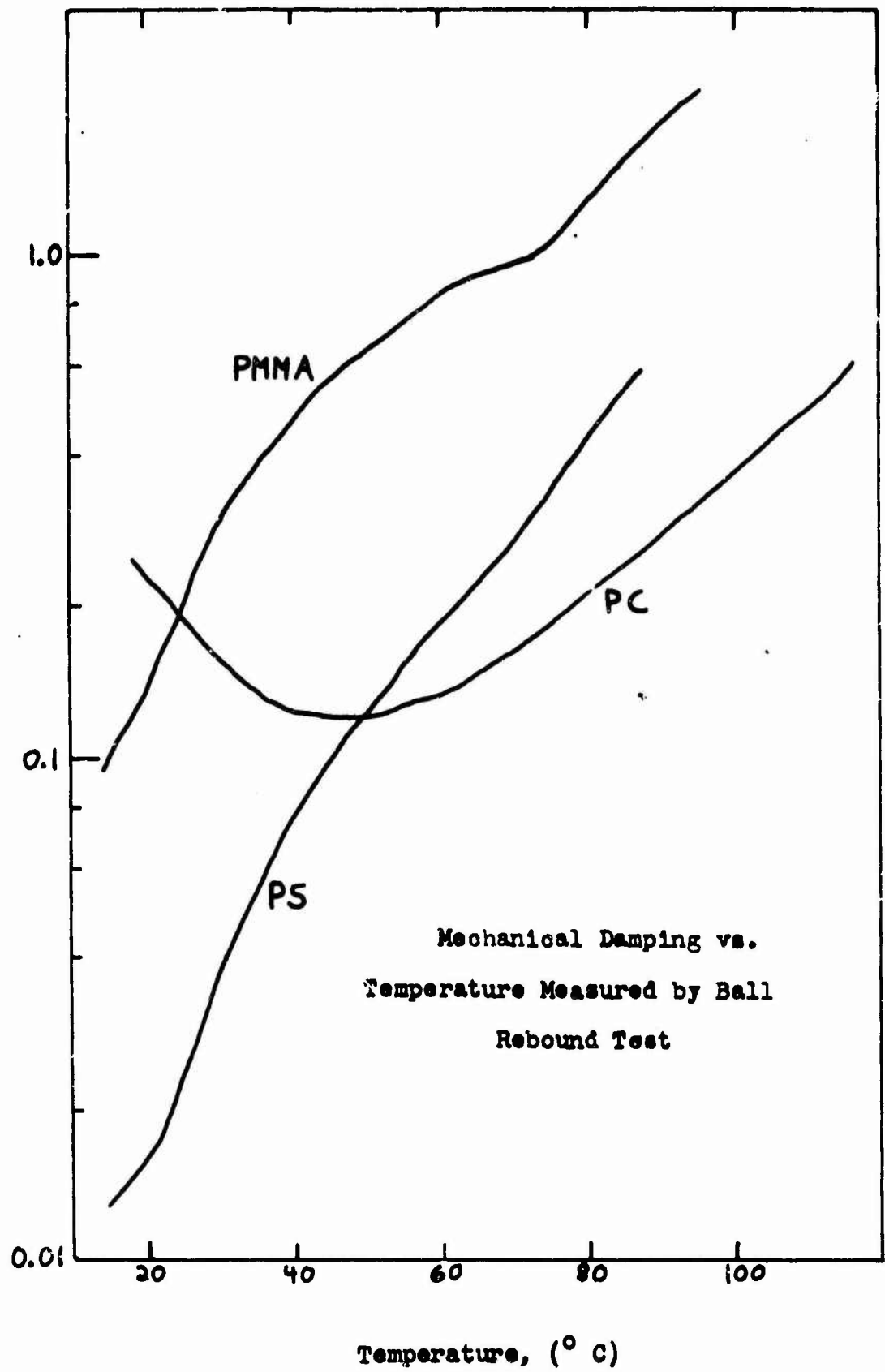
YIELD STRESS OF POLYSTYRENE vs. INCLINATION
BETWEEN STRESS AND ORIENTATION DIRECTIONS
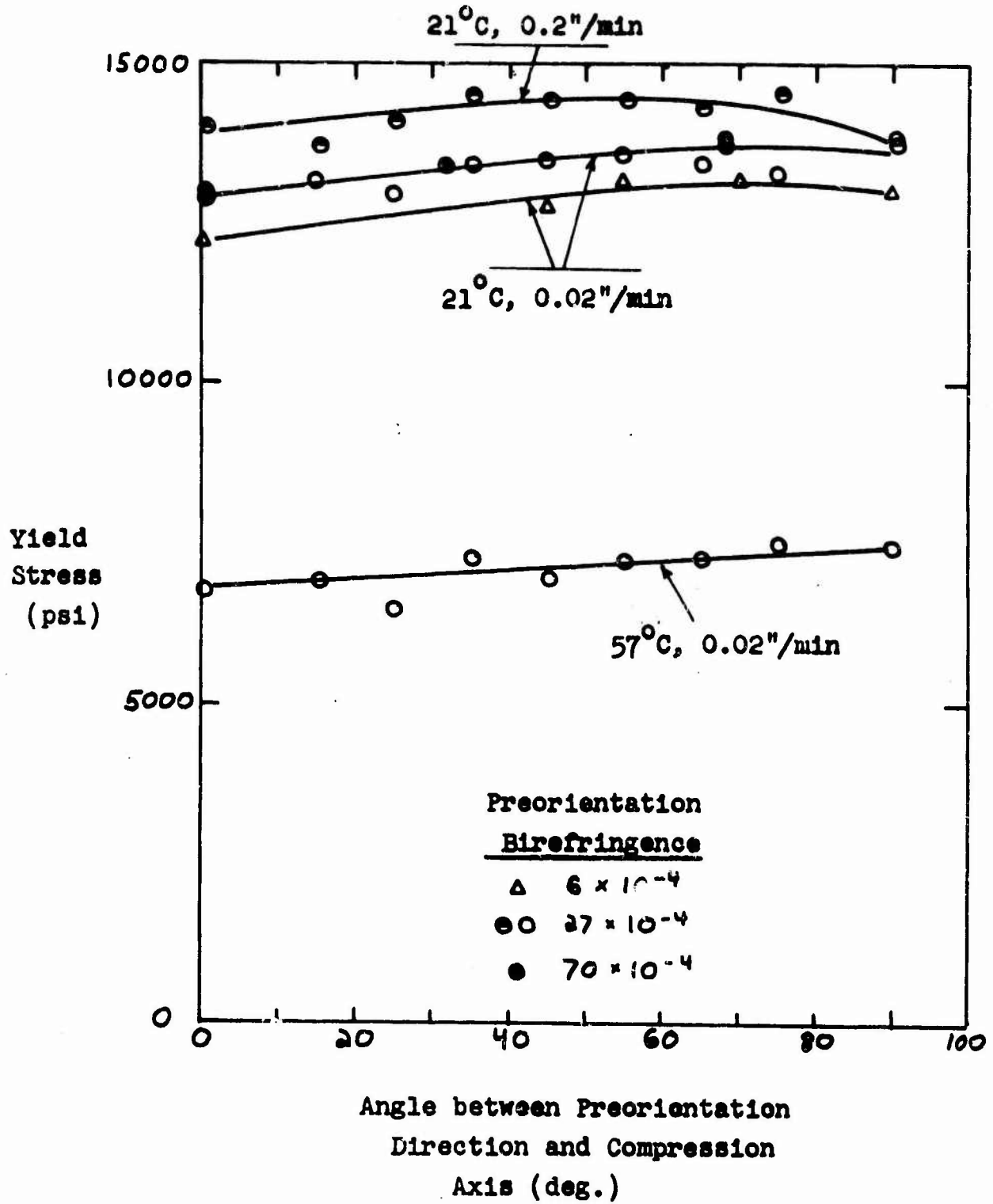
FIG. 4

Deformation Parameters vs. Inclination
Between Stress and Orientation Directions

POLYSTYRENE
$\Delta n_c = 27 \times 10^{-4}$

Total Strain @ Yield (%)

Plastic Strain @ Yield (%)

Modulus $(psi \times 10^{-5})$

Angle (deg.)
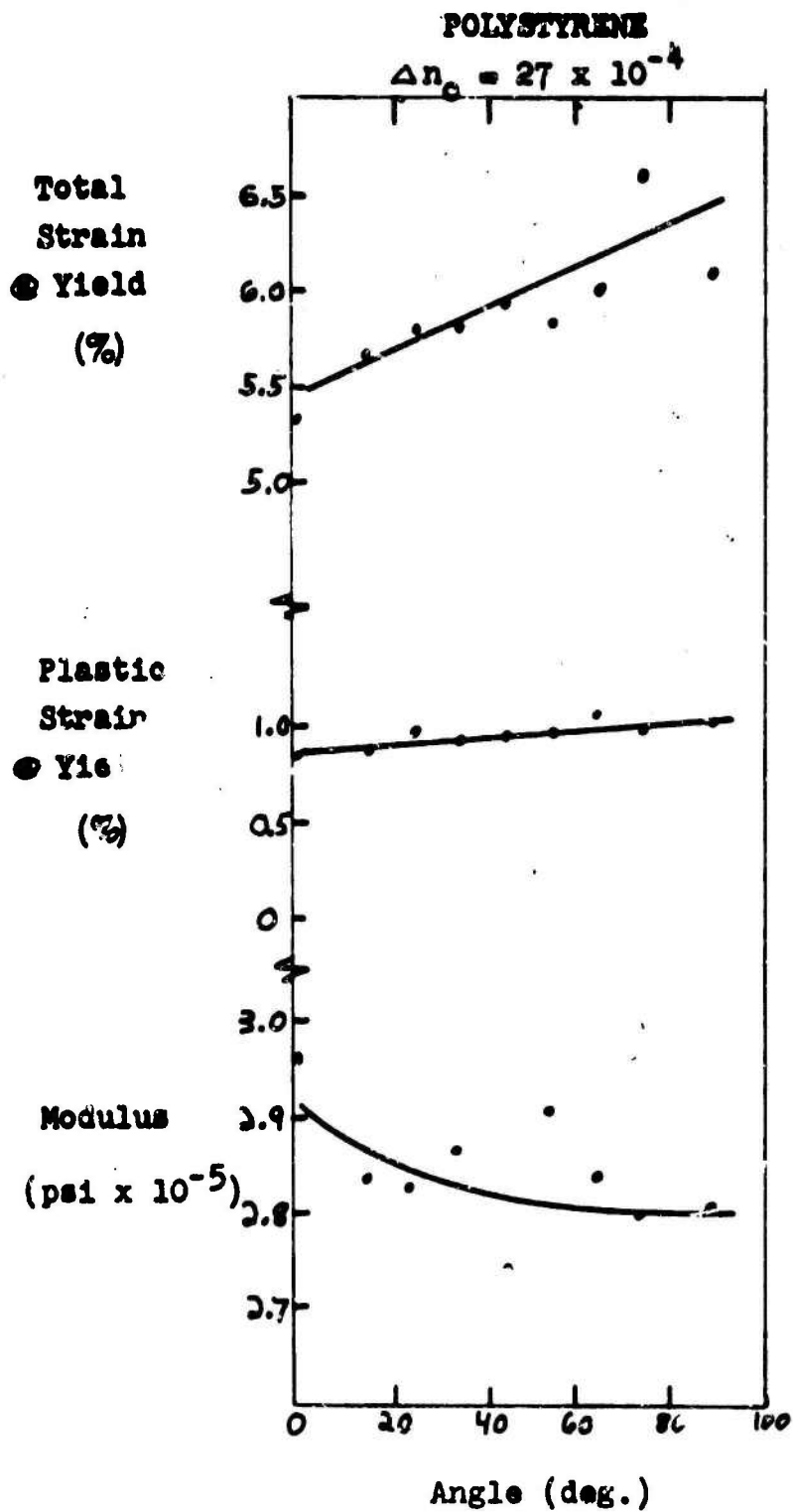
FIG. 5
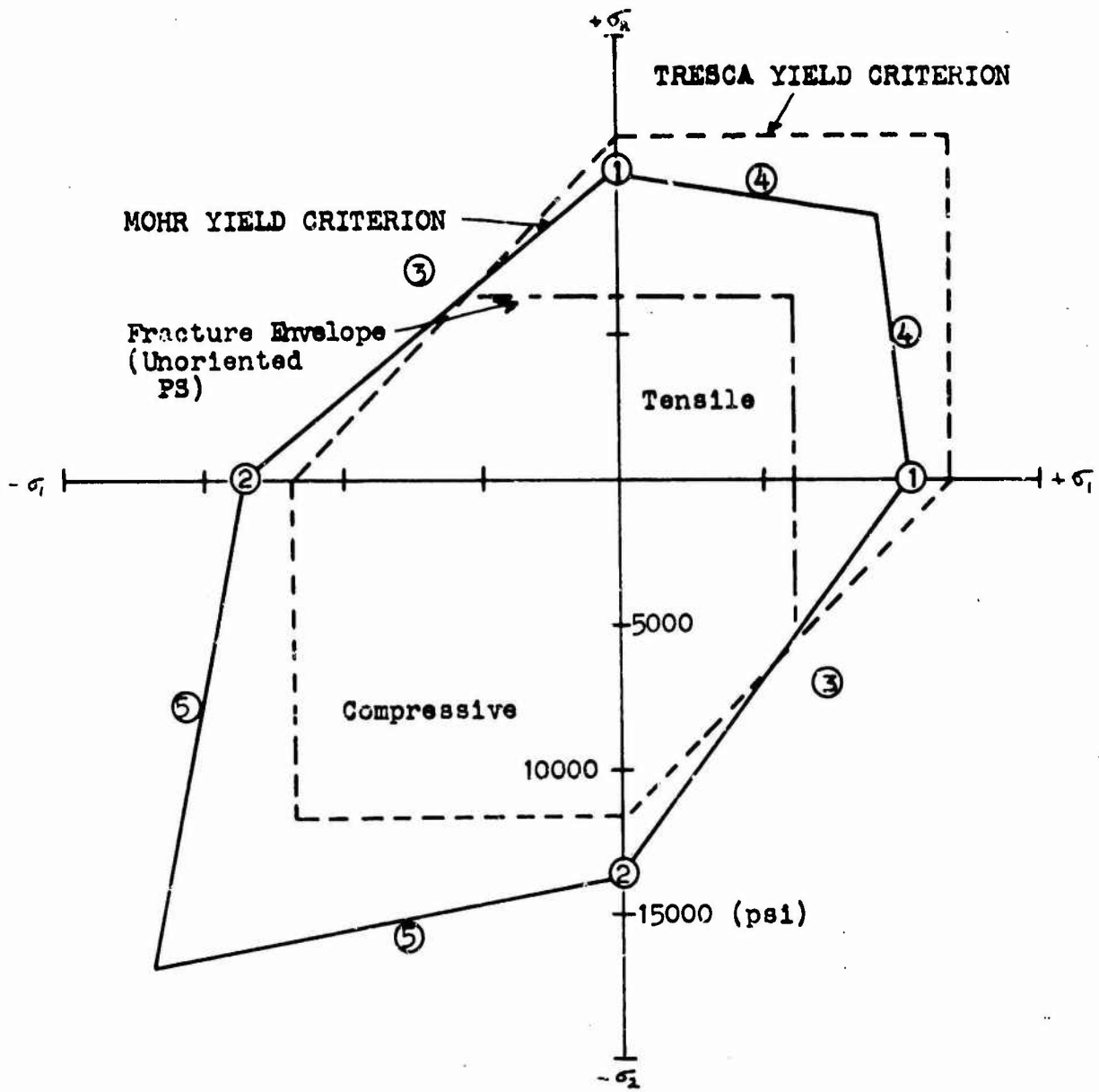
YIELDING OF POLYSTYRENE

FIG. 6

107
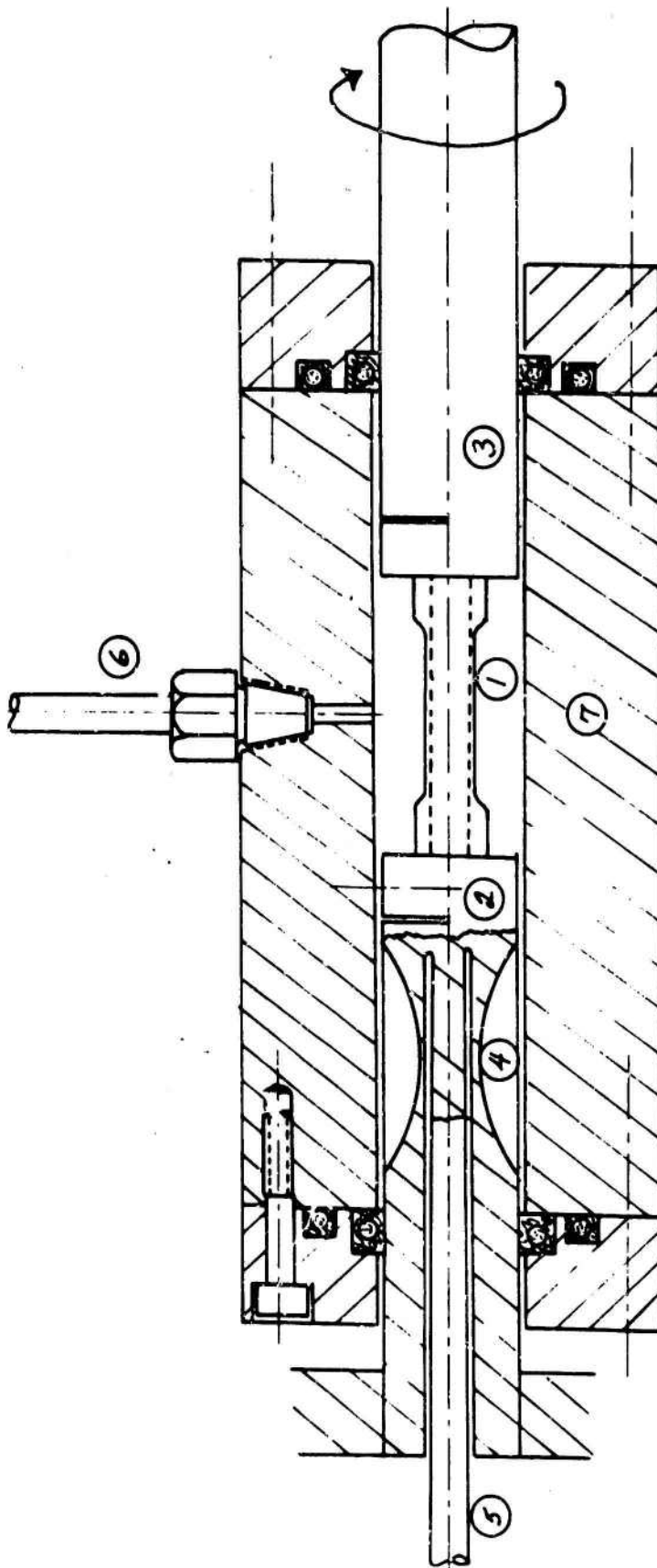
PRESSURE CHAMBER.

FOR

TORSION

EXPERIMENTS

FIG. 7

SEQUENTIAL STRESS RELAXATION OF POLYSTYRENE

POLYSTYRENE
Compression

Modulus
3.4×10^5 psi
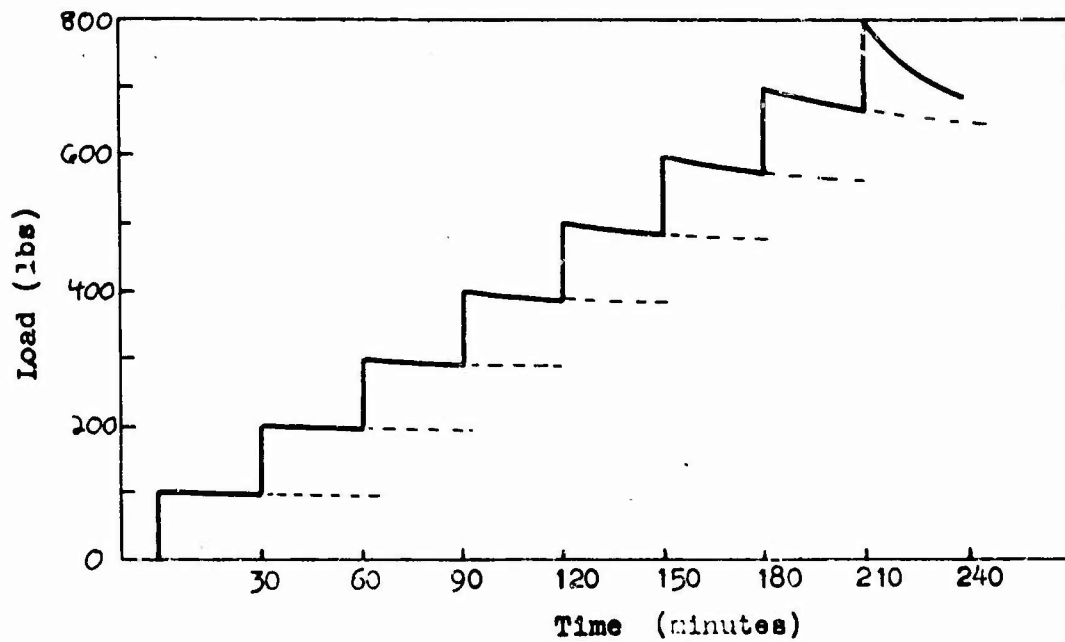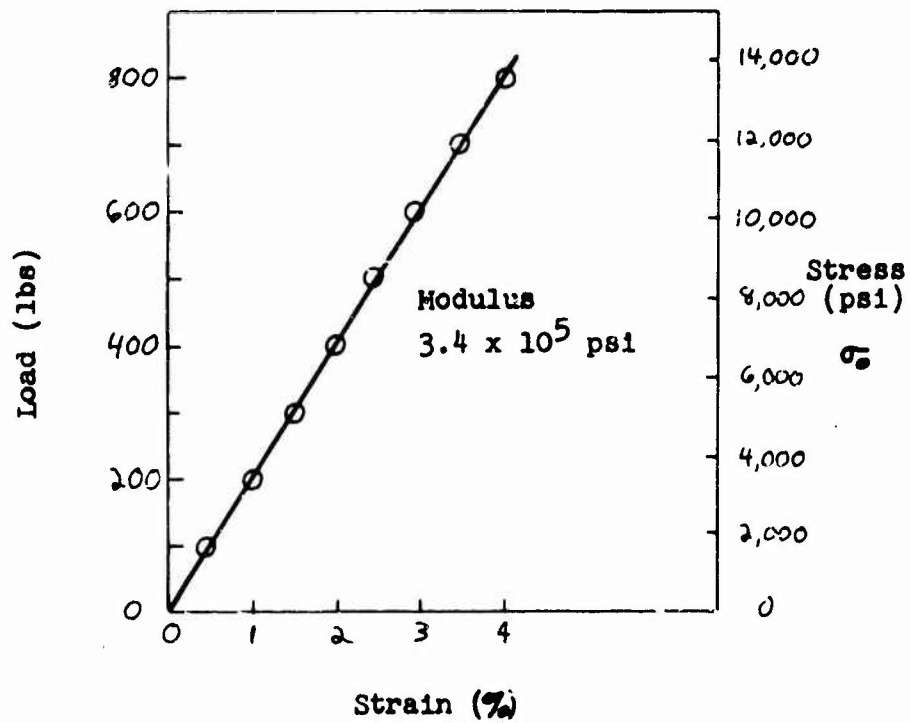
FIG. 8

STRESS RELAXATION OF POLYSTYRENE IN COMPRESSION

$\sigma_0 = 3370$ psi

$\sigma_0 = 10,150$ psi

$\sigma_0 = 11,740$ psi

$\sigma_0 = 13,550$ psi

Time (min)

STRESS RATIO $\sigma(t)/\sigma_0$
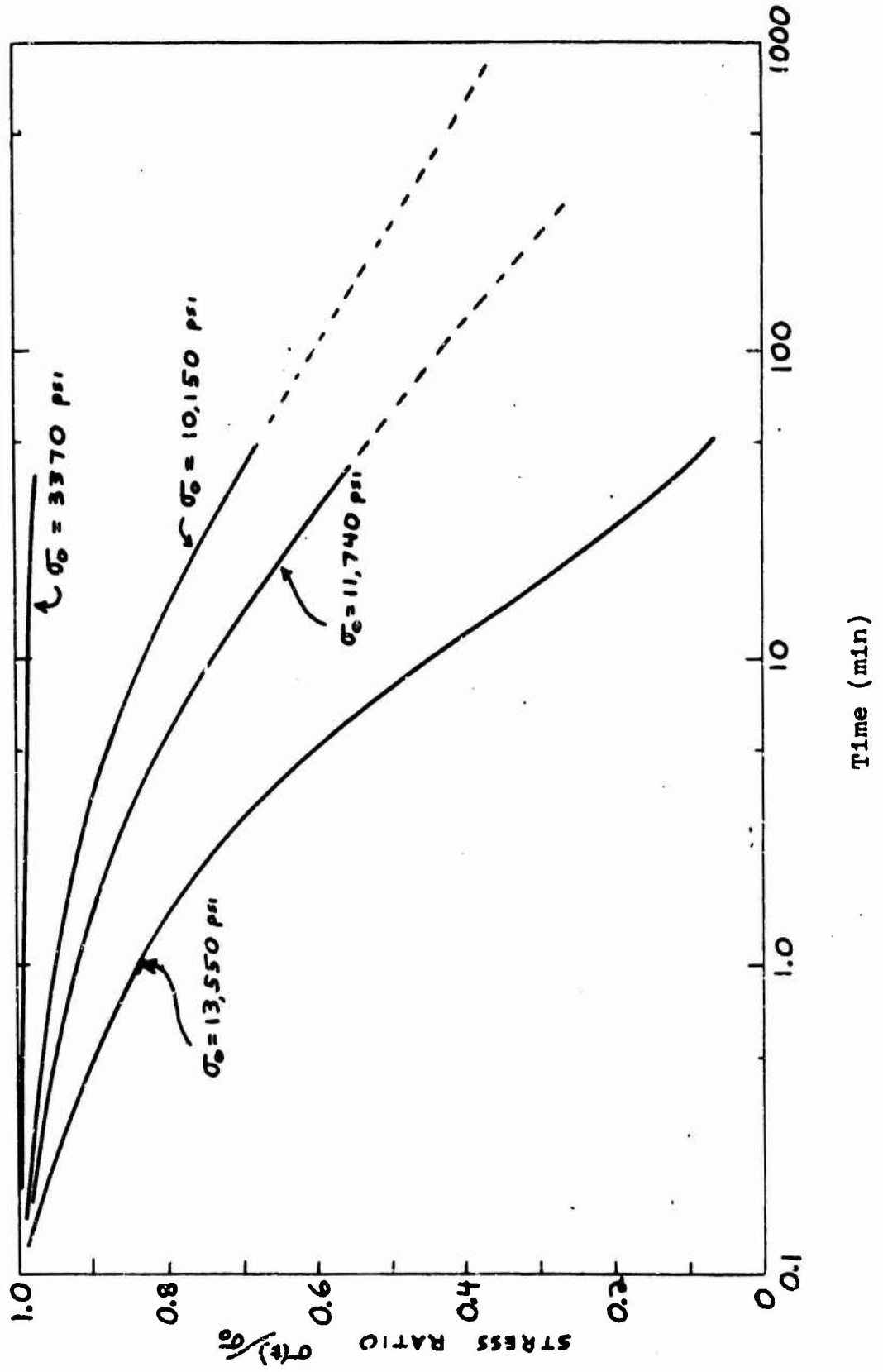
FIG. 9

STRESS-TIME BEHAVIOR IN VARIOUS TYPES OF TEST
OF POLYSTYRENE IN COMPRESSION AT ROOM TEMPERATURE
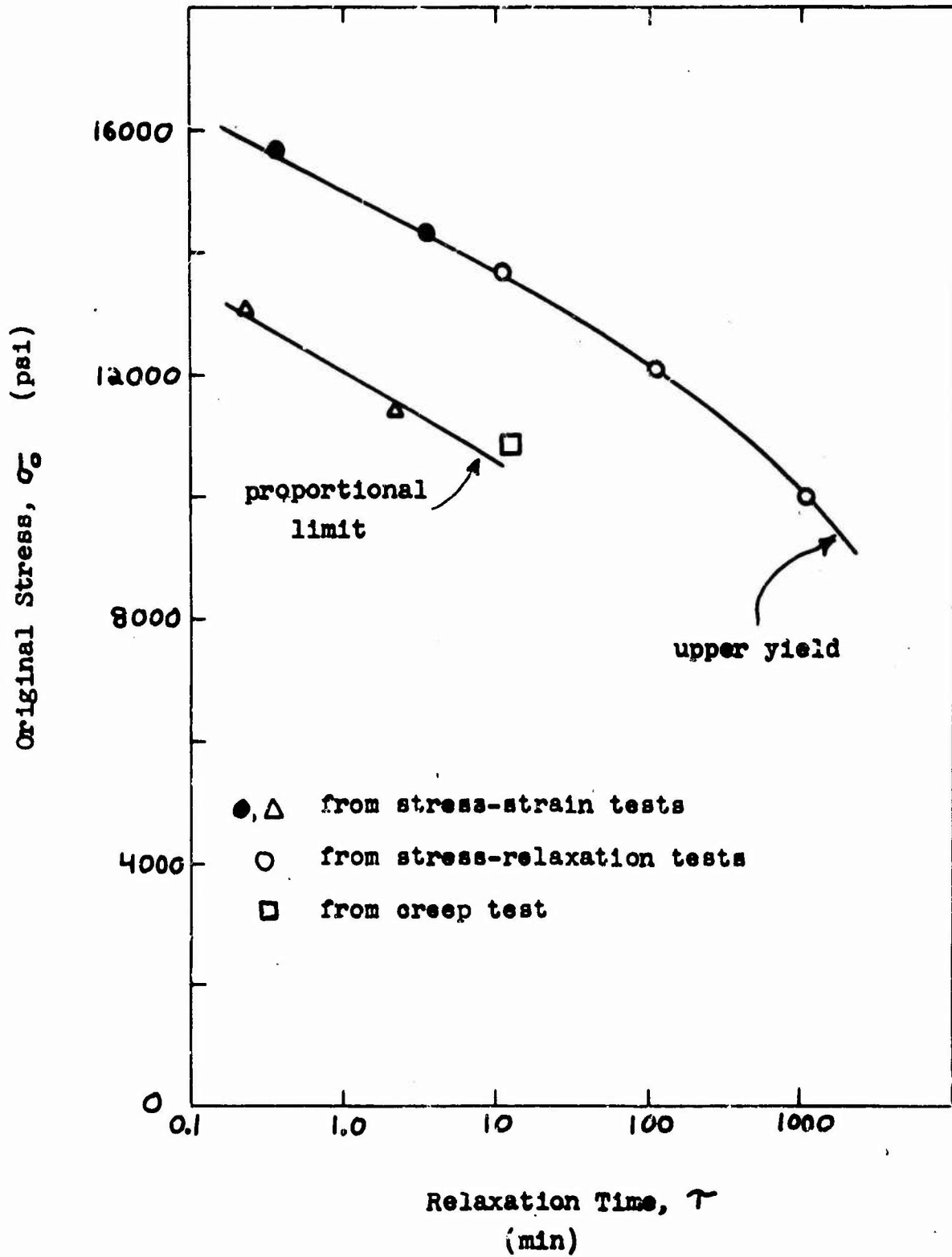
FIG. 10

STRESS RELAXATION OF POLYSTYRENE FILM

AT ROOM TEMPERATURE

Stress

Ratio

$\dfrac{\sigma(t)}{\sigma_o}$

$\sigma_o = 2200$ psi

$\sigma_o = 4430$ psi

$\sigma_o = 6200$ psi

Time (min)

FIG. 11

112
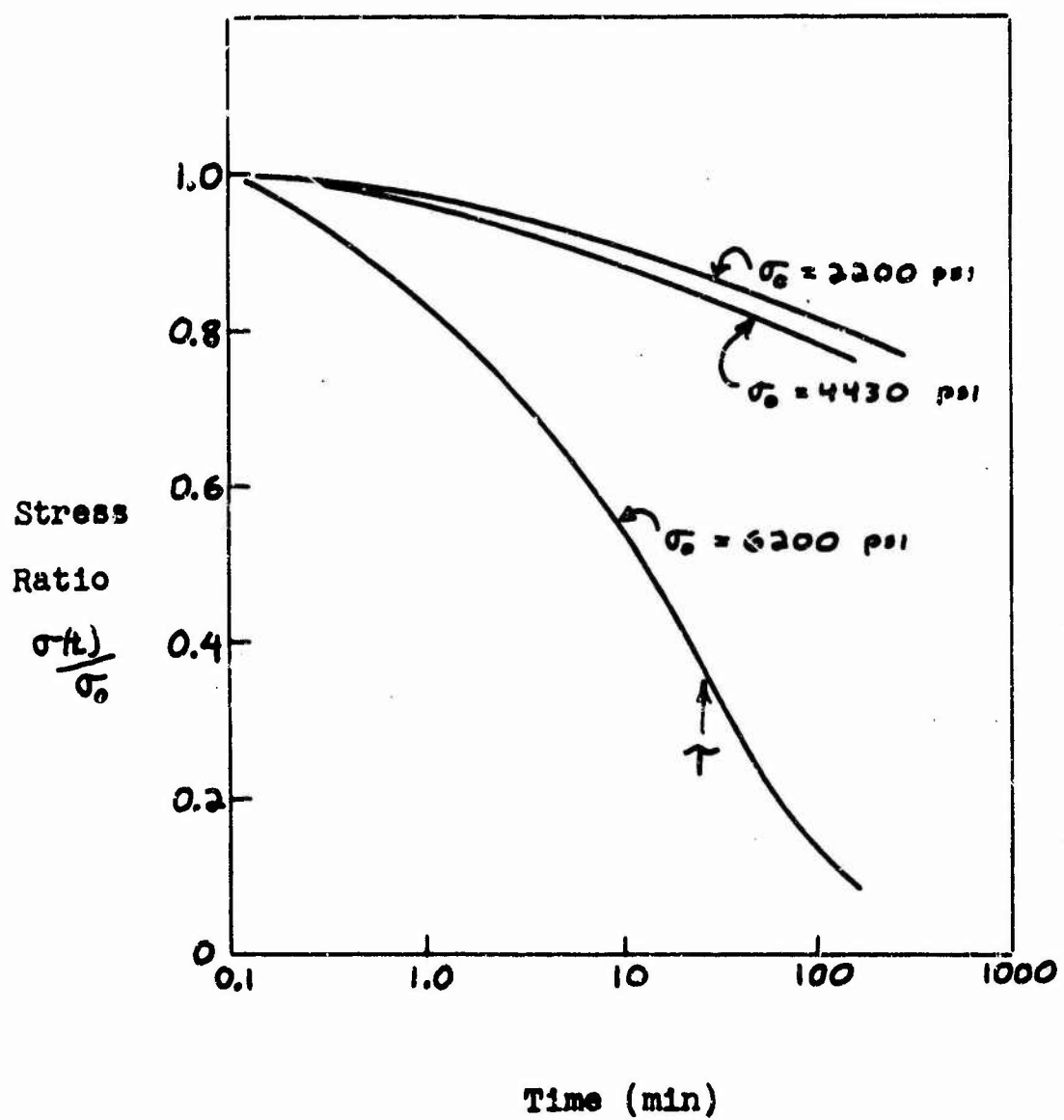
INTERRUPTED DRAWING OF POLYMERS (Schematic)
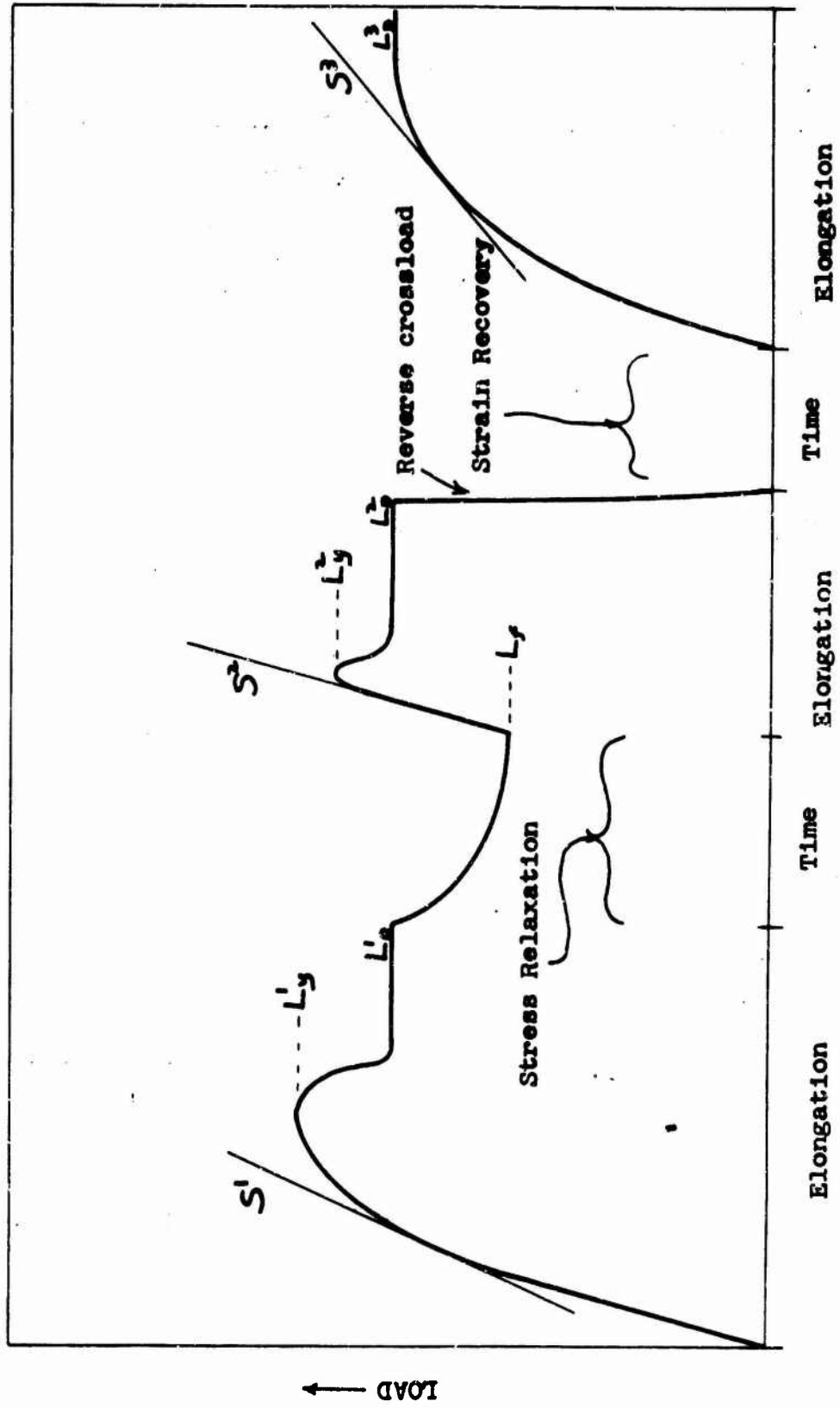
FIG. 12

113

REAPPEARANCE OF YIELD DROP AFTER VARIOUS TIMES OF
STRESS·RELAXATION IN INTERRUPTED DRAWING OF FORMVAR
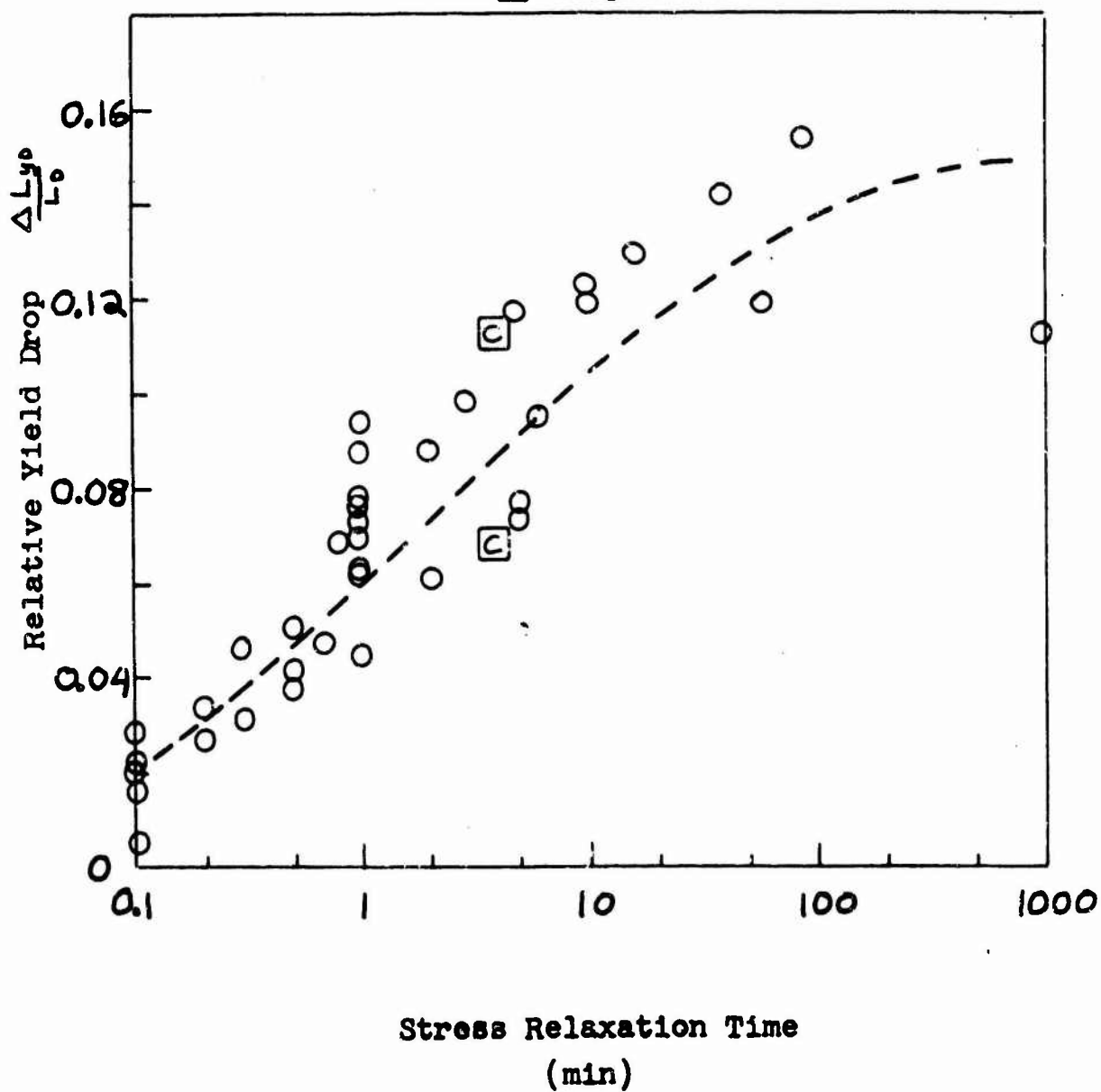
FIG. 13

REAPPEARANCE OF YIELD DROP AFTER VARIOUS TIMES OF
STRESS RELAXATION IN INTERRUPTED DRAWING OF NYLON
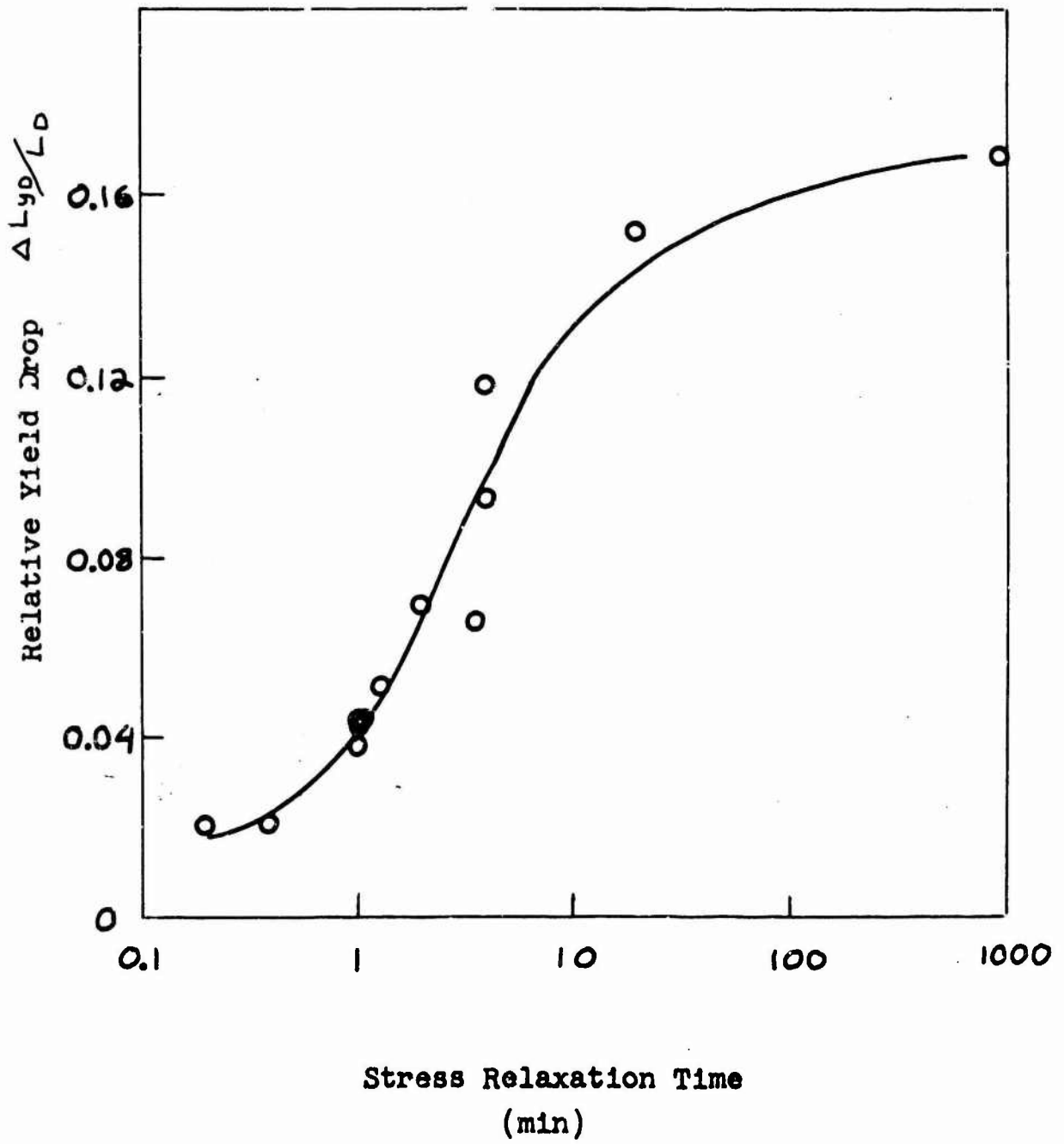
Stress Relaxation Time
(min)

FIG. 14

REAPPEARANCE OF YIELD DROP AFTER VARIOUS TIMES
OF STRESS RELAXATION IN INTERRUPTED
DRAWING OF LEXAN
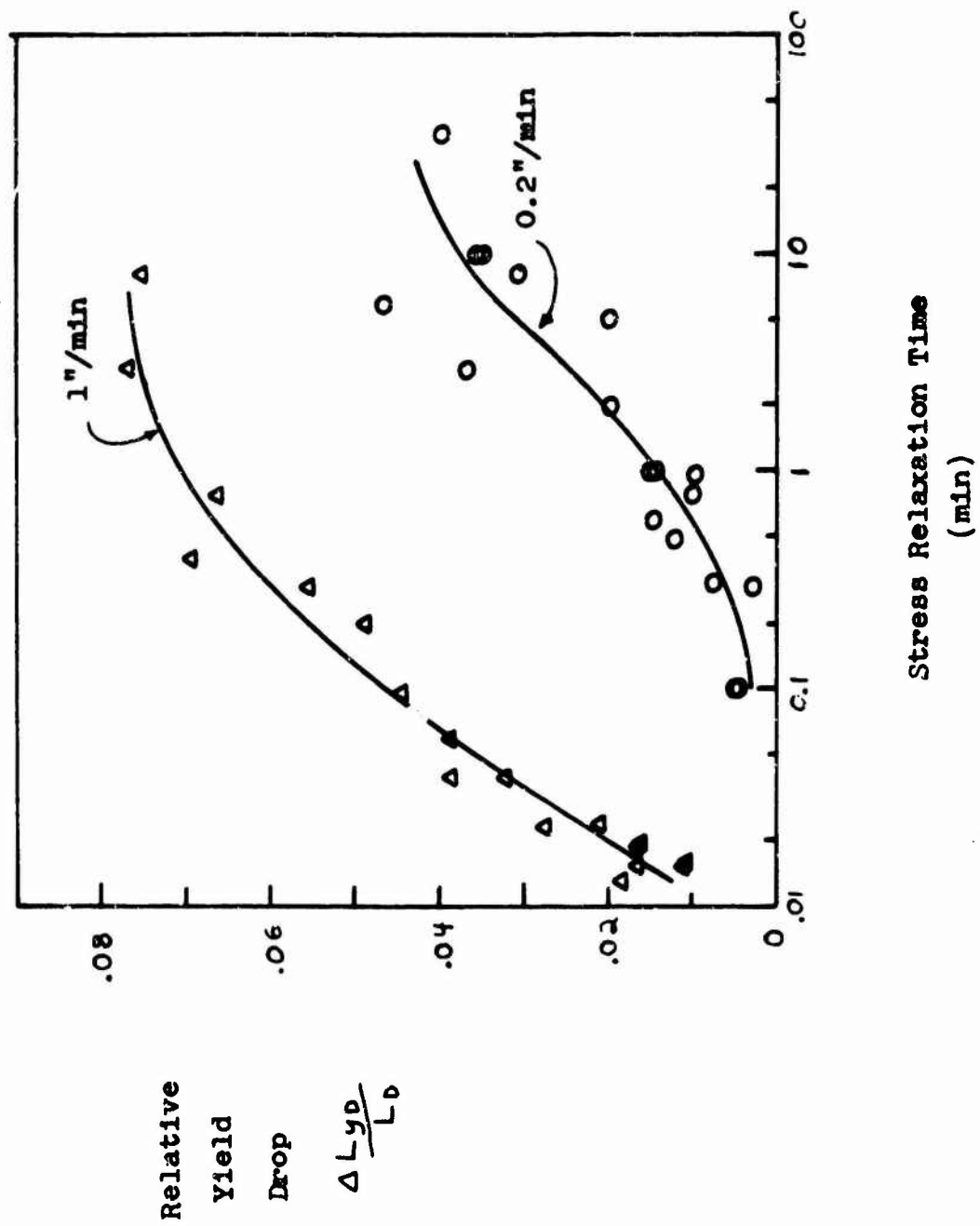
116   FIG. 15

REAPPEARANCE OF YIELD DROP AFTER VARIOUS TIMES OF
STRESS RELAXATION IN INTERRUPTED DRAWING OF SARAN

Stress Relaxation Time
(min)
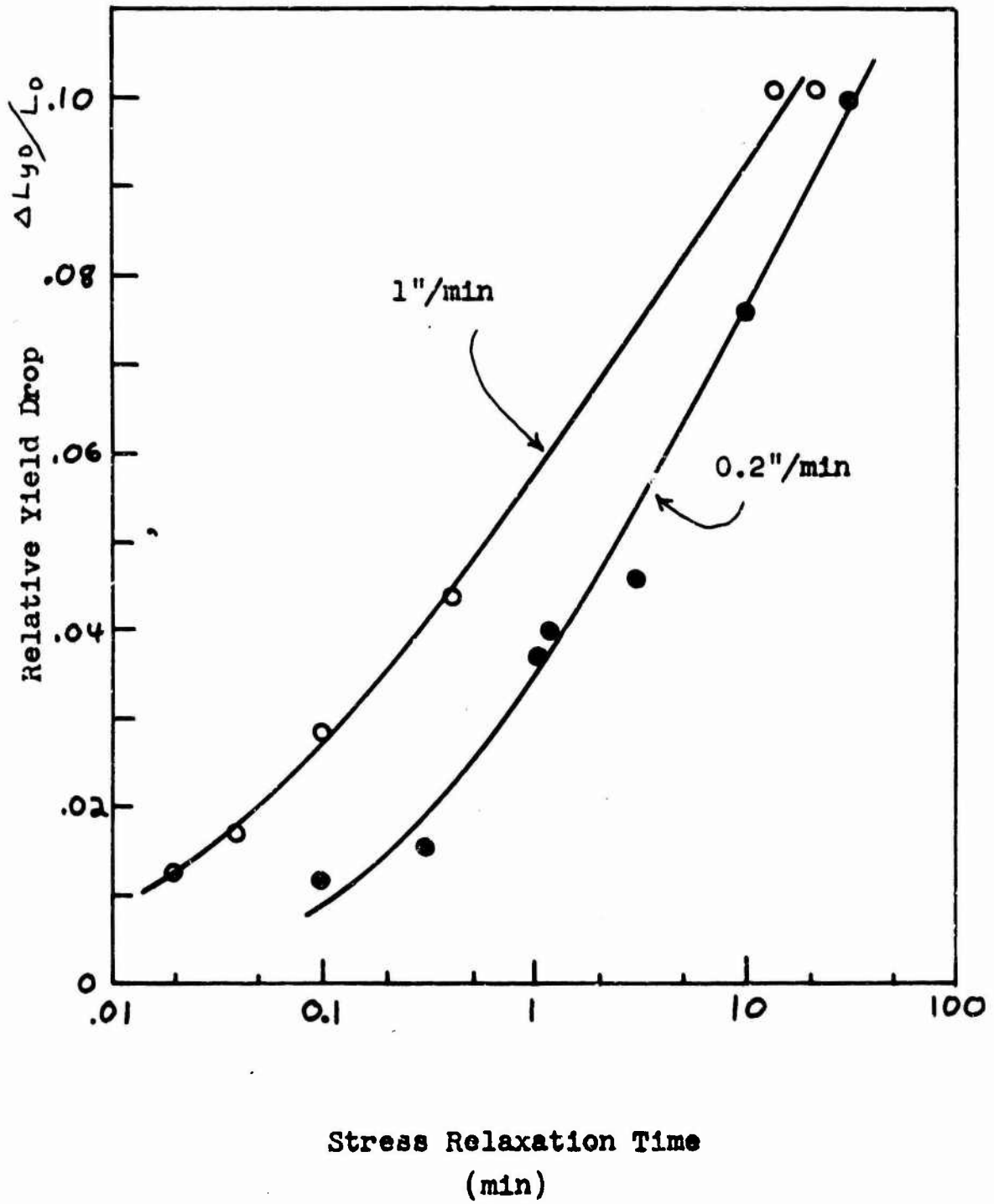
FIG.   16

ALTERNATING PERIODS OF DRAWING AND STRESS RELAXATION

SARAN

FIG. 17

118
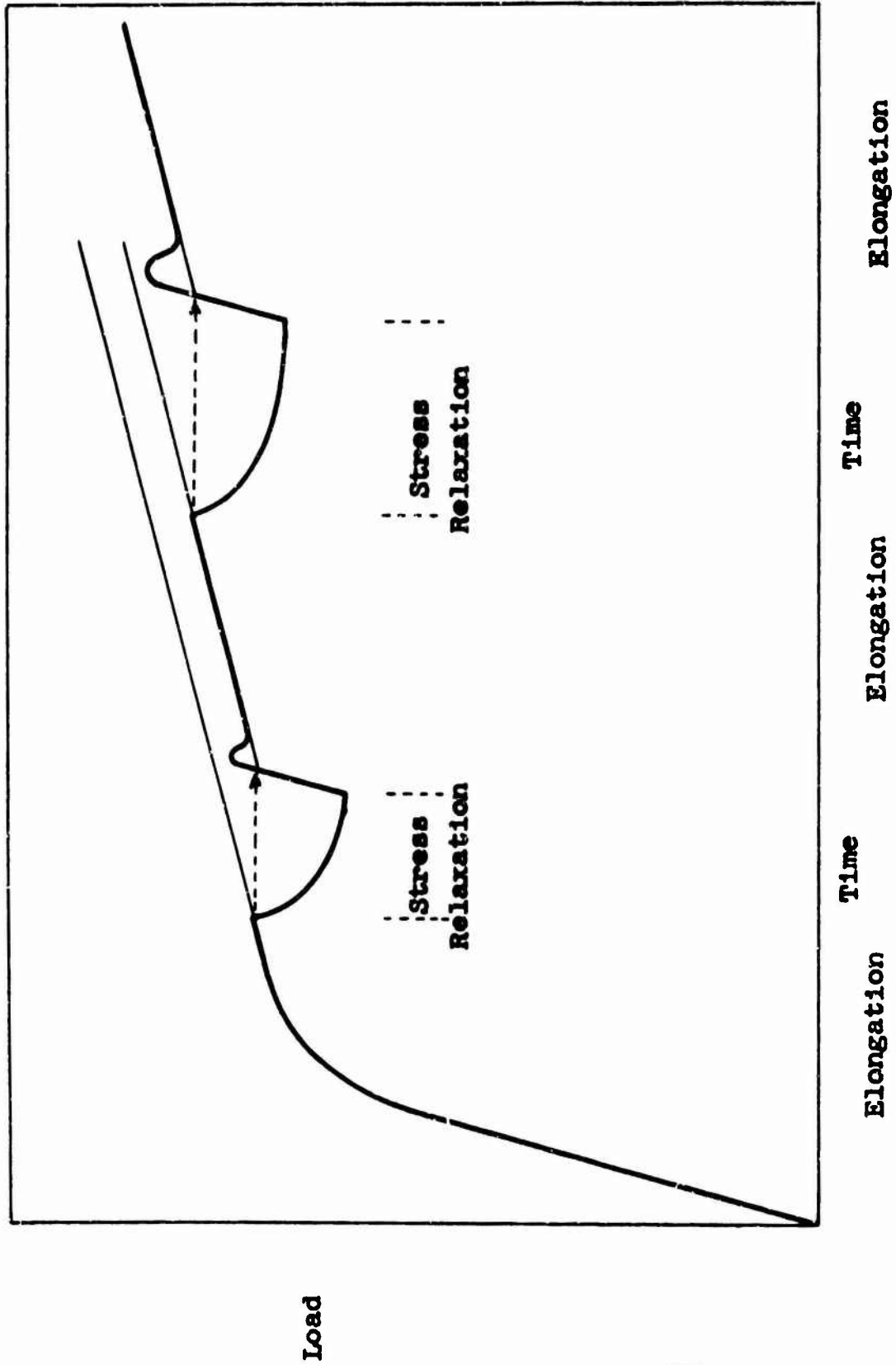
INTERRUPTED DRAWING WITH UNLOADING PERIOD

FORMVAR

Load
(lbs)

immediate
reload

reload after
20 min
at 0 Load

"Elongation" (inches)

"Bauschinger
elongation"
(inches)

Load (lbs)

FIG. 18

119
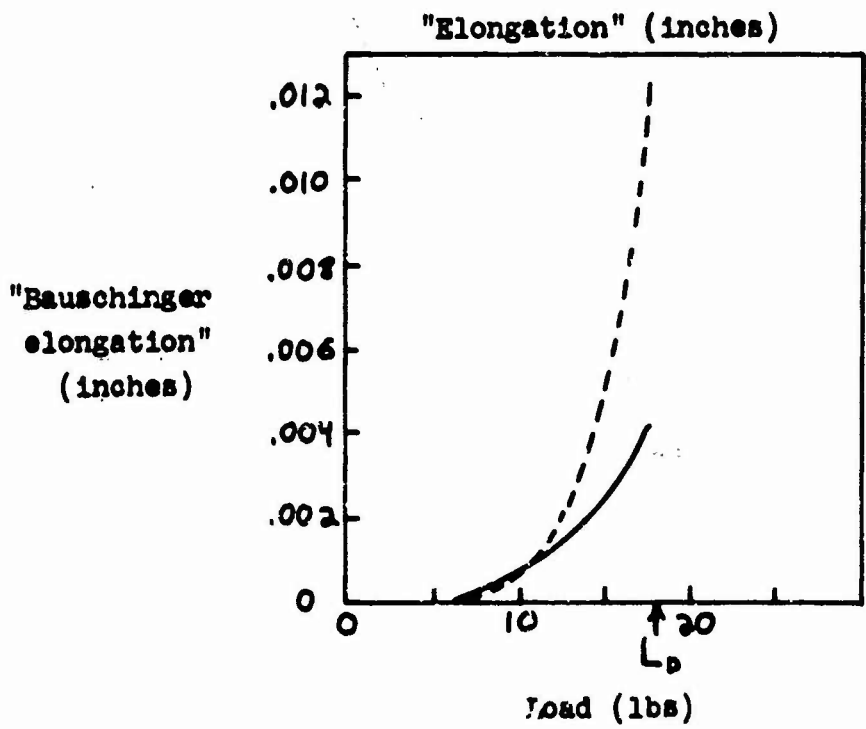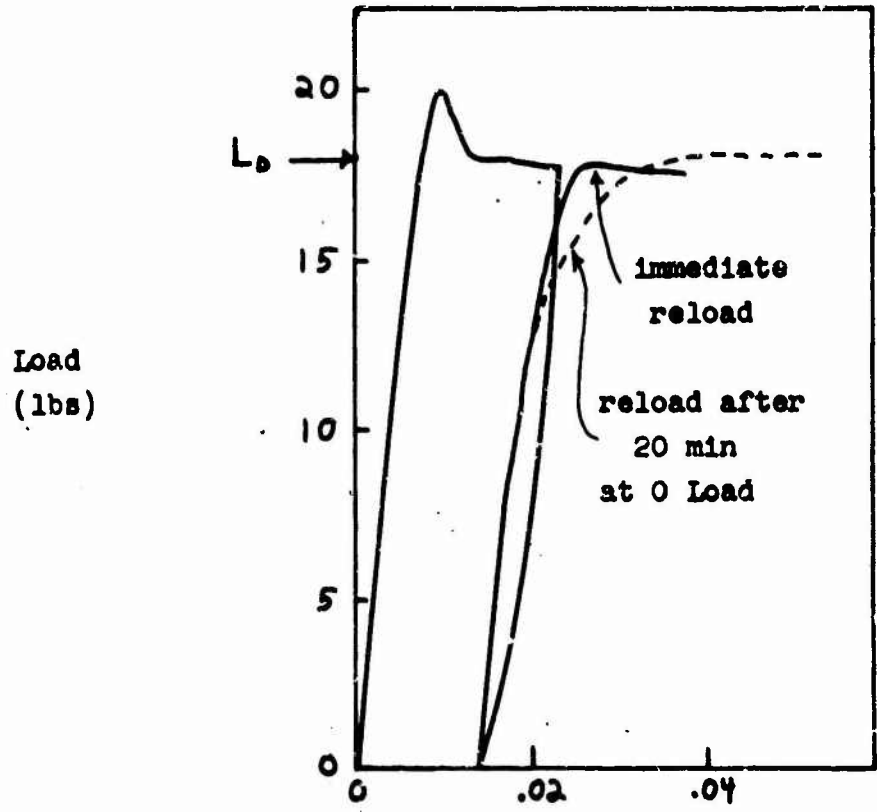
RELOADING SLOPES (S_3 of Fig. 14) vs. RECOVERY TIME

FIG. 19

120

RETRACTION UNDER ZERO LOAD AFTER DRAWING

FIG. 20

121
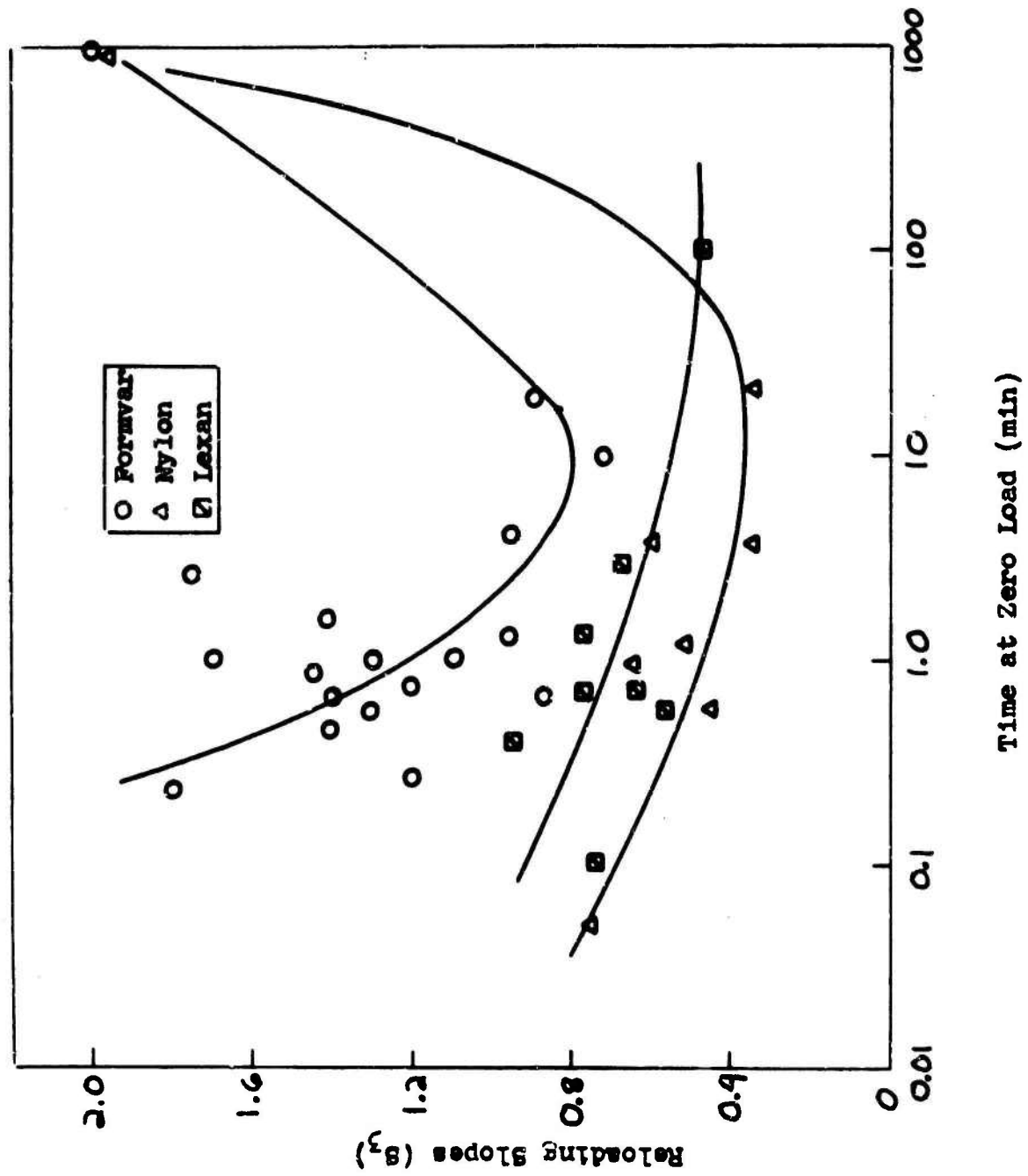
EFFECT OF COMBINED RELAXATION AND RECOVERY PERIODS
FORMVAR

FORMVAR

Load at Start of Stress Relaxation, L_o
(lbs)

FIG. 21

122
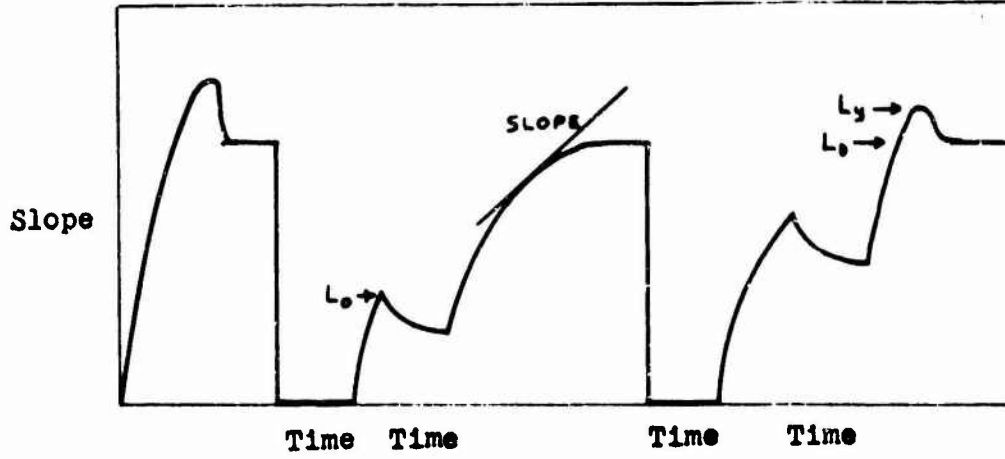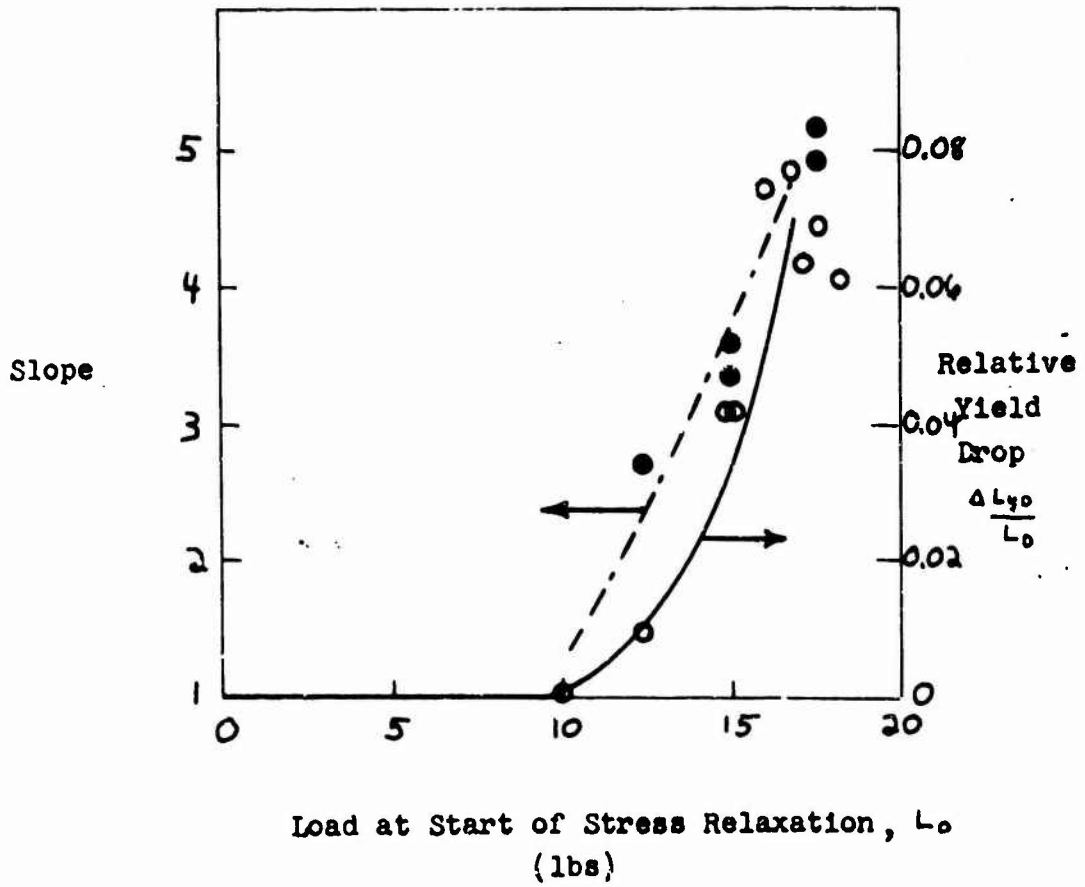
EFFECT OF COMBINED RELAXATION AND RECOVERY PERIODS
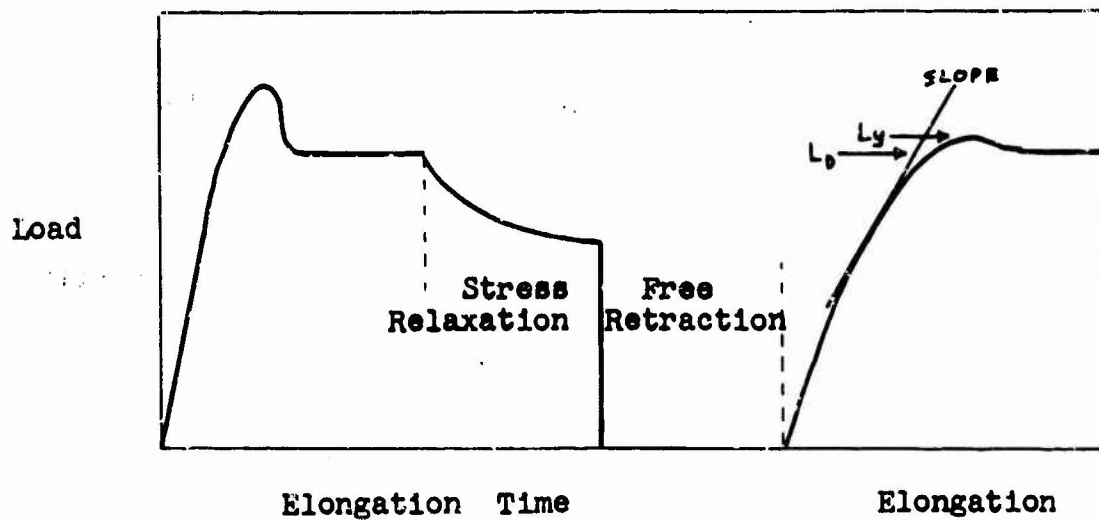
FORMVAR
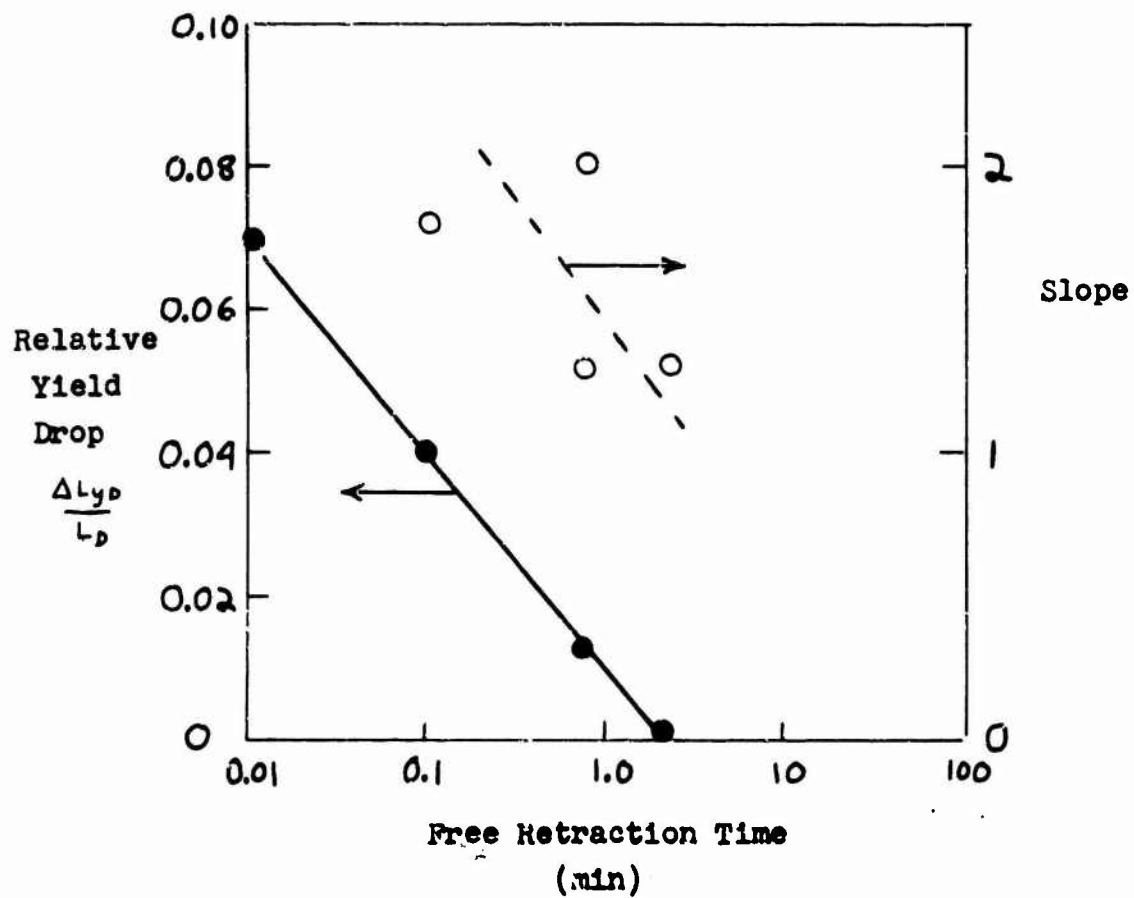
FIG. 22

Apparatus for Orienting Polymer Sheets

Upper Clamp

Heated Aluminum Plate

Polymer Sheet

Heated Aluminum Plate

Insulation

Table Top

Lower Clamp
mounted on
Sliding Plate

Track for Lower Clamp

FIG. 23

124

temperature
controller
air circulation

window
(rear and front)

specimen and
grips

heat exchanger

heater

blower

selector switch
for 6 thermo-
couples distri-
buted in box

recording drum

synchronous
motor

weights

frame

Apparatus for Creep Measurement
under Controlled Temperature

FIG. 24

125

TYPES OF ELONGATION VS. TIME CURVES OBSERVED
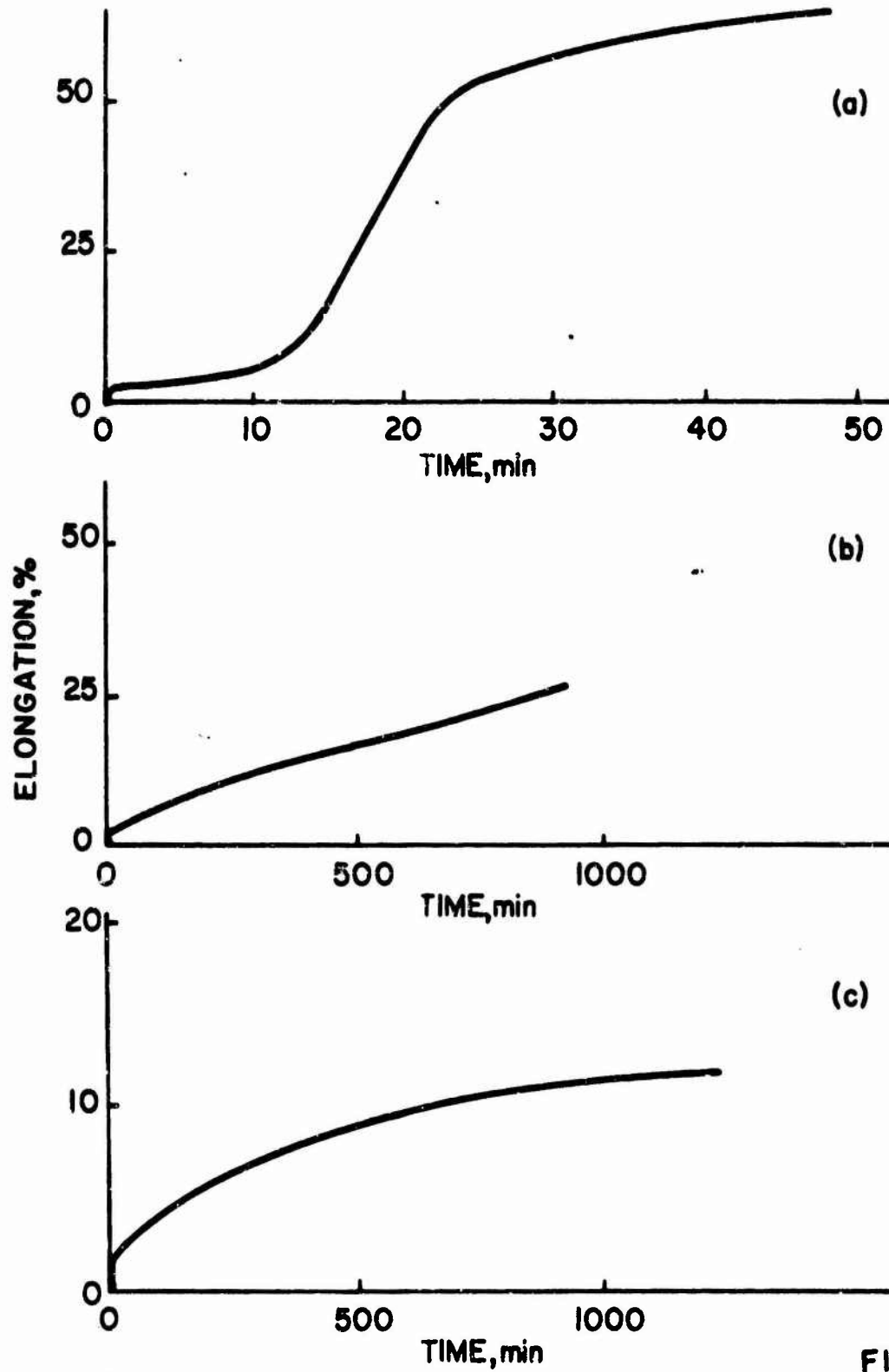
FIG. 25

CHARACTERISTIC PARAMETERS OF
DRAWING CURVES
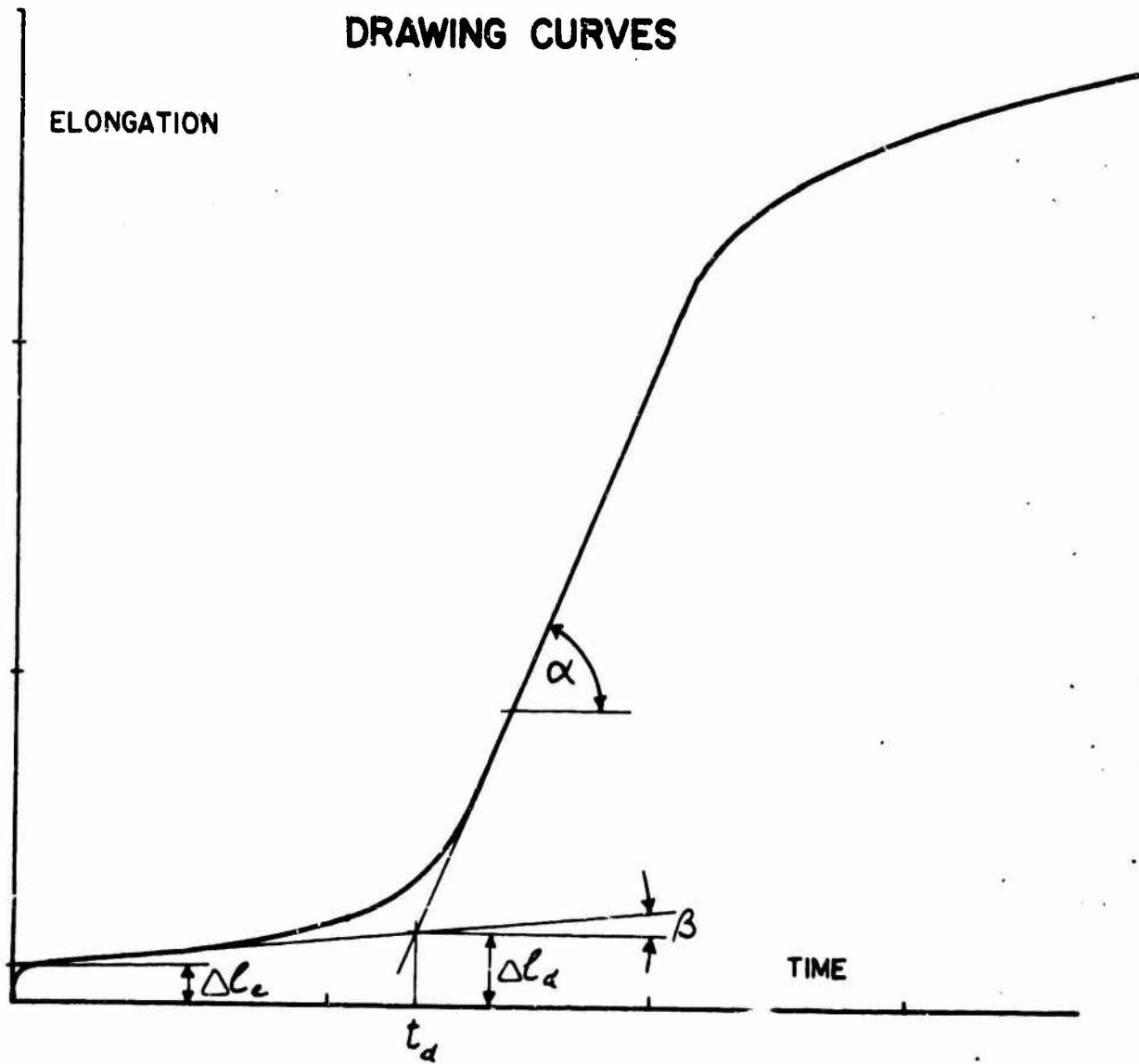
t_d = DELAY TIME

ε_d = DELAY STRAIN = $\Delta l_d / l_o$

ε_e = ELASTIC STRAIN = $\Delta l_e / l_o$

FIG. 26

127

DELAY TIMES AND REGIONS OF DEFORMATION TYPE
PREORIENTED POLYSTYRENE $\Delta n = 10 \cdot 10^{-3}$
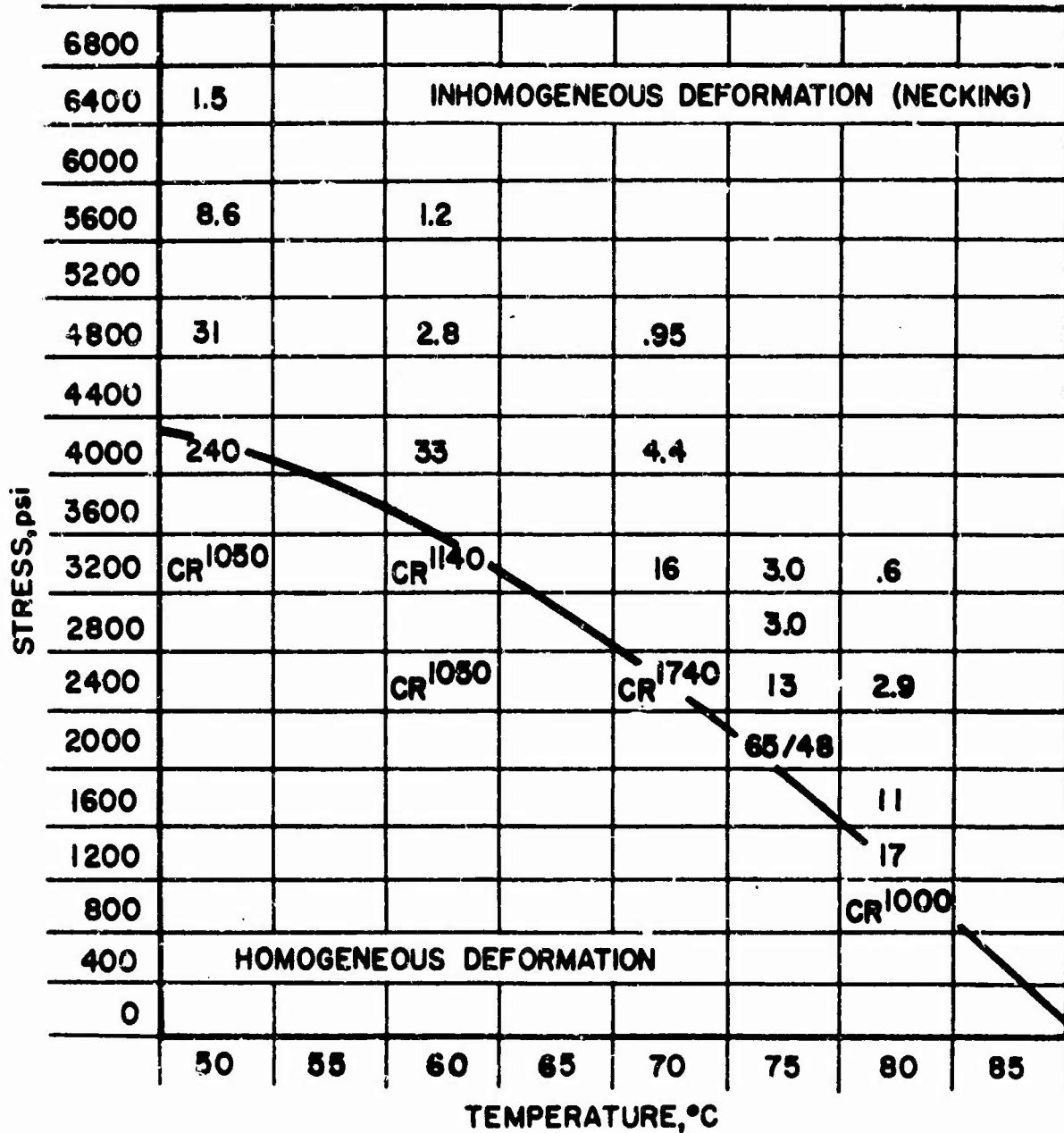
1. Delay times are listed in minutes.
2. CR^X indicates homogeneous deformation only was observed in an experiment
   lasting X minutes.

FIG. 27

DELAY ELONGATIONS (%) AND REGIONS OF DEFORMATION TYPE

PREORIENTED POLYSTYRENE
$(\Delta n = 10 \times 10^{-3})$

STRESS, psi								
6800								
6400	5.4		INHOMOGENEOUS DEFORMATION					
6000			(NECKING)					
5600	6.1		4.8					
5200								
4800	7.6		7.6		5.0			
4400								
4000	13.0		8.7		5.4			
3600								
3200	6.5 CR1050		20.6 CR1140		5.0		5.0	
2800								
2400			7.6 CR1050		22.8 CR1740		4.8	
2000								
1600							8.7	
1200								
800							25.0 CR1740	
400		HOMOGENEOUS DEFORMATION						
0								

TEMPERATURE, °C

50 55 60 65 70 75 60 85
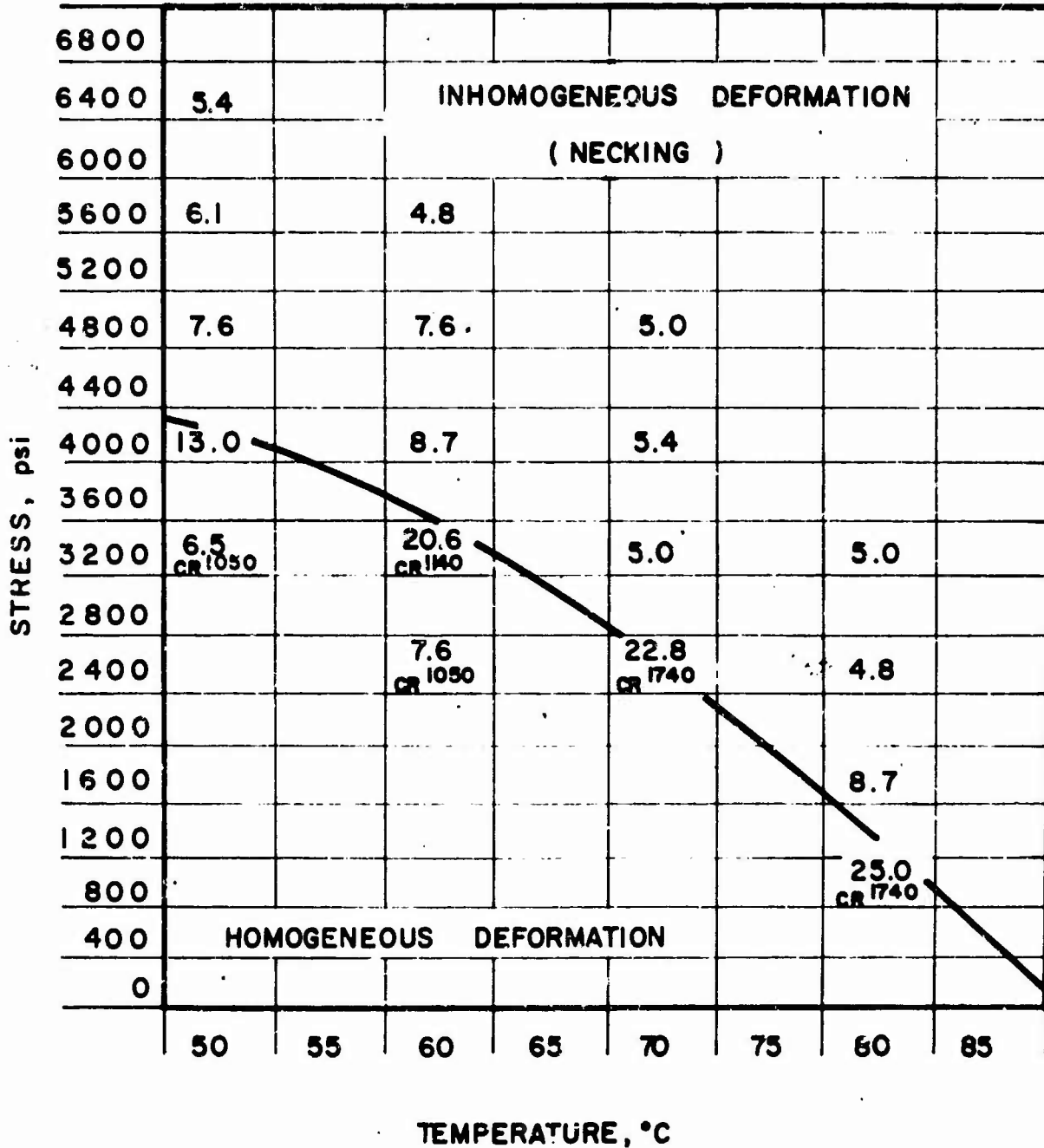
CR^x : elongation given was measured after x minutes of homogeneous drawing.

FIG. 28

129
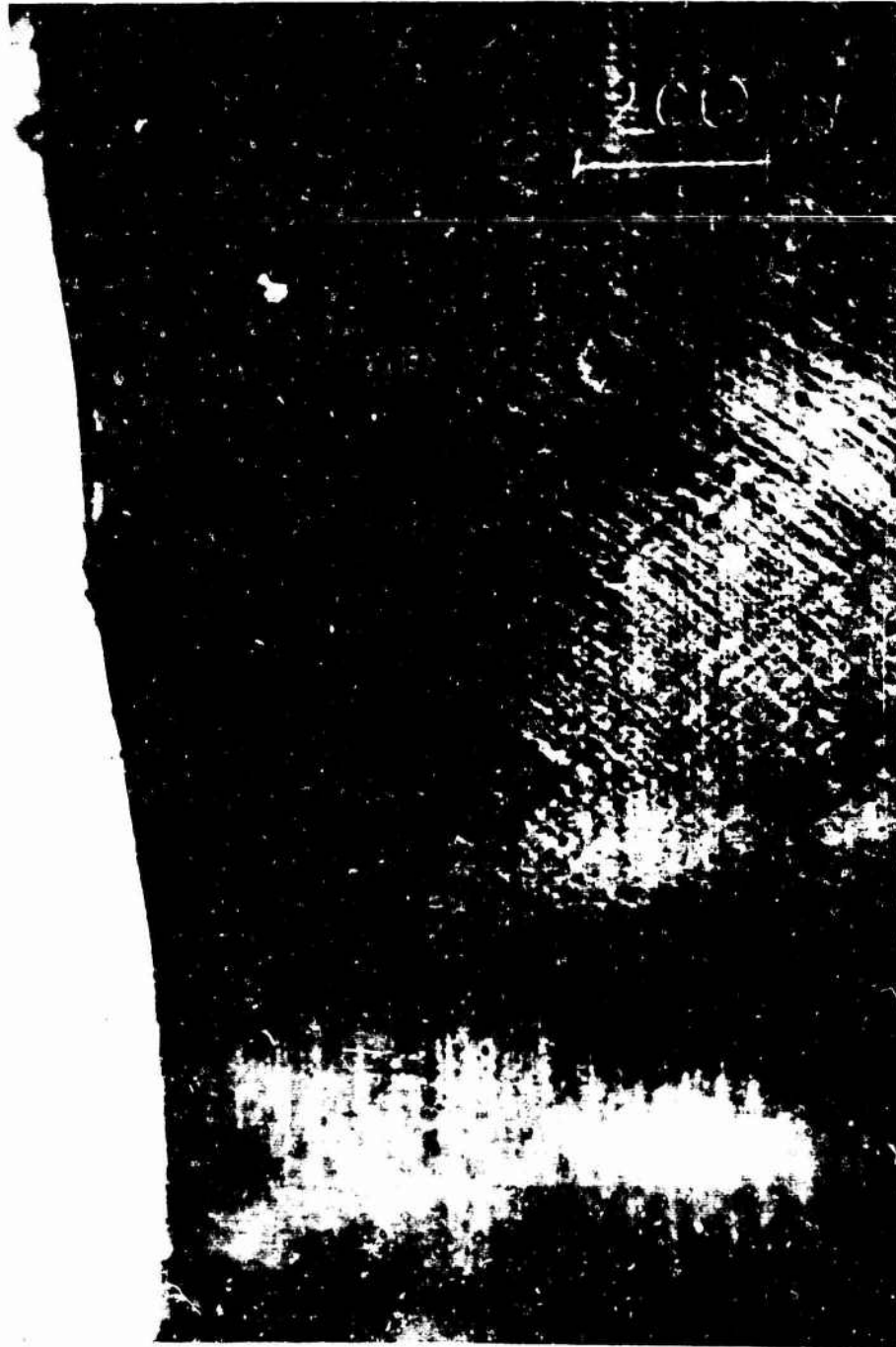
FIG. 29

SHEAR BAND FIELD IN NECK OF POLYSTYRENE

FIG. 30

DELAY TIMES AND REGIONS OF DEFORMATION TYPE
PMMA

STRESS, psi	50	60	70	80	90	100
7000						
6500		INHOMOGENEOUS DEFORMATION (NECKING)				
6000	64		0.7			
5500			1.4			
5000			6.7			
4500			18	0.4		
4000			44	4.8		
3500			168/780 4800	6.0	0.7	
3000			CR ^{4800}	62	2.1	0.3
2500				1400	4.4	1.5
2000				C R	166	4.1
1500					CR ^{1300}	55
1000						DR
500		HOMOGENEOUS DEFORMATION				CR ^{1000}
0						

TEMPERATURE, °C

1. Delay times are listed in minutes
2. CR^{x} indicates homogeneous deformation only was observed in an experiment lasting x minutes
3. DR indicates drawing was homogeneous

FIG. 31

DELAY ELONGATIONS(%) AND REGIONS OF DEFORMATION TYPE
PMMA

STRESS, psi	50	60	70	80	90	100
7000						
6500		INHOMOGENEOUS DEFORMATION (NECKING)				
6000	11.9		9.8			
5500			8.8			
5000			10.2			
4500			10.4			
4000			12.9	8.3		
3500			11.5/18.8 20.8	10.0	7.9	
3000			3.0 CR4800	10.4	7.9	8.4
2500				19.8	9.2	7.3
2000					20.8	10.4
1500					6.3 CR1300	10.9
1000						208 DR
500		HOMOGENEOUS DEFORMATION				7.3 CR1000
0						

TEMPERATURE, °C

1. CRx indicates homogeneous deformation only was observed in an experiment lasting x minutes
2. DR indicates drawing was homogeneous

FIG. 32

133

EFFECT OF MOISTURE ABSORPTION ON DELAY TIME

PMMA

% MOISTURE

TEMPERATURE : 80°C

0.6

2.0

DELAY TIME, minutes

STRESS, psi

FIG. 33

134
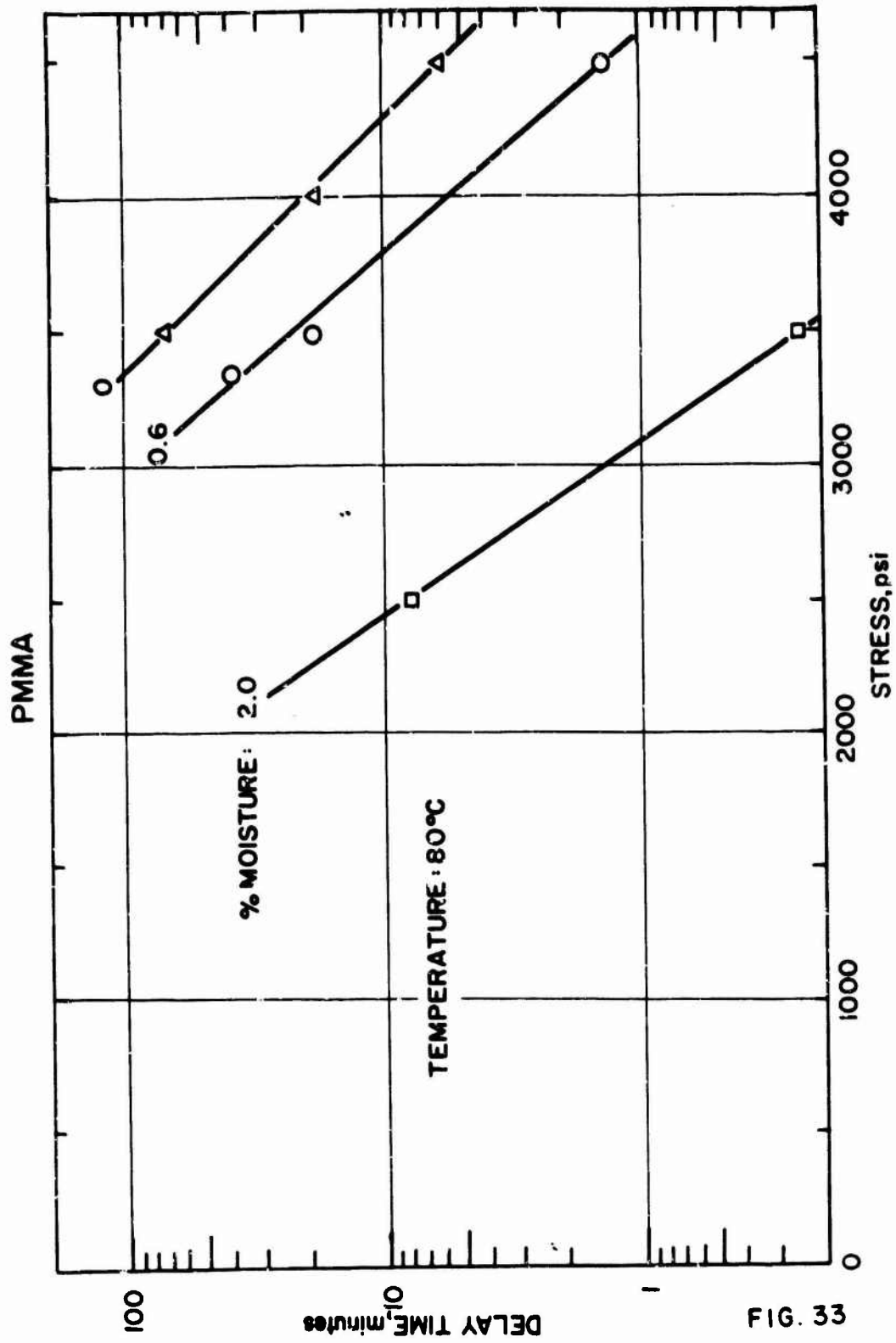
ELONGATION OF PMMA UNDER CONSTANT TENSILE LOAD
TEMPERATURE: 100°C
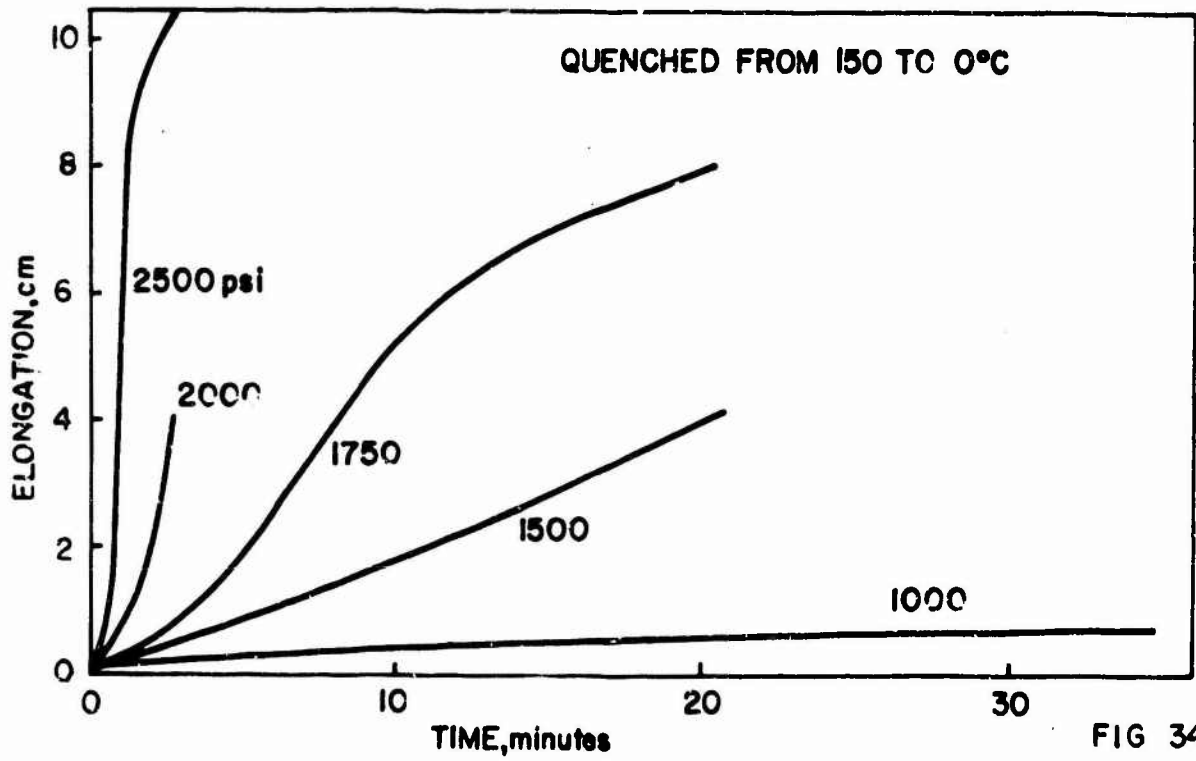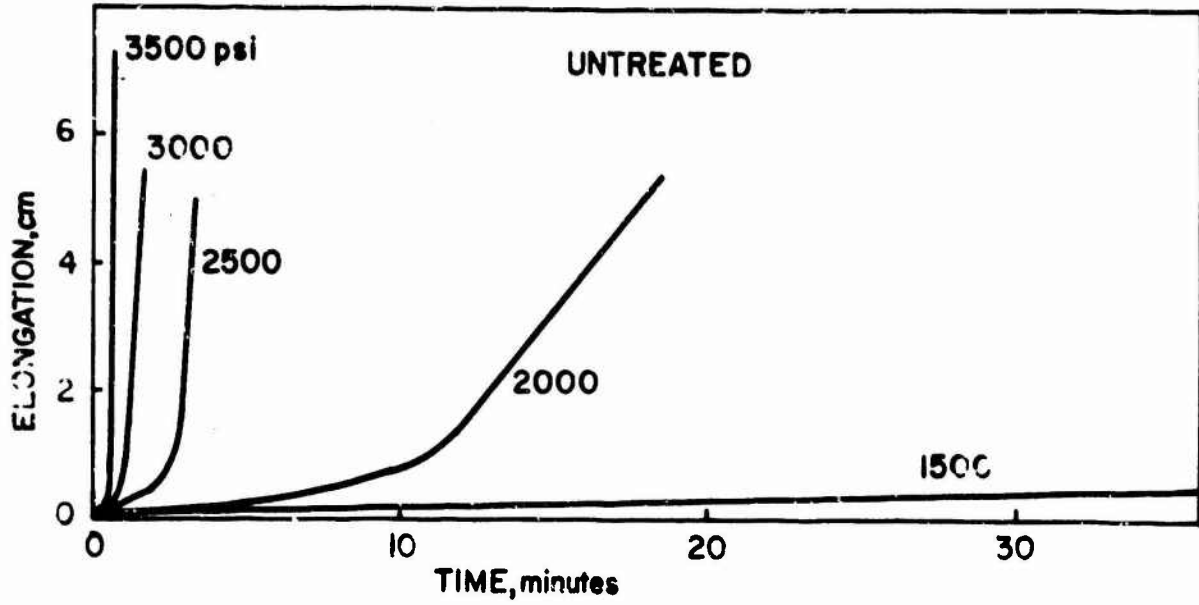
FIG 34

EFFECT OF THERMAL TREATMENT ON ELONGATION OF PMMA UNDER CONSTANT
TENSILE LOAD

LOAD: 2000psi
TEMPERATURE: 100°C

FIG. 35

136
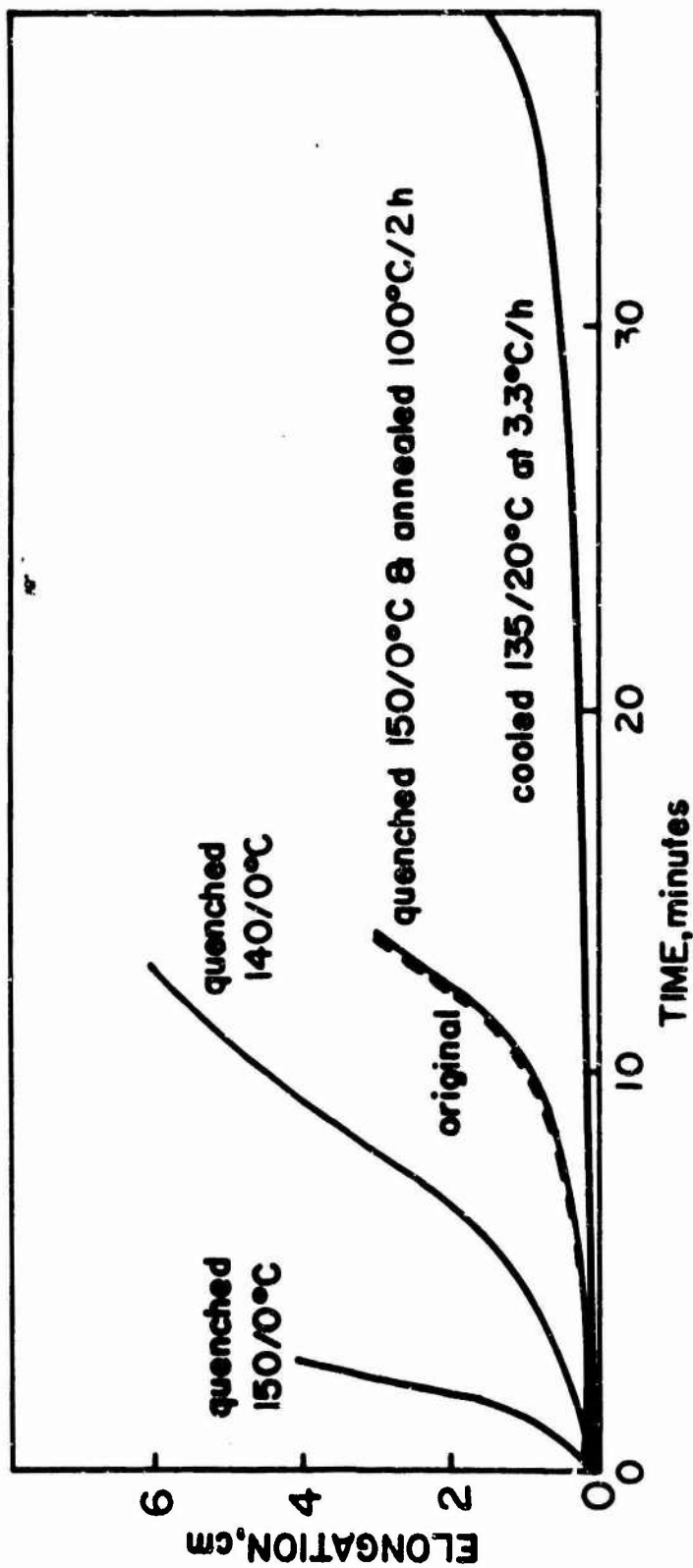
DEPENDENCE OF DELAY TIME ON STRESS LEVEL AT DIFFERENT TEMPERATURES – PREORIENTED POLYSTYRENE ($\Delta n = 5 \times 10^{-3}$)

FIG. 36

STRESS, psi
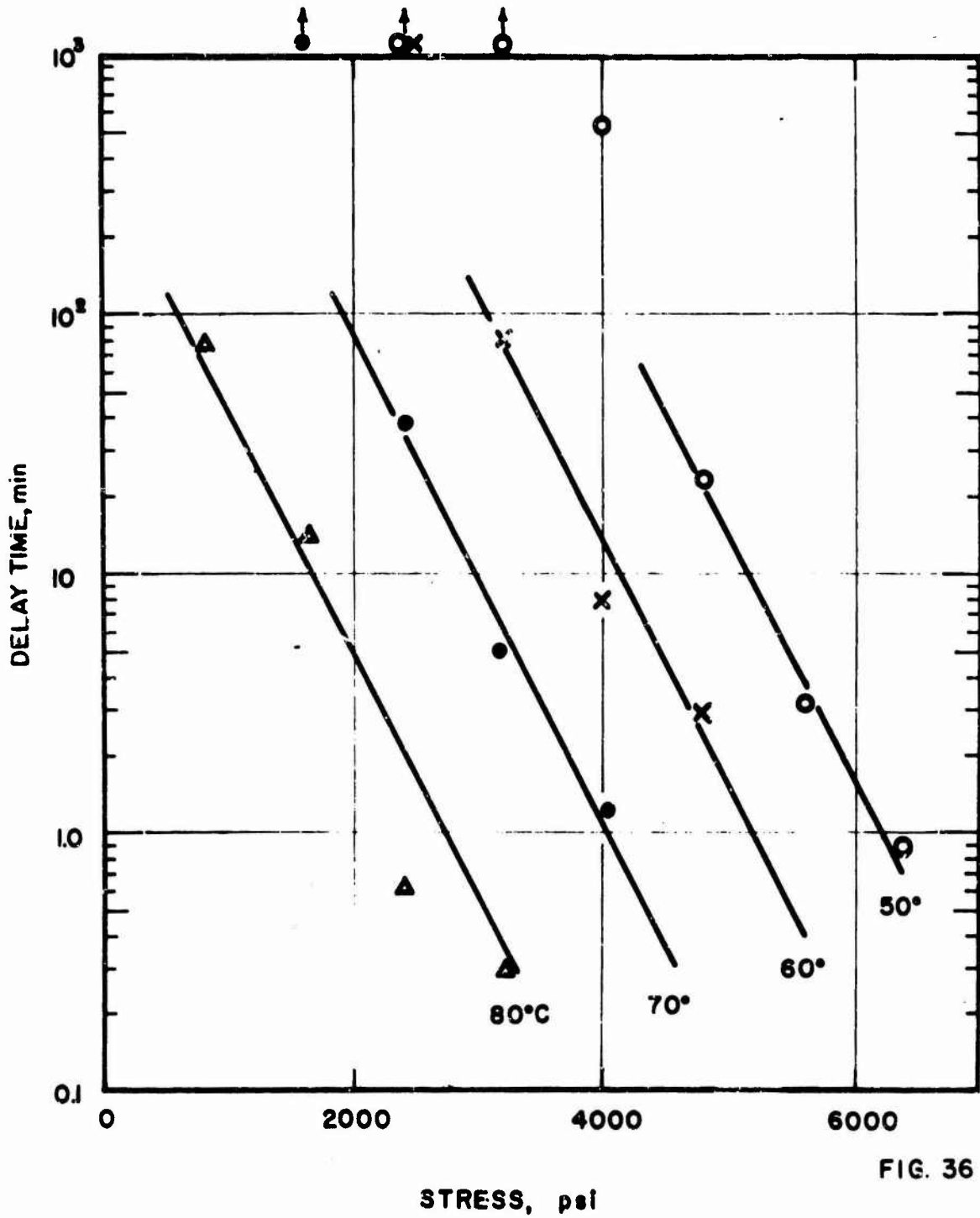
DEPENDENCE OF DELAY TIME ON STRESS LEVEL
AT DIFFERENT TEMPERATURES   PMMA

FIG. 37

138
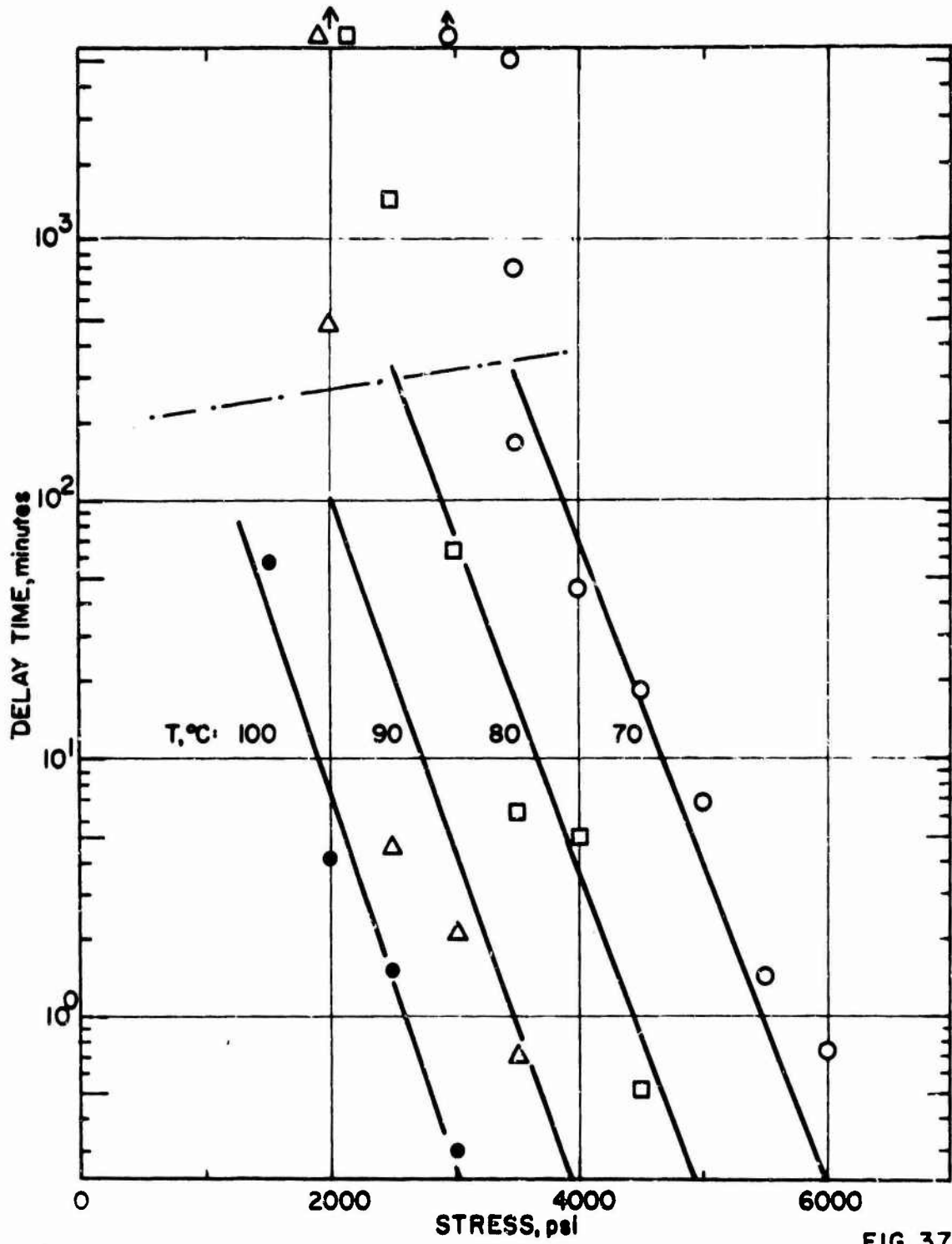
STRESS-STRAIN CURVES OF PMMA FOR VARIOUS EXTENSION RATES

FIG. 38
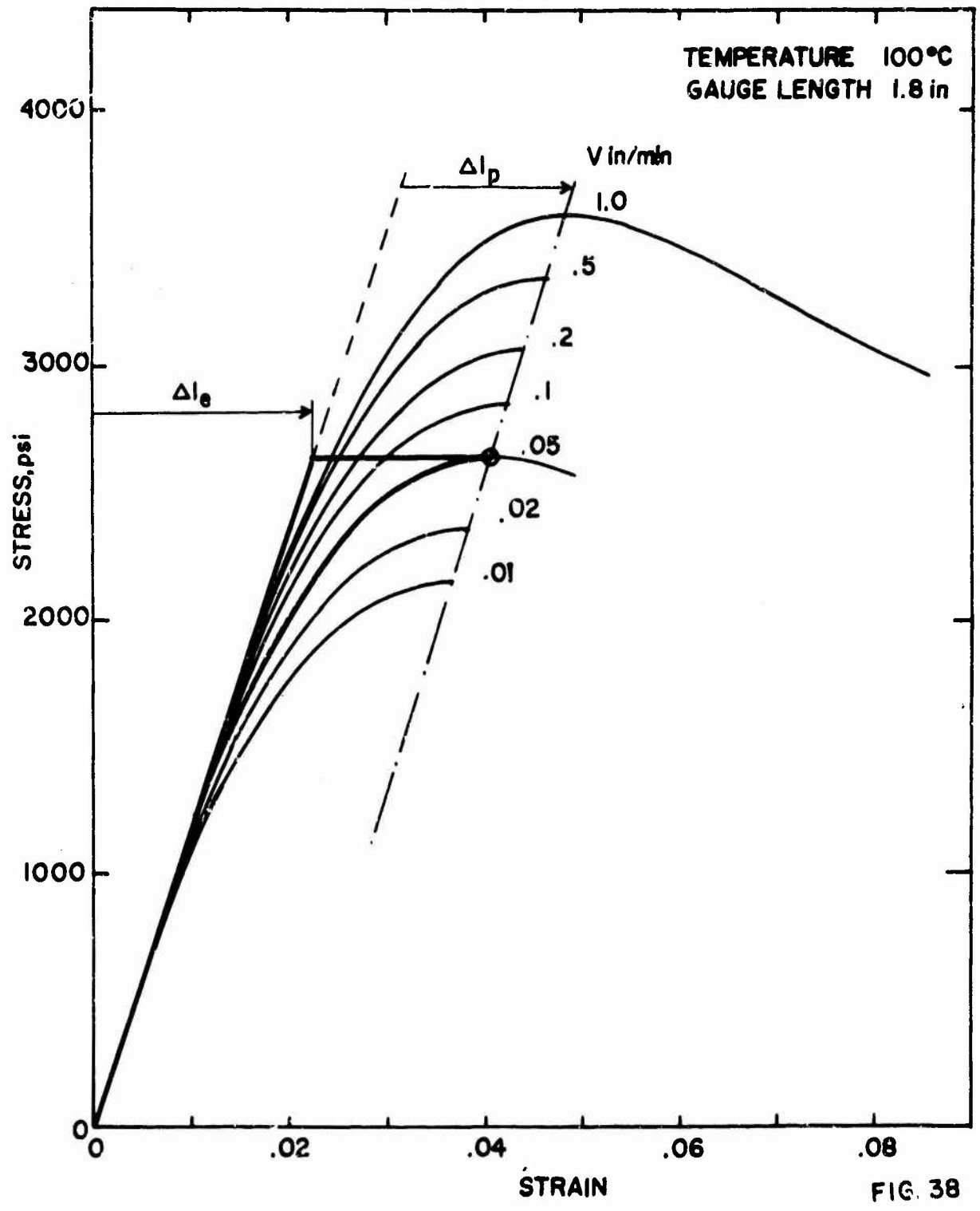
MEASURED AND PREDICTED DELAY TIMES
PMMA

FIG. 39
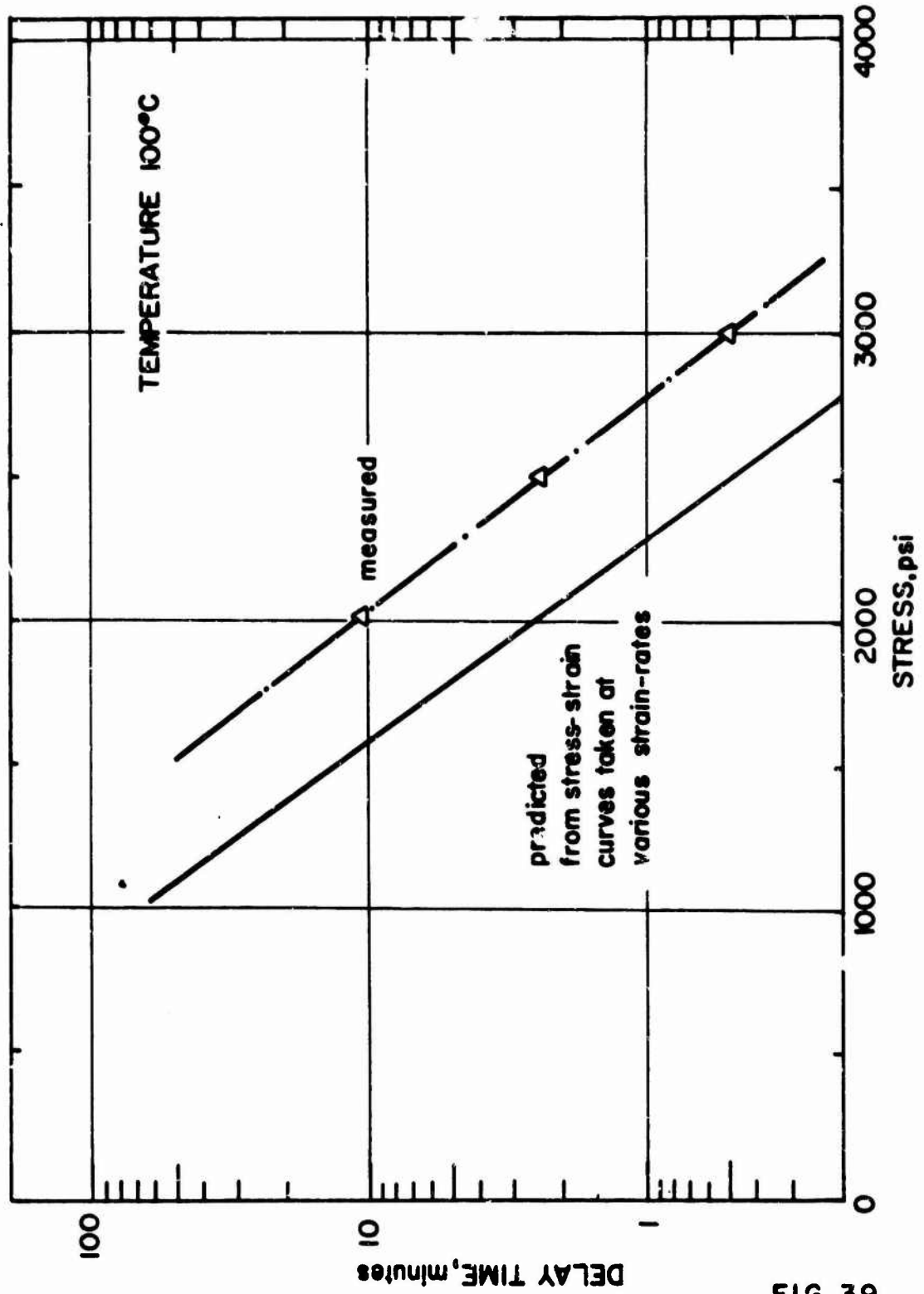
a. TYPICAL NECK PHOTOGRAPH

PMMA (PLEXIGLAS II UVA)

$\frac{D}{D_0}$

T = 93 °C
D_0 = 0.20 (in)
L_0 = 1.0 (in)
$\dot{e}$ = 0.2 (in/in/min)

DISTANCE ALONG SAMPLE AXIS (in.)

b. CORRESPONDING PROFILE PLOT

FIG. 40

141

NECK PROFILE SEQUENCE
T = 75°C
Δl = 0.2 in/min
PMMA

FIG. 41
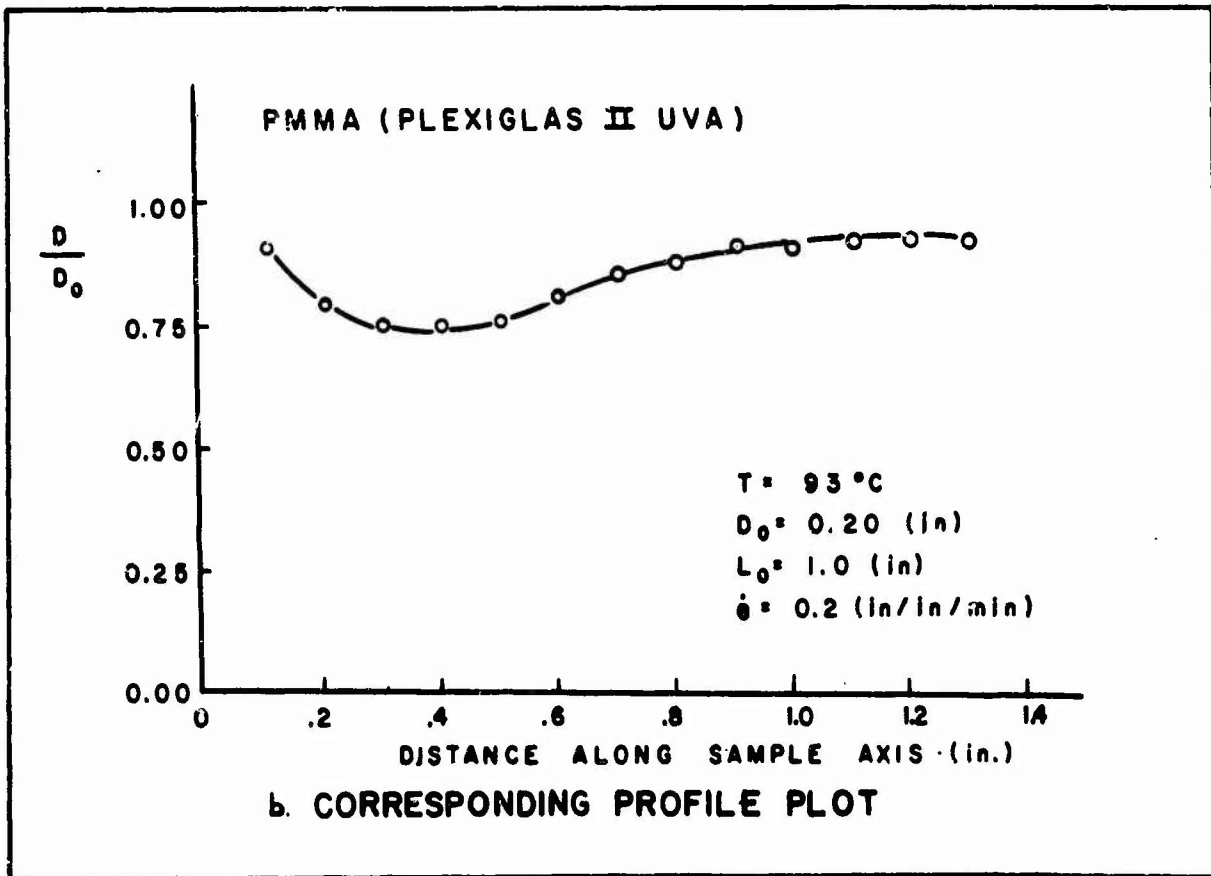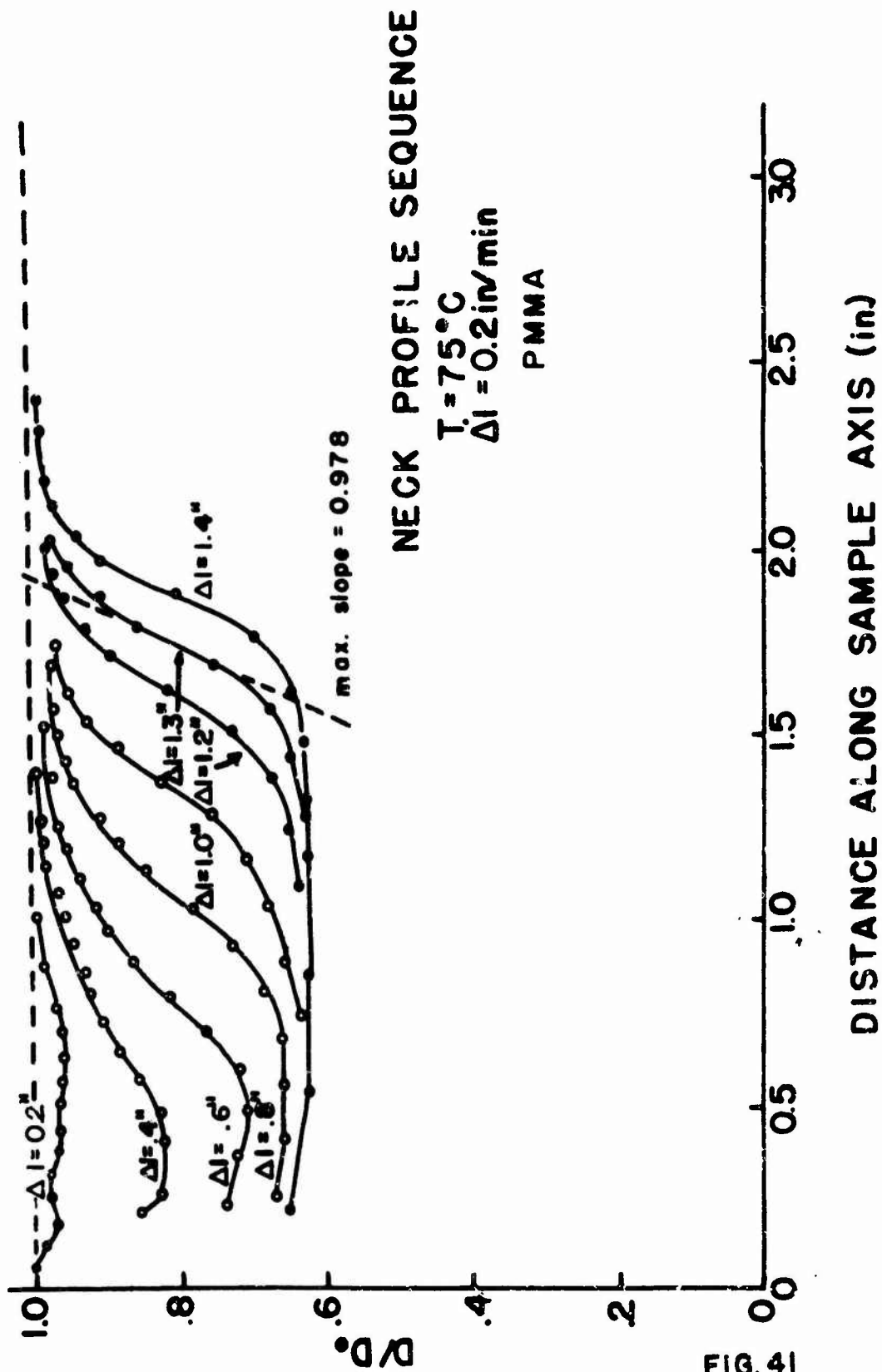
PMMA

VARIATION OF NECK
SHAPE WITH EXTENSION RATE

● T = 95°C
○ T = 75°C

NECK SLOPE

EXTENSION RATE (IN./MIN.)

FIG. 42

143
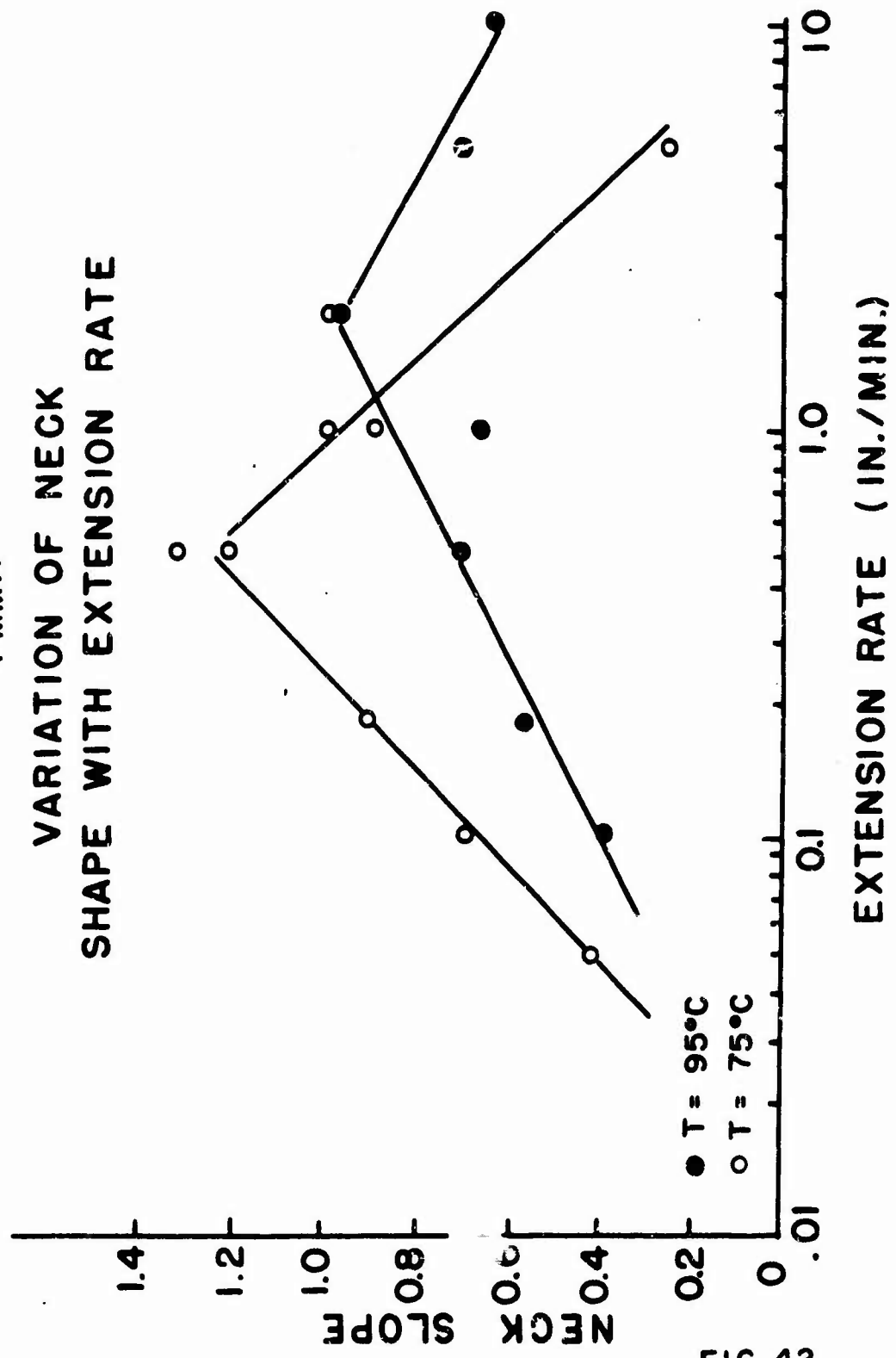
PMMA

VARIATION OF NECK SHAPE
WITH TEMPERATURE

FIG. 43

144
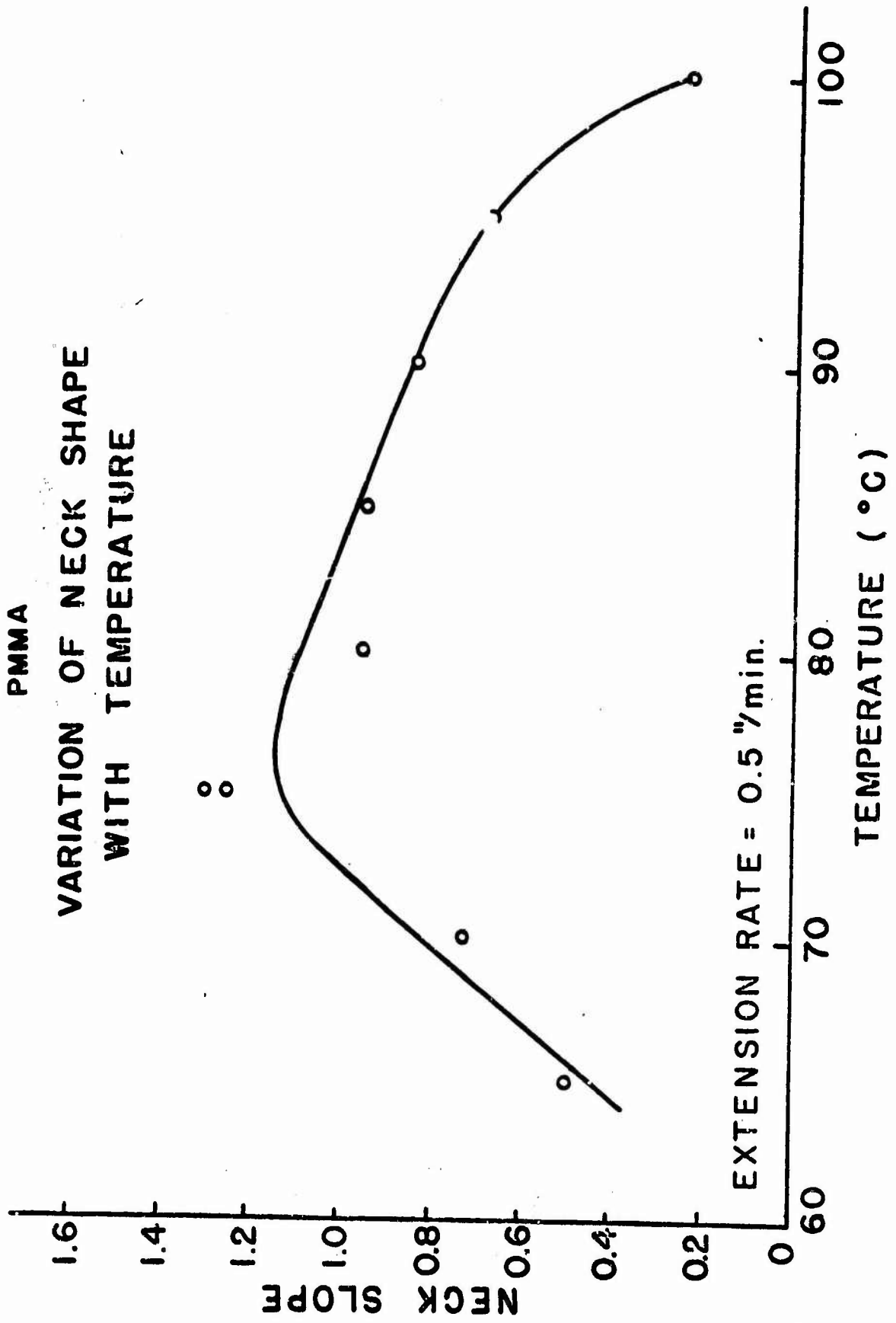
PMMA

THE VARIATION OF THE
NECK SLOPE WITH
PRE-ORIENTATION

FIG. 44

145

PMMA

VARIATION OF TRUE
STRESS - STRAIN CURVES
WITH EXTENSION RATE

FIG. 45

146

PMMA

TRUE STRESS vs.

TRUE STRAIN AT

CONSTANT EXTENSION RATE

$\dot{\Delta l}$ = 0.5in/min

T = 65°C
T = 75°C
T = 85°C
T = 95°C

TRUE STRESS x 10³, PSI

TRUE STRAIN

FIG. 46

147

PMMA

THE VARIATION OF THE
TRUE STRESS-STRAIN CURVE
WITH PRE-ORIENTATION

● Δn = 4.9 x 10⁻⁴   ■ Δn = 0.66 x 10⁻⁴
+ Δn = 1.45 x 10⁻⁴   ▲ Δn = 0

T = 75°C
Δḷ = 0.5 in/min.

FIG. 47

148

b.

c.

a.
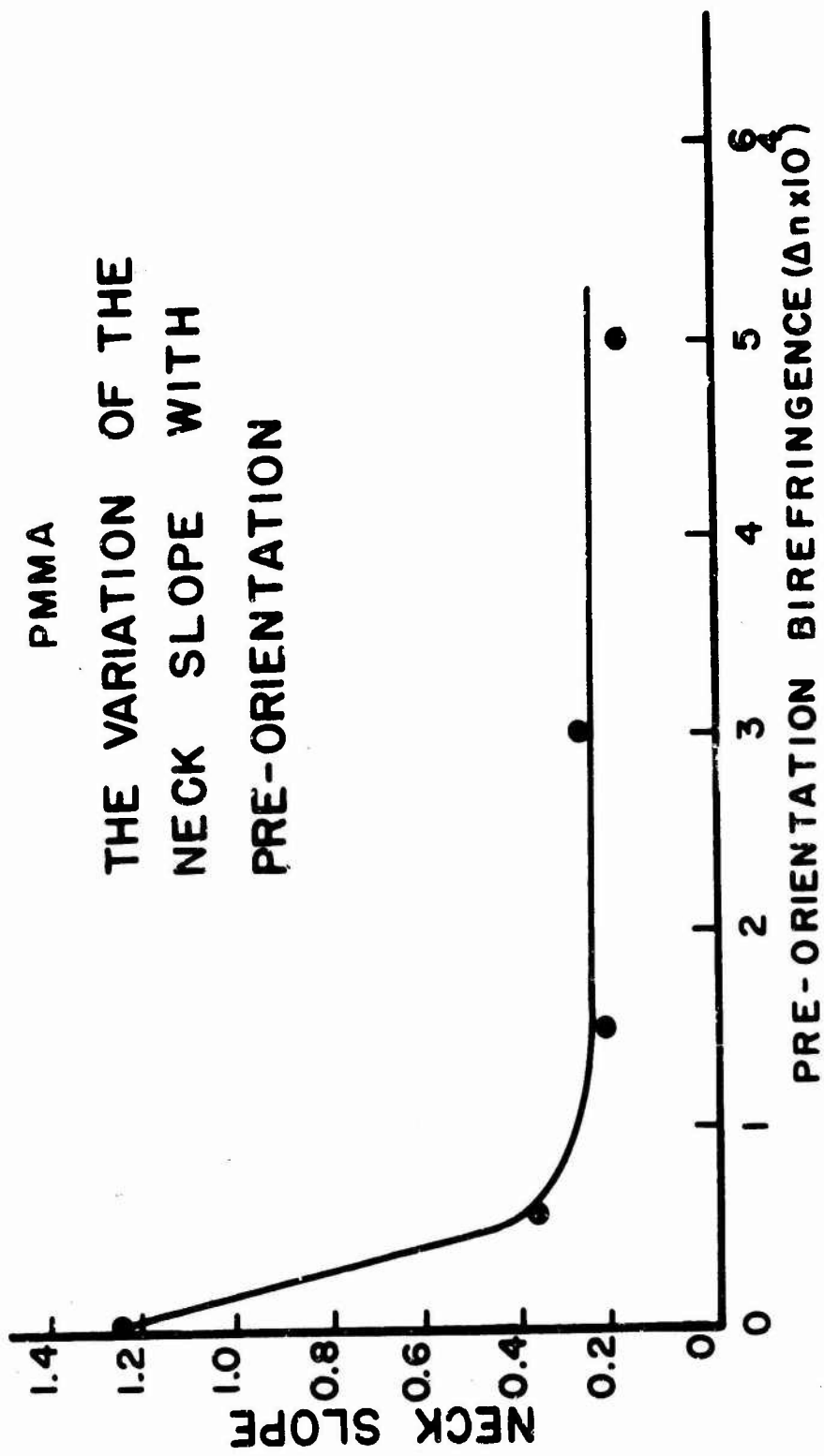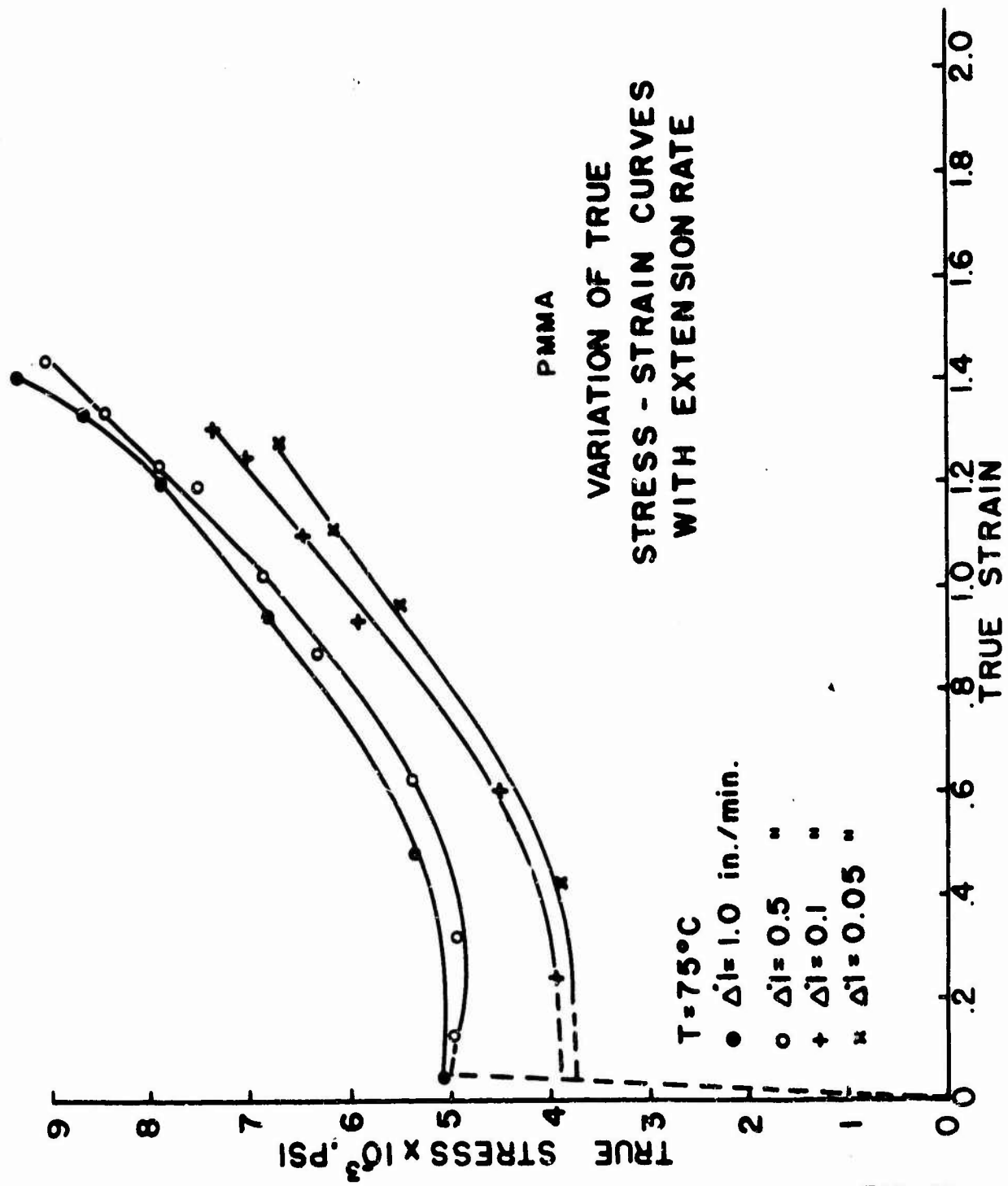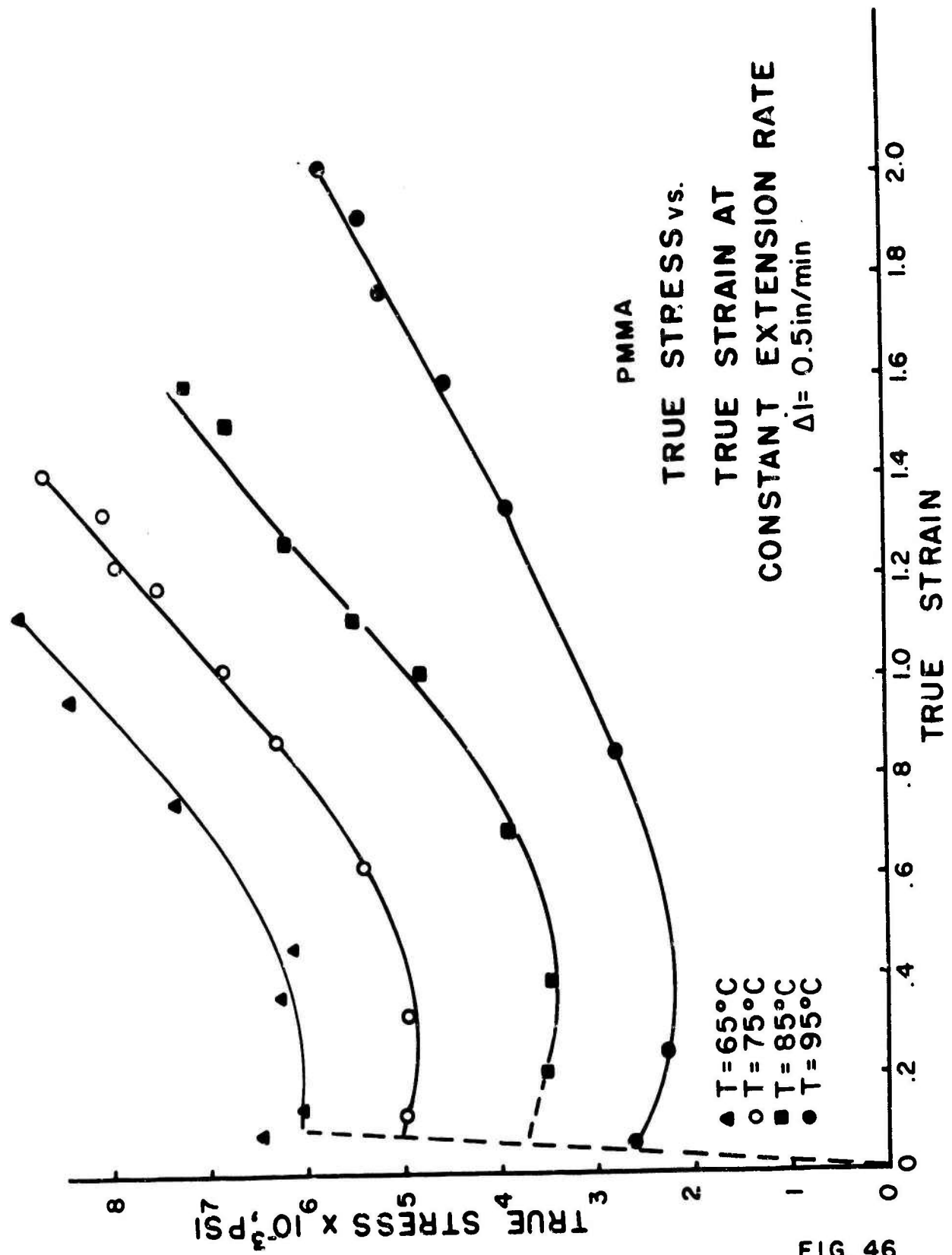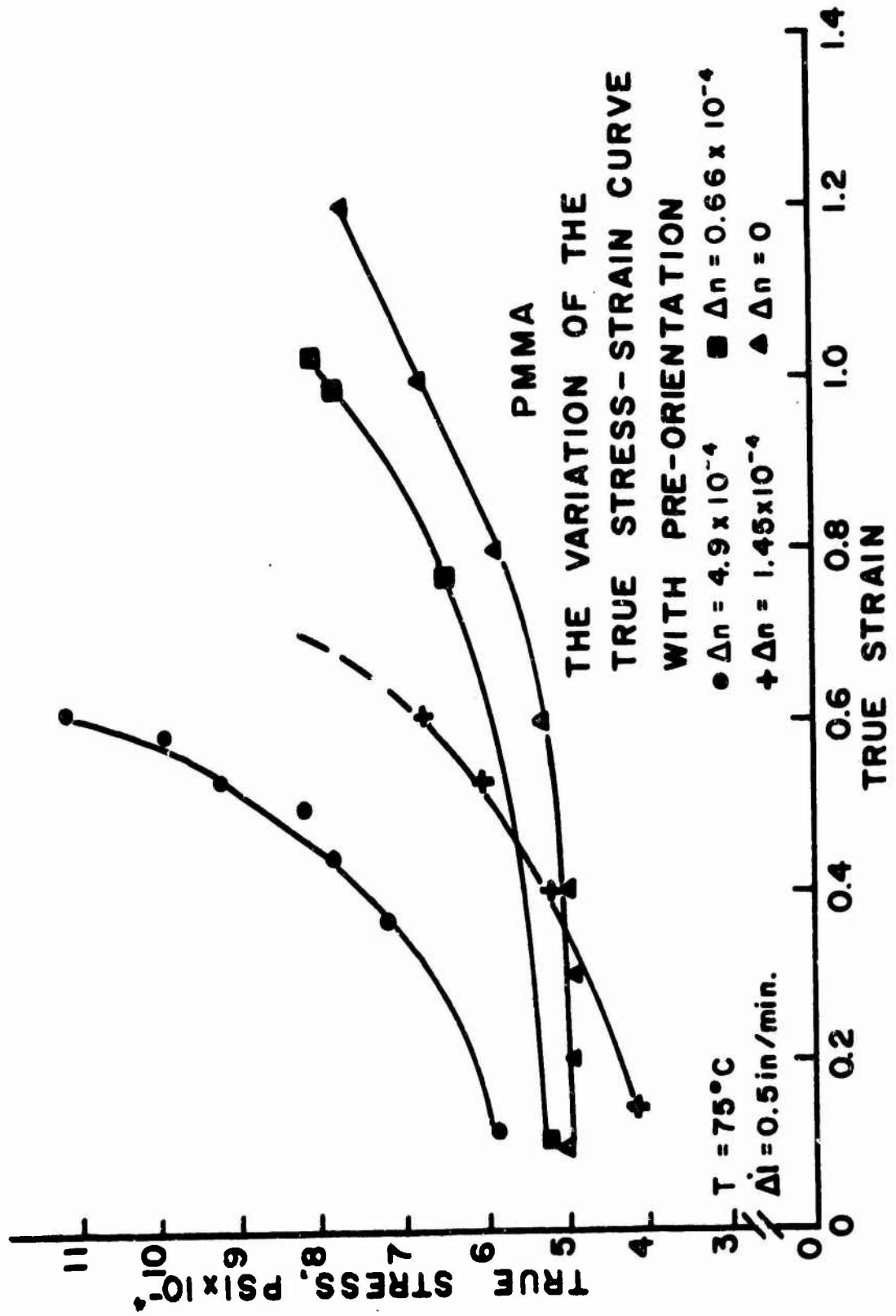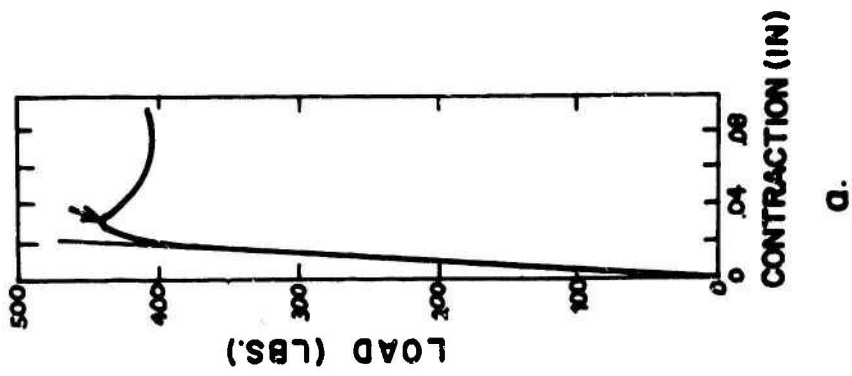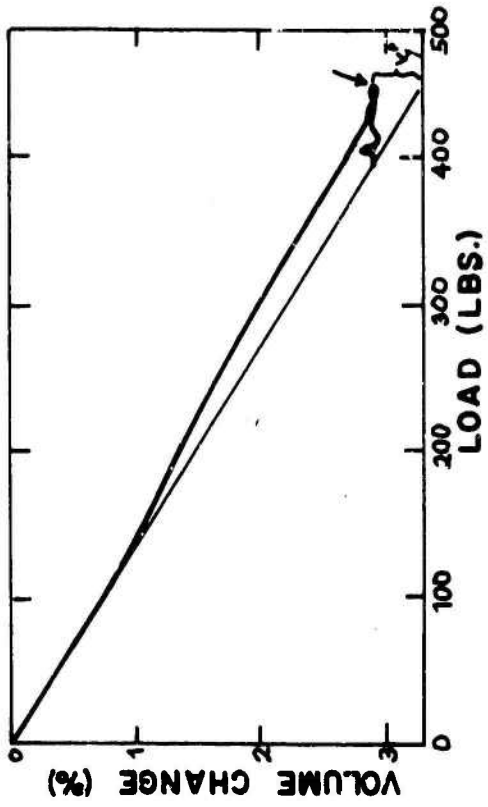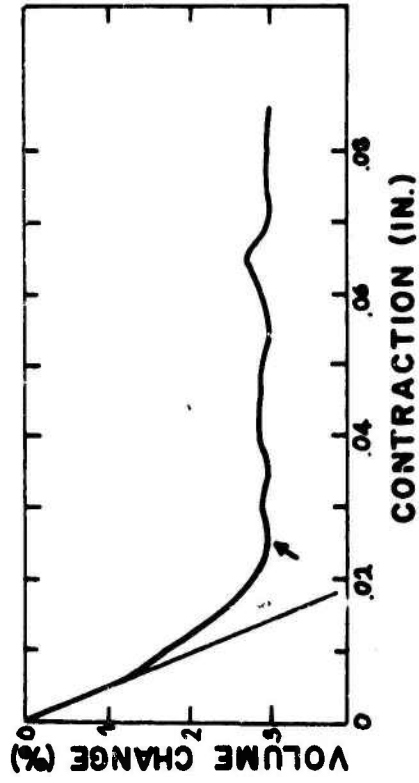
VOLUME CHANGES IN FORMVAR

FIG 48

149

NECKS AND BANDS IN FORMVAR FILM

FIG. 48

FIG. 49
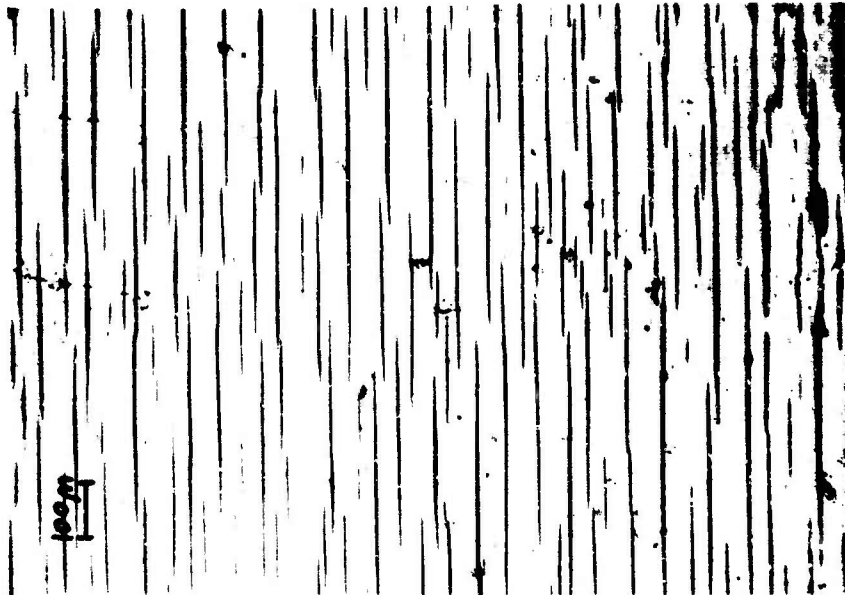
OPEN CRAZE IN POLYSTYRENE

FIG. 51

CRAZES IN POLYSTYRENE

FIG. 50
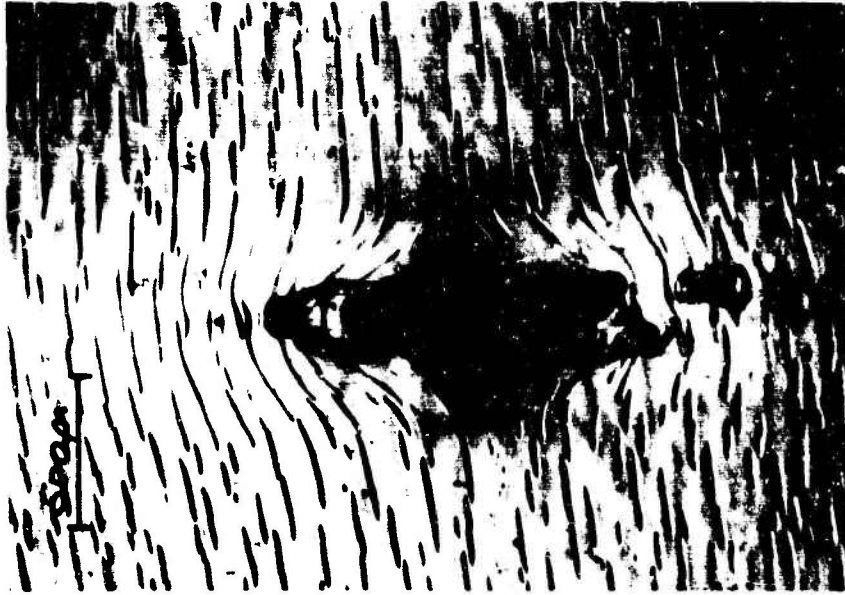
SURFACE OF POLYSTYRENE SPECIMEN

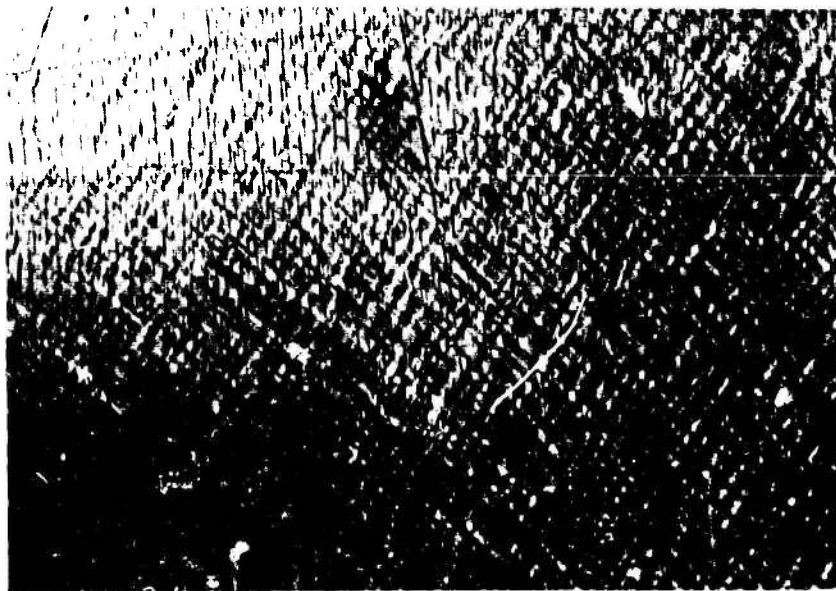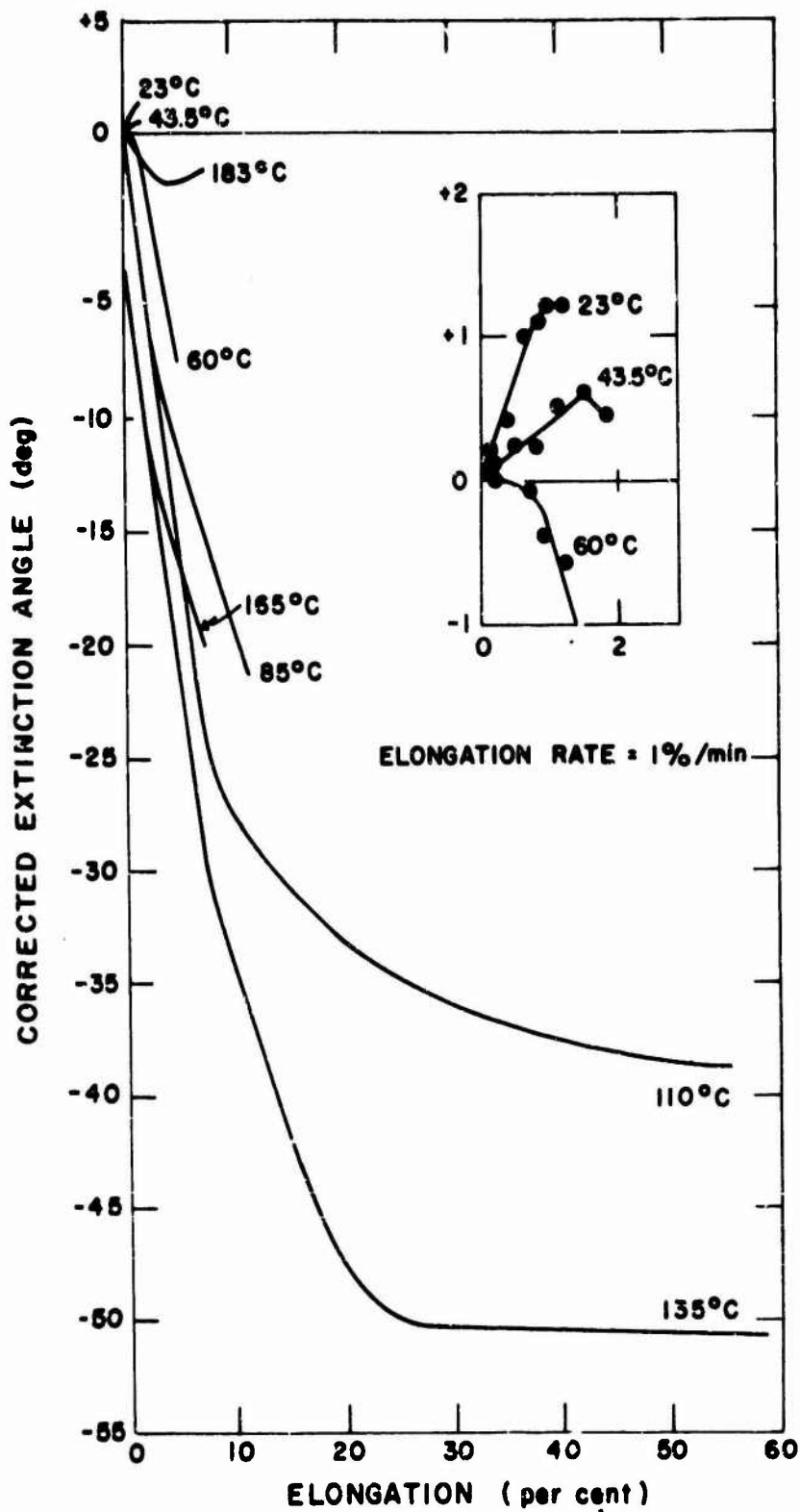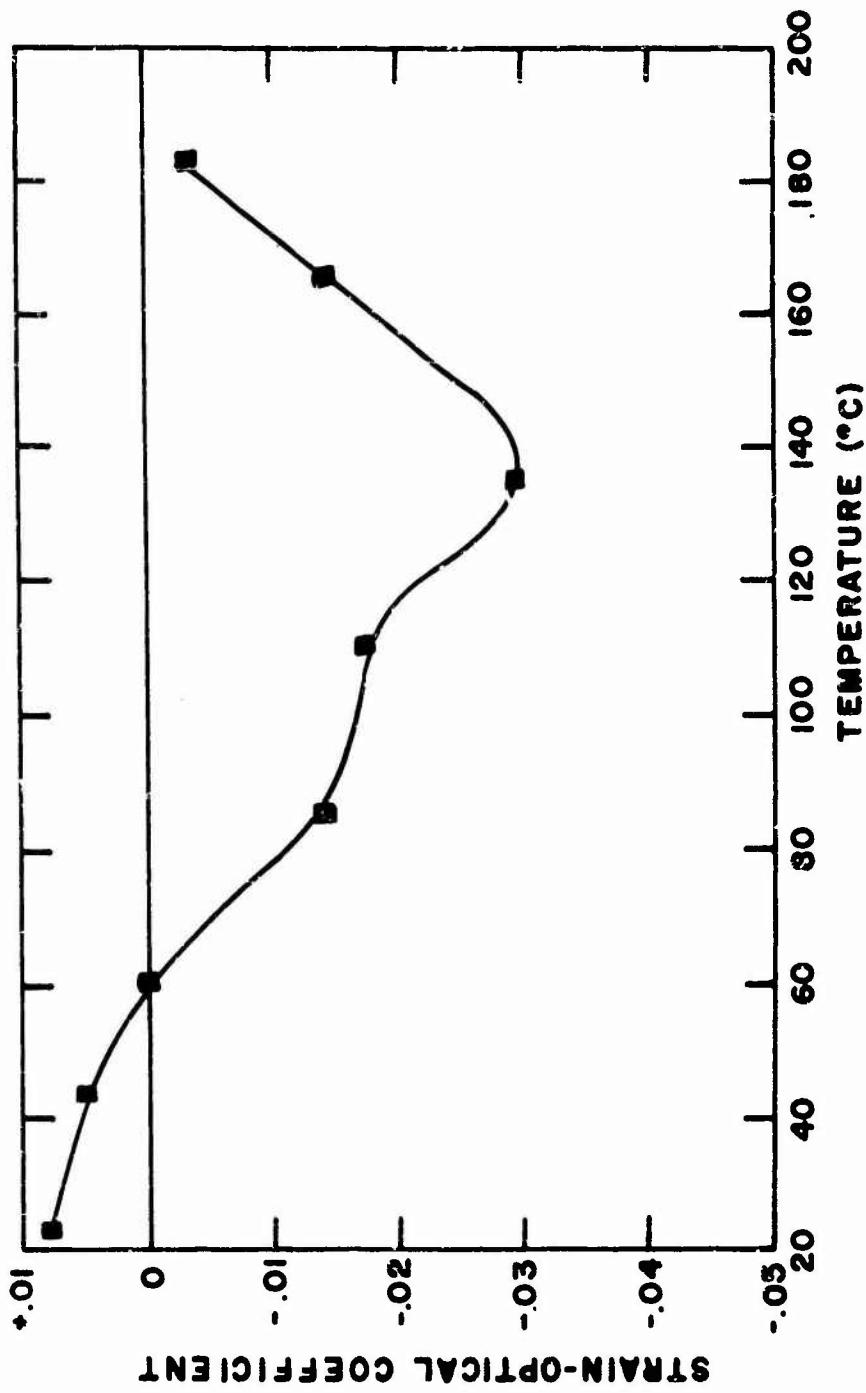AFTER COLD DRAWING
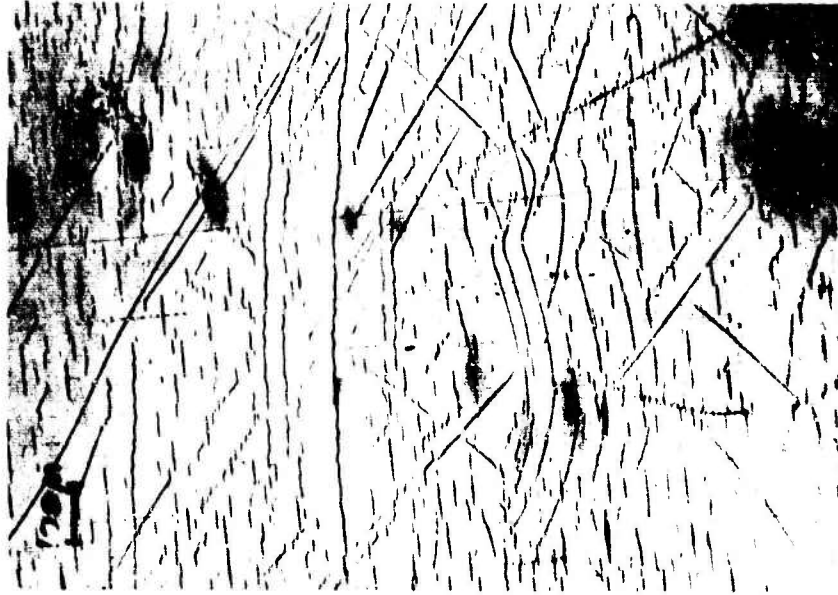
FIG. 53

DEFORMATION BANDS IN POLYSTYRENE

FIG. 52

152
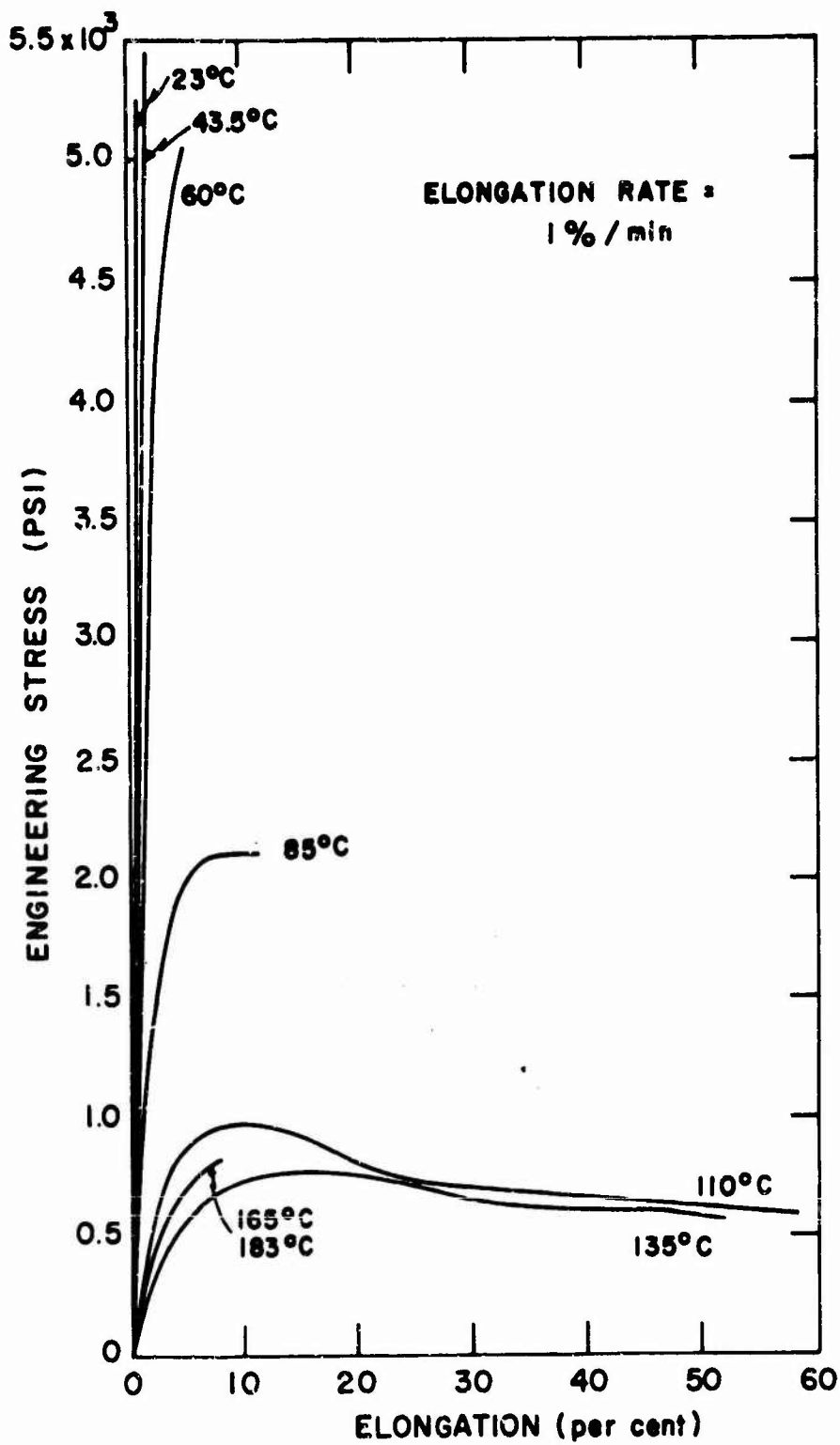
POLYACRYLONITRILE
ENGINEERING STRESS VS. ELONGATION
FIG. 54

153

POLYACRYLONITRILE
BIREFRINGENCE VS. ELONGATION

FIG. 55

154

POLYACRYLONITRILE
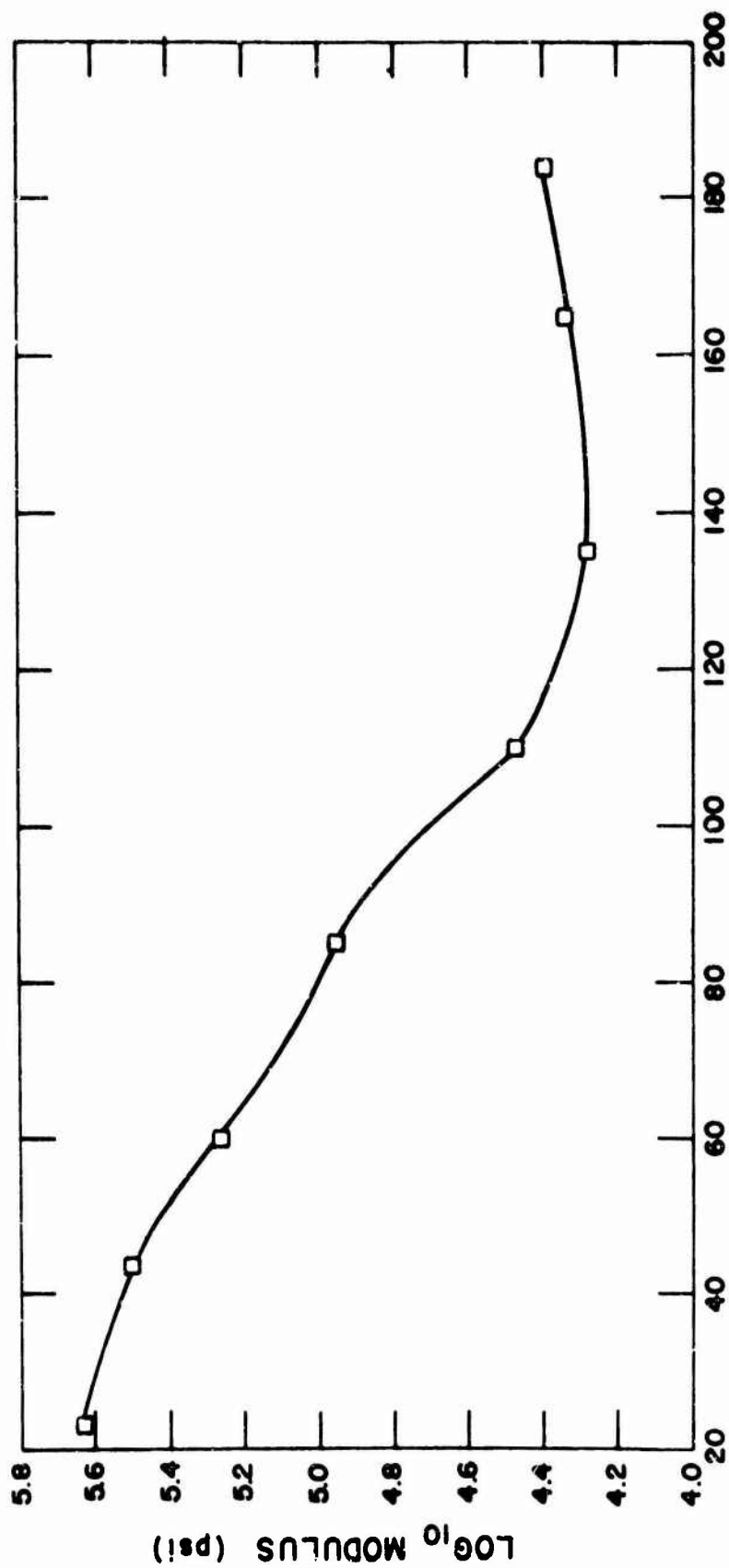
TEMPERATURE DEPENDENCE OF
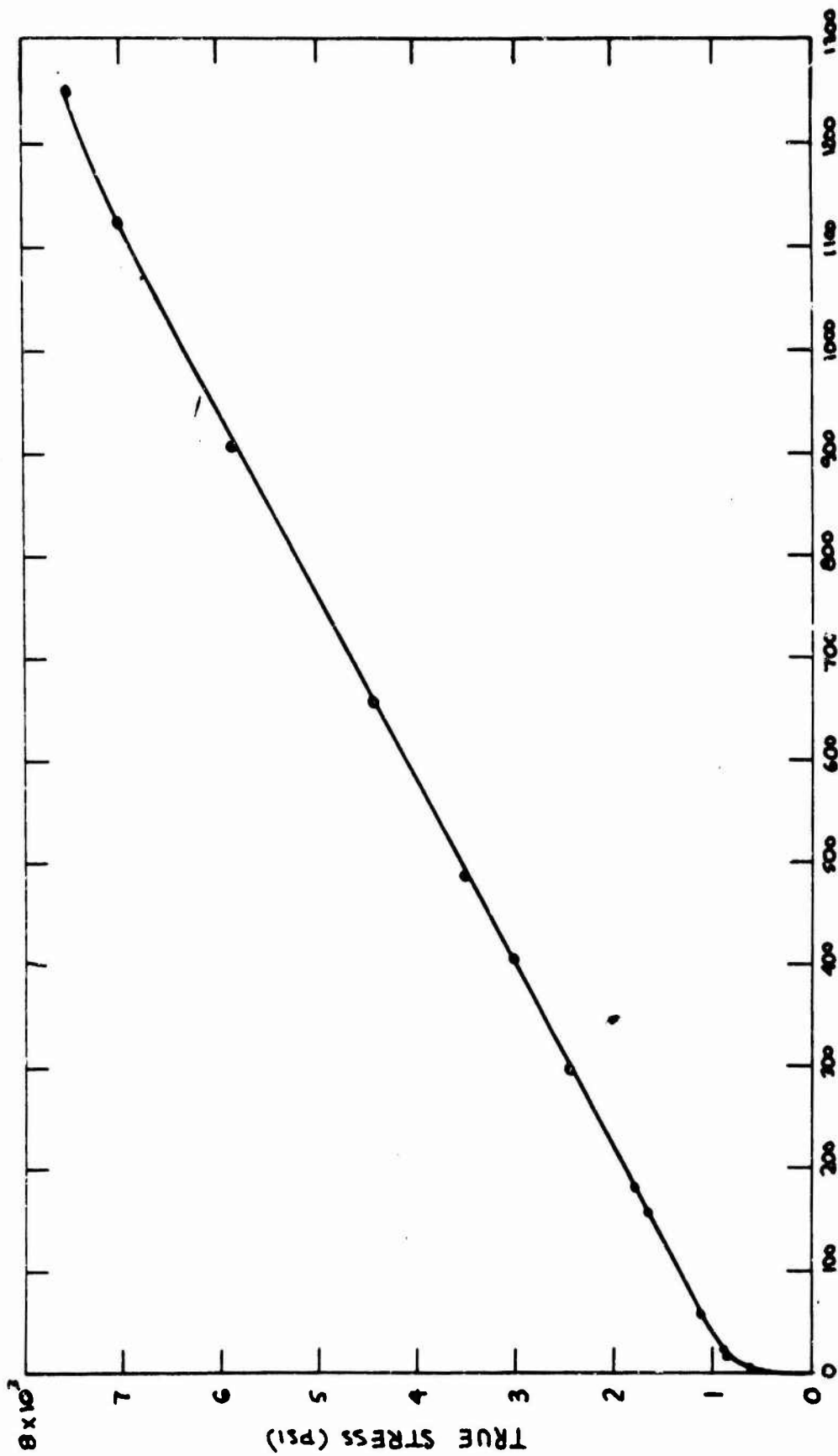STRAIN-OPTICAL COEFFICIENT

FIG. 56

TEMPERATURE (°C)

POLYACRYLONITRILE

TEMPERATURE DEPENDENCE OF MODULUS

FIG. 57

156

TRUE STRAIN (per cent)

POLYACRYLONITRILE

TRUE STRESS VS. TRUE STRAIN

NECKING AND DRAWING AT 135°C

TRUE STRESS (PSI)

FIG. 58

157
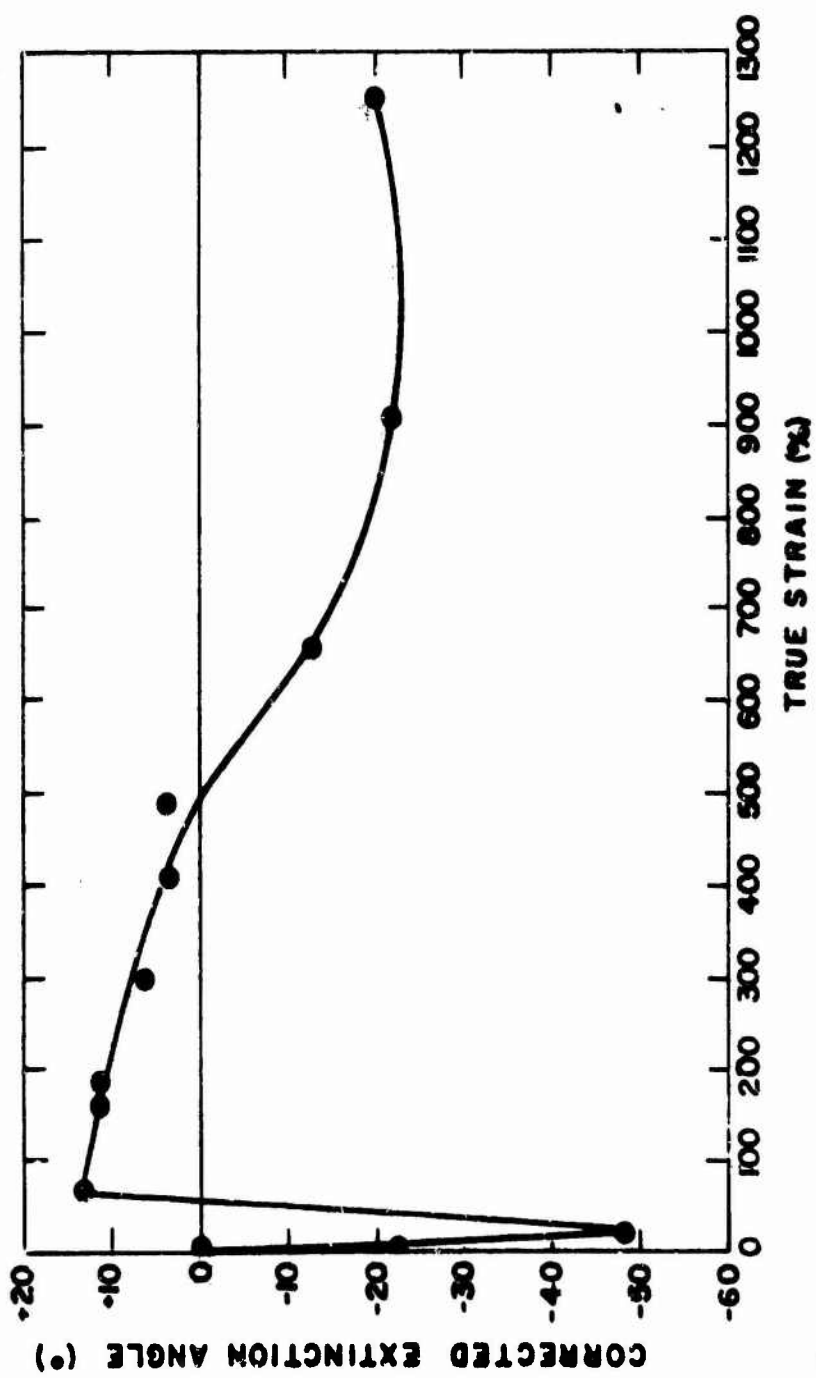
POLYACRYLONITRILE
NECKING AND DRAWING AT 135°C
BIREFRINGENCE VS. TRUE STRAIN

FIG. 59

158

BIREFRINGENCE vs. STRAIN DURING SHRINKAGE AT 105°C
PMMA

COLD DRAWN
80°C, 110%

HOT STRETCHED
144°C, 116%
PLUS
COLD DRAWN
80°C, 89%

HOT STRETCHED
150°C, 205%

BIREFRINGENCE x10⁴

% STRAIN

FIG. 60

159
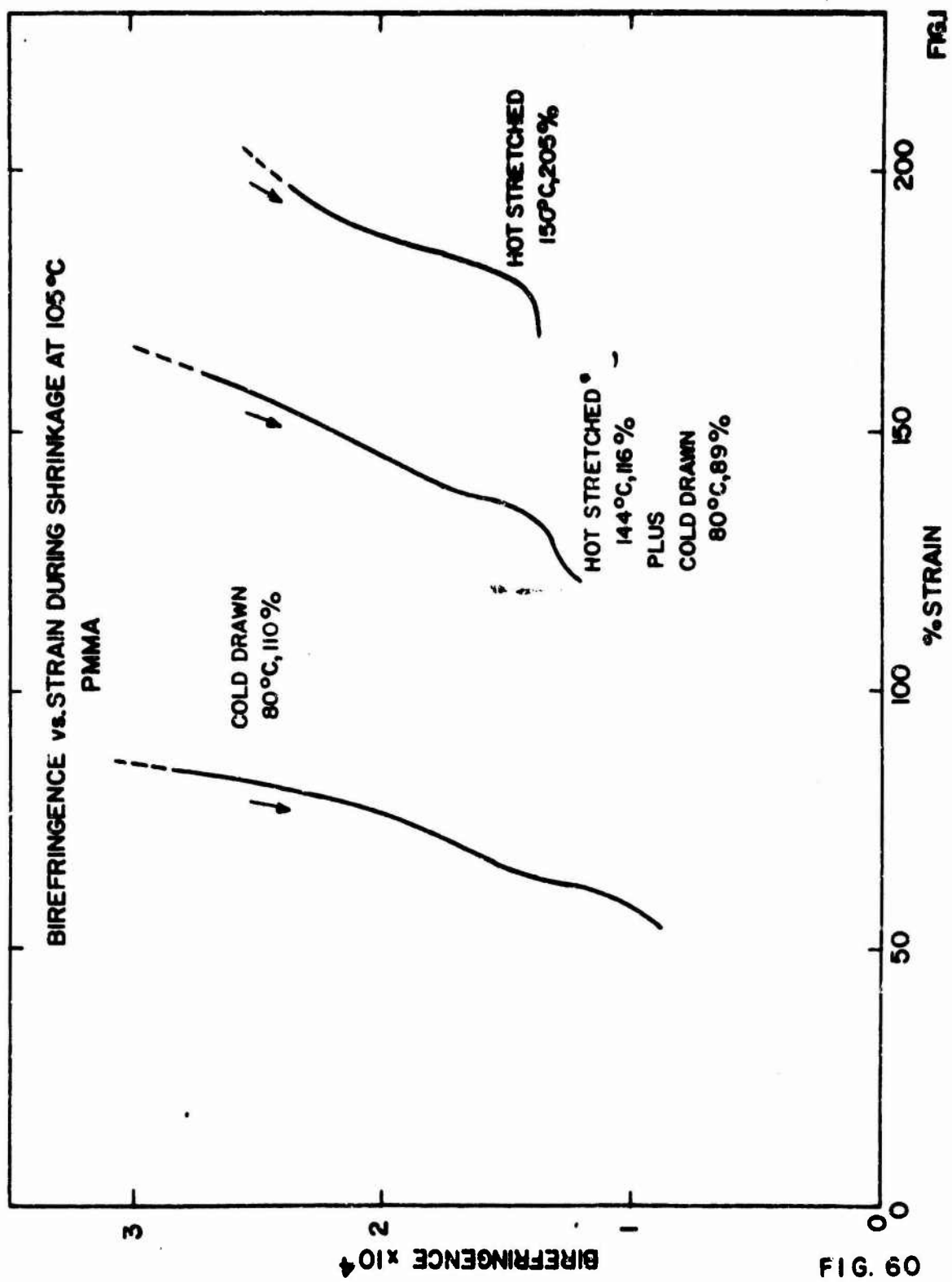
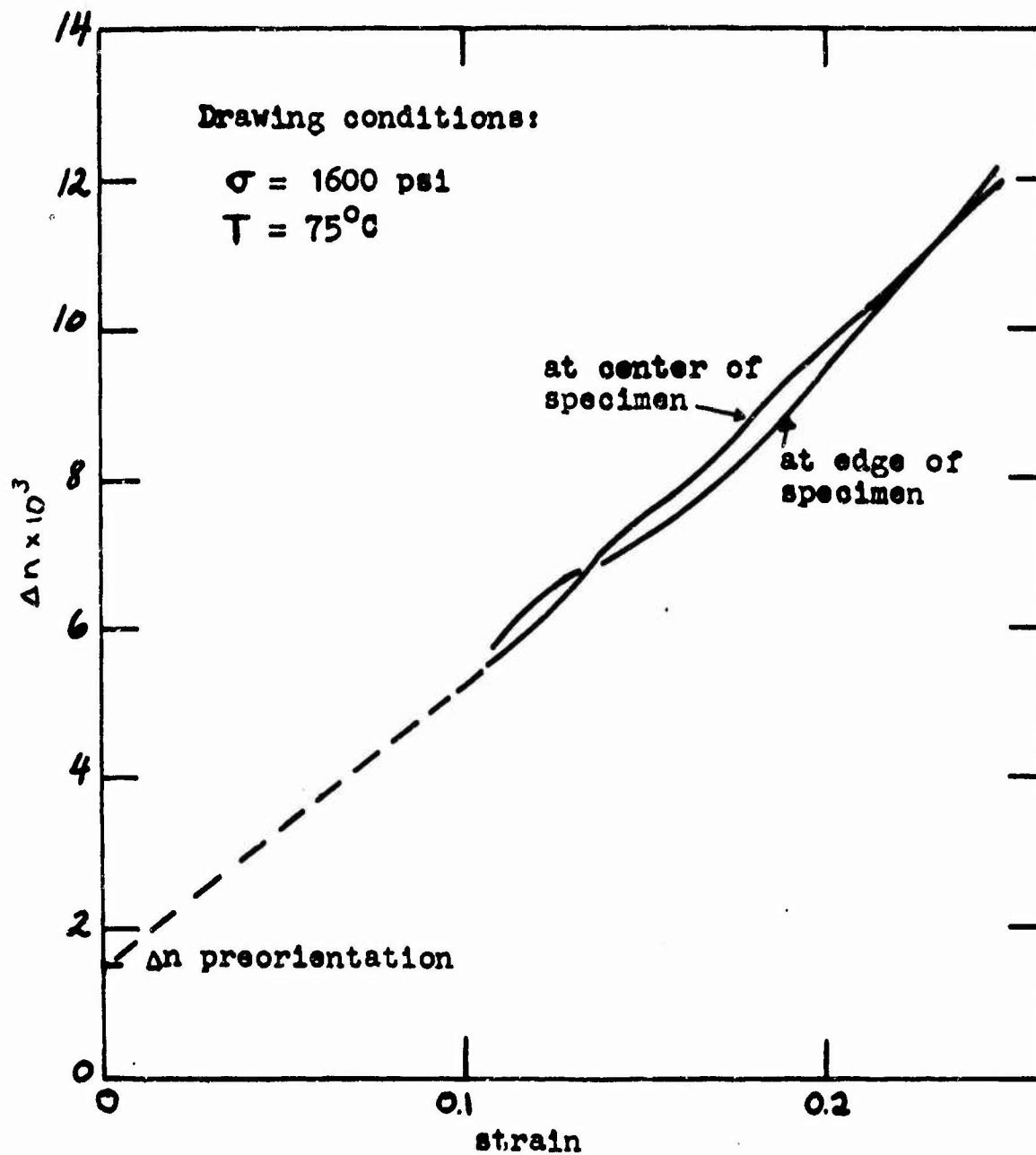BIREFRINGENCE vs. STRAIN OF PS MEASURED IN NECK OF PARTIALLY COLD-DRAWN SPECIMEN AT ROOM TEMPERATURE

FIG. 61

160

BIREFRINGENCE vs. STRAIN OF PMMA DURING
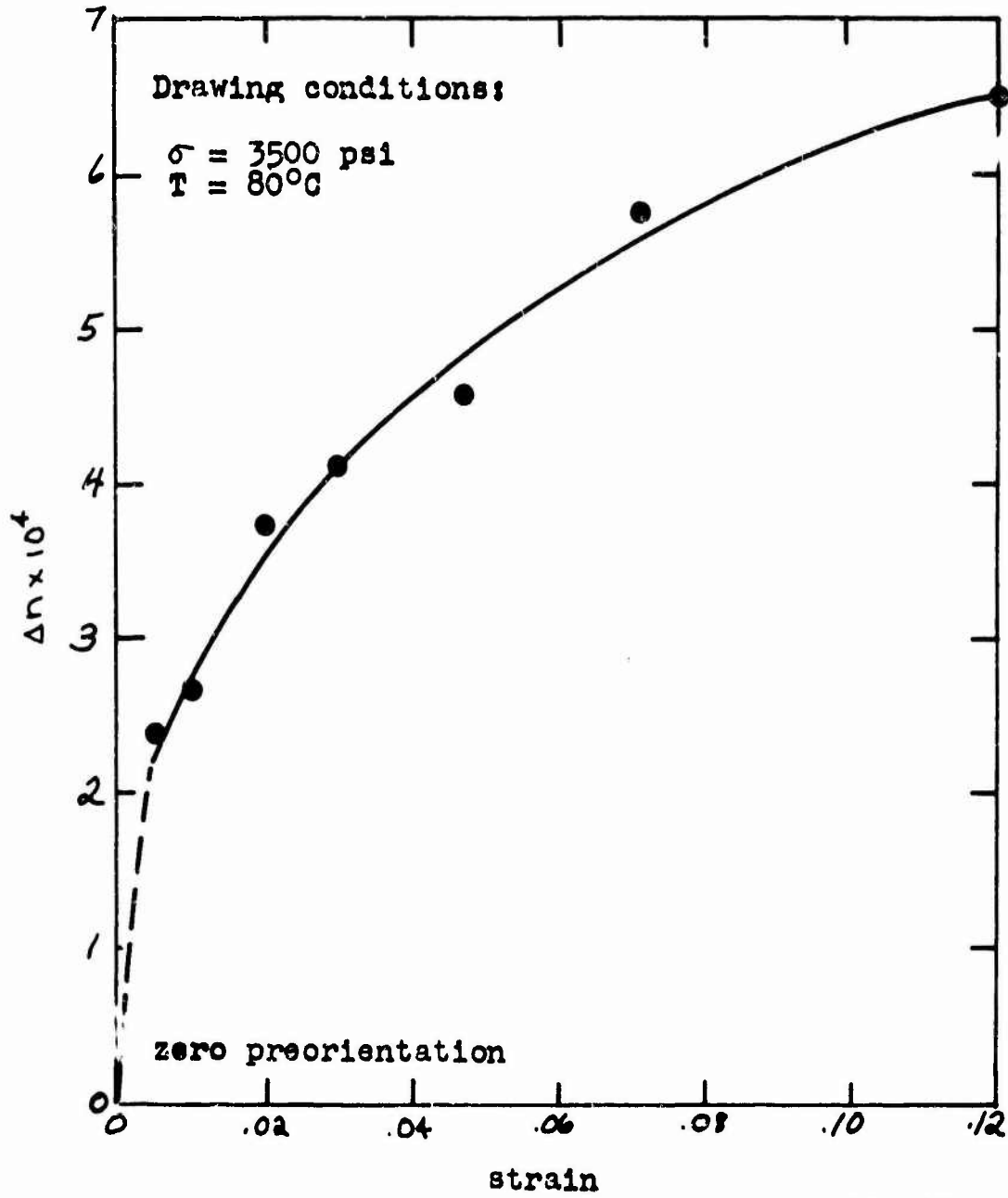INDUCTION PERIOD (HOMOGENEOUS DEFORMATION)

FIG. 62

DOCUMENT CONTROL DATA - R&D

(Security classification of title, body of abstract and indexing annotation must be entered when the overall report is classified)

1. ORIGINATING ACTIVITY (Corporate author)	2a. REPORT SECURITY CLASSIFICATION
Massachusetts Institute of Technology Fibers and Polymers Division, Dept. Mech. Engineering Cambridge, Massachusetts 02139	Unclassified
	2b. GROUP

3. REPORT TITLE

RESEARCH STUDY ON COLD DRAWING PHENOMENA IN HIGH POLYMERS

4. DESCRIPTIVE NOTES *(Type of report and inclusive dates)*

Final Report January 1964 - January 1966

5. AUTHOR(S) *(Last name, first name, initial)*

Andrews, R. D., Jr., Allison, S. W., Ender, D. H., Kimmel, R. M., and Whitney, W.

6. REPORT DATE	7a. TOTAL NO. OF PAGES	7b. NO. OF REFS
August 1966	166	41

8a. CONTRACT OR GRANT NO.	9a. ORIGINATOR'S REPORT NUMBER(S)
DA19-129-AMC-238(N)	
b. PROJECT NO.	
1K024401A113	
c.	9b. OTHER REPORT NO(S) (Any other numbers that may be assigned this report)
d.	67-10-CM C&OM-25

10. AVAILABILITY/LIMITATION NOTICES

Distribution of this document is unlimited. Release to CFSTI is authorized.

11. SUPPLEMENTARY NOTES	12. SPONSORING MILITARY ACTIVITY
	U. S. Army Natick Laboratories Natick, Massachusetts 01760

13. ABSTRACT

A fundamental study of the phenomenon of cold-drawing (plastic yield) in polymers has been carried out, through which a better understanding of several of the features of this process has been achieved. The effects of temperature, thermal history, stress-field, chemical structure and pre-orientation on the stress-strain behavior of both glassy and crystalline polymers have been explored. The behavior of several polymers, particularly polystyrene and polymethyl methacrylate, in stress relaxation, relation-recovery cycling and creep, especially with respect to delayed drawing, was investigated in detail. The geometry of neck formation has been quantitatively investigated by photographic techniques, and volume changes during compression have been measured using a mercury dilatometer. Microscopic modes of yielding, particularly the formation of deformation bands, are described. Birefringence changes during deformation of polyacrylonitrile under various conditions and during hot and cold extension of polystyrene and polymethyl methacrylate are presented and related to the molecular processes believed to be occurring. The development of a molecular theory of drawing is attempted through three different paths of approach: (1) a defect model analogous to dislocations, (2) a mathematical model of the "fiber bundle" type, and (3) a description in terms of the breakdown of secondary intermolecular cohesive bonding. General conclusions and recommendations for future studies in these areas are presented.

DD FORM 1473 1 JAN 64

14. KEY WORDS	LINK A		LINK B		LINK C	
	ROLE	WT	ROLE	WT	ROLE	WT
Plastic deformation	6					
Yield	6					
Plastics	9		9			
Polymers	9		c			
High	0		0			
Fracture (Mechanics)	7					
Strength	7					
Cold working	7		8			
Impact strength	7					
Creep (Materials)	7					
Drawing			8			

INSTRUCTIONS

1. ORIGINATING ACTIVITY: Enter the name and address of the contractor, subcontractor, grantee, Department of Defense activity or other organization (corporate author) issuing the report.

2a. REPORT SECURITY CLASSIFICATION: Enter the overall security classification of the report. Indicate whether "Restricted Data" is included. Marking is to be in accordance with appropriate security regulations.

2b. GROUP: Automatic downgrading is specified in DoD Directive 5200.10 and Armed Forces Industrial Manual. Enter the group number. Also, when applicable, show that optional markings have been used for Group 3 and Group 4 as authorized.

3. REPORT TITLE: Enter the complete report title in all capital letters. Titles in all cases should be unclassified. If a meaningful title cannot be selected without classification, show title classification in all capitals in parenthesis immediately following the title.

4. DESCRIPTIVE NOTES: If appropriate, enter the type of report, e.g., interim, progress, summary, annual, or final. Give the inclusive dates when a specific reporting period is covered.

5. AUTHOR(S): Enter the name(s) of author(s) as shown on or in the report. Enter last name, first name, middle initial. If military, show rank and branch of service. The name of the principal author is an absolute minimum requirement.

6. REPORT DATE: Enter the date of the report as day, month, year; or month, year. If more than one date appears on the report, use date of publication.

7a. TOTAL NUMBER OF PAGES: The total page count should follow normal pagination procedures, i.e., enter the number of pages containing information.

7b. NUMBER OF REFERENCES: Enter the total number of references cited in the report.

8a. CONTRACT OR GRANT NUMBER: If appropriate, enter the applicable number of the contract or grant under which the report was written.

8b, 8c, & 8d. PROJECT NUMBER: Enter the appropriate military department identification, such as project number, subproject number, system numbers, task number, etc.

9a. ORIGINATOR'S REPORT NUMBER(S): Enter the official report number by which the document will be identified and controlled by the originating activity. This number must be unique to this report.

9b. OTHER REPORT NUMBER(S): If the report has been assigned any other report numbers (either by the originator or by the sponsor), also enter this number(s).

10. AVAILABILITY/LIMITATION NOTICES: Enter any limitations on further dissemination of the report, other than those imposed by security classification, using standard statements such as:

(1) "Qualified requesters may obtain copies of this report from DDC."

(2) "Foreign announcement and dissemination of this report by DDC is not authorized."

(3) "U. S. Government agencies may obtain copies of this report directly from DDC. Other qualified DDC users shall request through

_____."

(4) "U. S. military agencies may obtain copies of this report directly from DDC. Other qualified users shall request through

_____."

(5) "All distribution of this report is controlled. Qualified DDC users shall request through

_____."

If the report has been furnished to the Office of Technical Services, Department of Commerce, for sale to the public, indicate this fact and enter the price, if known.

11. SUPPLEMENTARY NOTES: Use for additional explanatory notes.

12. SPONSORING MILITARY ACTIVITY: Enter the name of the departmental project office or laboratory sponsoring (paying for) the research and development. Include address.

13. ABSTRACT: Enter an abstract giving a brief and factual summary of the document indicative of the report, even though it may also appear elsewhere in the body of the technical report. If additional space is required, a continuation sheet shall be attached.

It is highly desirable that the abstract of classified reports be unclassified. Each paragraph of the abstract shall end with an indication of the military security classification of the information in the paragraph, represented as (TS), (S), (C), or (U).

There is no limitation on the length of the abstract. However, the suggested length is from 150 to 225 words.

14. KEY WORDS: Key words are technically meaningful terms or short phrases that characterize a report and may be used as index entries for cataloging the report. Key words must be selected so that no security classification is required. Identifiers, such as equipment model designation, trade name, military project code name, geographic location, may be used as key words but will be followed by an indication of technical context. The assignment of links, rules, and weights is optional.